2013

# Roles of manganese and protein kinase signaling in cell culture and animal models of prion disease

Dustin Paul Martin
*Iowa State University*

# Roles of manganese and protein kinase signaling in cell culture and animal models of prion disease

by

**Dustin Martin**

A dissertation submitted to the graduate faculty

in partial fulfillment of the requirements for the degree of

DOCTOR OF PHILOSOPHY

Co-majors: Molecular, Cellular, and Developmental Biology; Neuroscience

Program of Study Committee:

Anumantha G. Kanthasamy, Major Professor

Arthi Kanthasamy

Eric Rowe

Jesse Hostetter

M. Heather Greenlee

Iowa State University

Ames, Iowa

2013

## TABLE OF CONTENTS

# CHAPTER 1: GENERAL INTRODUCTION

## Dissertation Organization

This dissertation is written in an alternative thesis format and consists of manuscripts that have been published, in peer review, or are being prepared for submission. The references for the background and literature review section and each manuscript chapter are listed at the end of that specific section.

This dissertation contains the experimental results obtained by the author during his graduate study under the supervision of his major professor, Dr. Anumantha G. Kanthasamy in the department of Biomedical Sciences, affiliated with the Neuroscience and Molecular, Cellular, and Developmental Biology Interdepartmental Graduate Programs at Iowa State University of Science and Technology.

## Introduction

Despite several decades of dedicated research by a diverse array of researchers from around the globe, the molecular mechanisms underlying neuronal loss during transmissible spongiform encephalopathy (TSE) remain to be elucidated. Additionally, the etiology of so-called “sporadic” cases of TSE, which represents the

vast majority of cases in both humans and animals, remains unknown. Several recent advancements in the understanding of other protein misfolding neurodegenerative disorders including Alzheimer's Disease (AD), Parkinson's Disease (PD), Amyotrophic Lateral Sclerosi (ALS), and TSE have highlighted the similarities between disease etiopathogenesis which may broaden the diversity of potential future therapies. As our understanding of each disease state increases, the potential of advancements from one disease state applying to another is tantalizingly possible. Conversely, the public health implications of the discovery that AD, PD, and ALS may be transmitted in a prion-like manner highlight the urgency in elucidating the mechanisms underlying these devastating disorders. Although the metal binding capacity of $PrP^C$ and other amyloidogenic proteins is well documented, the environmental contribution to TSE pathogenesis, including the role of divalent metals such as manganese, is unknown. Herein we report that neuronal cells infected with TSE are less susceptible to Mn-induced toxicity than uninfected cells. Mn treatment also induces cytosolic localization of $PrP^C$ in cell and animal models, thus providing a mechanism that incorporates inhibition of the protein degradation machinery with metal dyshomeostasis. Additionally, we have discovered proteolytic activation of the delta isoform of protein kinase C (PKCδ) and changes in the phosphorylation of PKCδ at two regulatory sites in multiple brain regions in a mouse-adapted scrapie model. Knockout of PKCδ causes a significant delay in the onset of motor symptoms associated with TSE and an altered pattern of oxidative damage. These discoveries provide further mechanistic insight into TSE-related

neuronal degeneration.

Metals and Neurodegenerative Disorders

Our understanding of the role of metals in key neurobiological processes as well as in the pathogenesis of various neurodegenerative diseases has continued to expand over the last two decades. Although it is well known that elemental metals are required for normal functioning of cells, the degree at which the central nervous system (CNS) uses metals in synaptic signaling and the loss of metal homeostasis during neurodegenerative diseases was, until recently, unknown. Dyshomeostasis of transition metals such as iron, copper, and zinc have been implicated in major neurodegenerative conditions such as Parkinson's disease (PD), Alzheimer's disease (AD), amyotrophic lateral sclerosis (ALS or Lou Gherig's disease), and Huntington disease (HD) (Bishop et al., 2002; Bossy-Wetzel et al., 2004; Brown, 2009; Bush and Curtain, 2008; Cahill et al., 2009; Gaeta and Hider, 2005; Molina-Holgado et al., 2007; Sayre et al., 1999). Another common pathological feature of neurodegenerative diseases is aggregation of β-sheet rich proteins associated with each specific disease (e.g., α-synuclein in PD, a-beta and tau in AD, and huntingtin in HD) (Tyedmers et al., 2010). Alarmingly, the exposure of amyloidogenic proteins or their cleavage products to metals has been shown to induce their aggregation. Copper has been linked to aggregation of α-synuclein and a-beta (Brown, 2009). Zinc has been implicated in the aggregation of a-beta and manganese was shown to

seed aggregation of recombinant $PrP^C$ (Brown, 2009). Studies overwhelmingly demonstrate metal dyshomeostasis, protein aggregation, and oxidative stress are interconnected mechanisms key to the neurodegeneration in PD, AD, HD, and ALS. Despite this clear association, the molecular mechanisms underlying these phenomena are still poorly understood; however, a clearer picture is beginning to emerge.

Molecular pathways of neurodegeration

Although several of the major programmed cell death signals including extracellular receptors and internal stress receptors have been identified, the molecular pathways leading to DNA fragmentation, lysosome formation, and zeiosis continue to be a target of dedicated investigation. Various signaling pathways have been identified that involve tightly controlled cascades of posttranslational modifications of proteins that lead to apoptosis (Bossy-Wetzel et al., 2004). Many of the key molecules involved in these pathways, such as the proteolytic caspases, remain in a dormant state prior to the activation of the cell death cascade (Jellinger, 2009). However, several proteins that serve normal endogenous functions within the cell are conscripted once the programmed cell death machinery has been activated. The delta isoform of protein kinase C has been implicated in cellular differentiation, proliferation, and secretion; however, cleavage by proapoptotic capspase-3 separates the regulatory domain of the protein from the catalytic domain producing a

constitutively active kinase that can induce PCD (Kanthasamy et al., 2003; Reyland, 2007). The disruption of the delicate interplay between these and other signaling pathways caused by TSE must be more clearly understood if effective treatments are to be designed.

Are all proteinaceous neurodegenerative disorders prion diseases?

Recent evidence elucidated by multiple groups studying a variety of neurodegenerative diseases including Alzheimer's disease, Parkinson's disease, and amyotrophic lateral sclerosis (ALS or Lou Gherig's disease), have established the possibility that the pathogenic proteins implicated in each of these diseases are prions as well. Specifically, α-synuclein, tau, and Mn-superoxide dismutase, the amyloidogenic proteins associated with Parkinson's disease, Alzheimer's disease, and amyotrophic lateral sclerosis, respectively, can catalyze the conversion from their endogenous conformation to their disease isoforms and can therefore be considered prions (Jucker and Walker, 2011; Lee et al., 2010; Moreno-Gonzalez and Soto, 2011; Walker and LeVine, 2012). Our group has focused on understanding the molecular pathways of neurodegeneration in Parkinson's disease in an effort to elucidate the etiology of the disease and to provide targets for pharmaceutical intervention. In an effort to more clearly understand the multilayer connectivity amongst neurodegenerative diseases, we examined the consequence of metal dyshomeostasis and kinase signaling on the progression of TSE-related

neurodegeneration.

Conclusion of background information

Classically, “TSE” and “prion disease” have been used interchangeably to refer to the multitude of diseases caused by the infectious isoform of prion protein ($PrP^{Sc}$). This choice of nomenclature must be reevaluated since it is clear that many, if not all, amyloidogenic proteins associated with neurodegenerative disorders are transmissible pathogens. For the purposes of this document, TSE will refer to the prion disease caused by pathogenic misfolding of the prion protein.

**Literature Review**

Prion Protein

The endogenous prion protein ($PrP^{C}$) is ubiquitously expressed with the highest concentrations in the central nervous system (CNS) and lymphatic system, although its biological function still remains unclear. $PrP^{C}$ has been suggested to function as an antioxidant, a cellular adhesion molecule, a signal transducer, and a metal binding protein (Brown, 2004; Chen et al., 2003; Chiarini et al., 2002; Mange et al., 2002; Sakudo et al., 2004). While the function of the $PrP^{C}$ is not well defined, the hallmark of transmissible spongiform encephalopathy (TSE) is conversion of the

soluble α-helix rich form of cellular $PrP^{C}$ to the insoluble β-sheet rich infectious isoform of the protein ($PrP^{Sc}$) through a still unknown mechanism (Bolton et al., 1985; Collinge, 2005; Prusiner and DeArmond, 1990). The Prnp gene is found on chromosome 20 in humans and encodes for a 254 amino acid sequence before processing (Kretzschmar et al., 1986). The first 22 amino acid residues of the N-terminus are cleaved shortly after translation, and the last 23 amino acid residues of the C-terminus are cleaved prior to the addition of a glycophosphatidylinositol (GPI) anchor (Kretzschmar et al., 1992; Stahl et al., 1987). Properly folded prion protein is present on lipid membrane rafts, and is believed to be internalized via clathrin-mediated endocytosis with a half-life of about 3 hrs (Nunziante et al., 2003; Peters et al., 2003; Prado et al., 2004). Internalized $PrP^{C}$ is rapidly degraded via the ubiquitin proteasomal system (UPS) or recycled back to the cell surface (Ciechanover and Brundin, 2003; Kang et al., 2004; Laszlo et al., 1992). $PrP^{C}$ is a highly conserved protein among mammals, with protein homology scores greater than 90% in all observed species (Martins and Brentani, 2002).

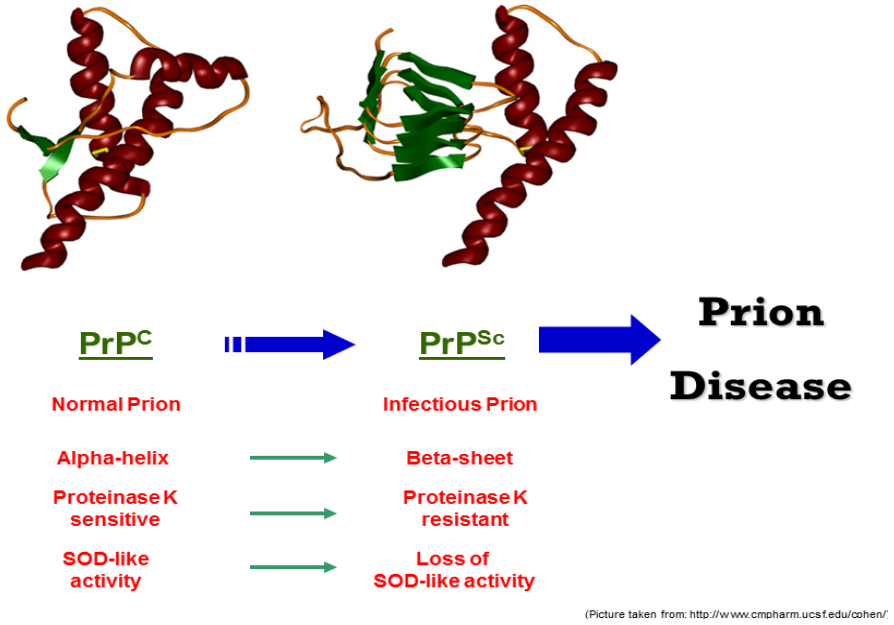


Figure 1 Overview of TSE

Prion Disease and TSE

Prions are pathogenic molecules formed solely from misfolded isomers of endogenous proteins (Alpers and Isselbacher, 1967; Prusiner, 1982). Prions act as a template to induce the misfolding of normal conformers to the pathogenic isoform, that can then propagate more conversions, yet the mechanism by which this change occurs is unknown. Transmissible spongiform encephalopathy (TSE) is a fatal neurodegenerative disorder caused by misfolding of the endogenous prion protein ($PrP^C$) induced by exposure to the pathogenic conformational isomer of PrP ($PrP^{Sc}$) or by heritable mutation of $PrP^C$ (Prusiner, 1991a; Prusiner, 1991b; Prusiner, 1991c).

TSE affects both humans and animals, and transfer between species has been recorded (Belay and Schonberger, 2005). TSE is characterized by accumulation of aggregated, proteolytically-resistant $PrP^{Sc}$, gliosis, neuronal loss, and vacuolation of the CNS (Belay and Schonberger, 2005; Wadsworth and Collinge, 2011). When examined histologically, the neuronal loss and vacuolation observed in TSE gives affected tissue a diagnostic spongy appearance. Reactive astrocytic gliosis, microglial activation, and spongiform degeneration co-localize with accumulation of $PrP^{Sc}$ *in vivo* (DeArmond et al., 1987). Interestingly, different conformational isomers with identical primary sequences can display widely varying pathology indicating that the secondary and tertiary structure of $PrP^{Sc}$ can encode different strains of TSE (Gambetti et al., 2011; Parchi et al., 2010; Weissmann et al., 2011). Recent findings have uncovered the possibility that the amyloid plaque forming proteins involved in Parkinson's disease, Alzheimer's disease, and amyotrophic lateral sclerosis are prions as well (Braak and Del Tredici, 2011; Desplats et al., 2009; Guo and Lee, 2011; Kordower et al., 2008; Munch et al., 2011). A detailed understanding of the prion mechanism that leads to protein aggregation and accumulation may help demystify the etiology of all amyloidogenic neurodegenerative disorders.

TSE and public health

The unique nature of the proteinaceous pathogen that is the causative agent of TSE is highly resistant to classic sterilization methods that affect nucleic acids

(Bellinger-Kawahara et al., 1987; Gibbs et al., 1978). Additive to this is the resistance of $PrP^{Sc}$ to denaturation and proteolysis (Prusiner et al., 1980). Iatrogenic transmission of PrP through blood transfusions and grafts of human tissue have been confirmed (Belay and Schonberger, 2005). $PrP^{Sc}$ binds readily to metal surfaces such as stainless steel surgical instruments and can be readily transmitted if not properly decontaminated (Flechsig et al., 2001; Zobeley et al., 1999). Insidiously, exposure of normal uninfectious brain homogenate to steel wires produced de novo infectious $PrP^{Sc}$ that could be transmitted to animals (Edgeworth et al., 2010). This spontaneous mechanism of $PrP^{Sc}$ generation clearly demonstrates the need to better understand the pathogenesis of this diabolical disease.

Characterization of prion disease

Pathogenically misfolded $PrP^{Sc}$ has been identified as the causative agent of TSE, yet the various forms of this disease do not share a common etiology or pathology. Studies have demonstrated that $PrP^{C}$ undergoes a conversion from endogenous membrane-bound protein to a misfolded transmissible neurodegenerative pathogen through changes to its secondary and tertiary structure by an as yet unidentified process (Prusiner, 1982). Both exposure to pathogenic $PrP^{Sc}$ and mutations within $PrP^{C}$ have been shown to cause TSE (Belay and Schonberger, 2005).

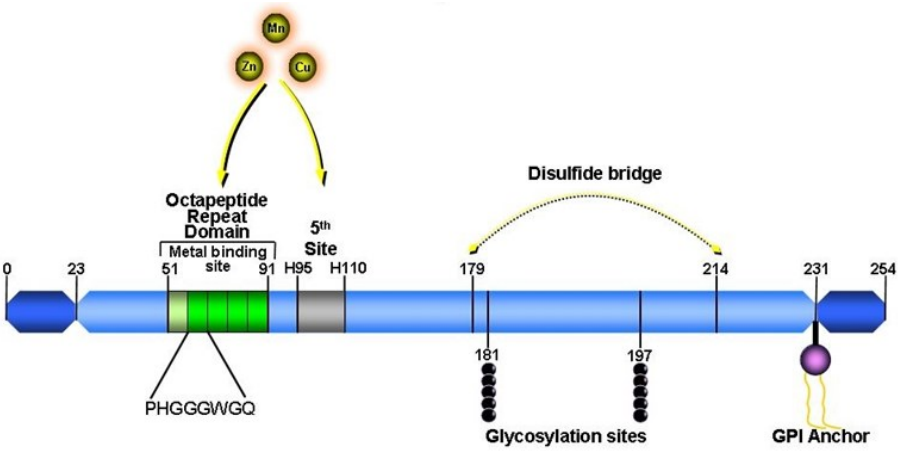


Figure 2 Schematic of $PrP^C$

$PrP^C$ structure and function

Endogenous $PrP^C$ is a glycophosphatidylinositol anchored membrane protein located primarily in lipid raft domains (Lakhan et al., 2009; Naslavsky et al., 1997; Stahl et al., 1987). Structural studies have suggested that the N-terminus of prion protein is unstructured, while the C-terminus is highly structured, with two α-helices linked via disulfide bond, a shorter α-helix, and two short strands of β-sheet structures (Di Natale et al., 2005; Jones et al., 2005; Renner et al., 2004; Viles et al., 2001). The C-terminal domain also contains two N-linked glycosylations on the asparagines in positions 181 and 197 (mouse numbering); however, the protein is found in unglycosylated, monoglycosylated, and diglycosylated forms that produce three distinct bands in immunoblot assays (Kretzschmar et al., 1986). The role the

glycosylations play in the endogenous function of the protein, if any, is currently unknown. However, a recent study has shown the glycosylation state of $PrP^C$ does not affect the metal binding affinity of $PrP^C$ (Davies and Brown, 2009).

Although the metal binding capacity of $PrP^C$ has been demonstrated by multiple studies, the endogenous function of $PrP^C$ is still a matter of debate. It has been suggested to function as an antioxidant, a cellular adhesion molecule, a signal transducer, and a metal regulatory protein (Brown, 2004; Chen et al., 2003; Chiarini et al., 2002; Mange et al., 2002; Sakudo et al., 2004). Cu bound to the N-terminus of $PrP^C$ is able to undergo full and reversible redox chemistry, which allowed for the detoxification of superoxide and the reduction of hydroxyl radicals in *in vitro* assays (Nadal et al., 2007). A variety of approaches have identified possible ligands for $PrP^C$. $PrP^C$ interacts with the cell adhesion molecules NCAM and lamanin to promote neurite outgrowth (Beraldo et al., 2011; Santuccione et al., 2005). The interaction of $PrP^C$ and stress inducible protein 1 (STI1) has been linked to the induction of cell survival under apoptotic stress and the modulation of both short and long term memory performance (Coitinho et al., 2007; Zanata et al., 2002). Although GPI anchored $PrP^C$ does not contain an intracellular domain, initial studies found that the binding of anti-PrP antibodies to cell surface $PrP^C$ induced a calveolin-dependent coupling of PrP to Fyn kinase that resulted in an increase in Fyn kinase activity (Mouillet-Richard et al., 2000). Binding of $PrP^C$ specific antibodies to surface $PrP^C$ has also been shown to selectively modulate 5-HT receptor signaling (Mouillet-Richard et al., 2005). Induced dimerization of $PrP^C$ through binding of the anti-PrP

antibody 6H4 in human neurons resulted in alterations of the mitogen activated protein kinase (MAPK) signaling pathways (Arsenault et al., 2012). Additionally, in the same study a peptide corresponding to residues 106-126 of $PrP^{C}$ activated growth factor related signaling pathways including vascular endothelial growth factor (VEGF) signaling and the phosphoinositide-3 kinase (PI3K) pathway. Recent evidence has also linked $PrP^{C}$ signal transduction to Alzheimer's disease pathogenesis. In this study, Aß was shown to directly interact with cell surface $PrP^{C}$ to modulate the distribution of NMDA receptors through a Fyn kinase-dependent mechanism (Um et al., 2012; Um and Strittmatter, 2012). These studies and others indicate that $PrP^{C}$ must interact with a transmembrane signaling protein to transmit information into the cell; however the identity of this elusive molecule or molecules remains a mystery.

Aggregation and amyloidogenesis of $PrP^{Sc}$

Similar to other amyloidogenic proteins, $PrP^{Sc}$ often undergoes truncation prior to the formation of amyloid fibrils (Kitamoto et al., 1991). Sequencing of peptides obtained through purification of amyloid plaques found in GSS using formic acid identified the amyloid core of $PrP^{Sc}$ resides in the $PrP^{Sc}$ binding domain between residues 90-140 (Piccardo et al., 1996). The structure of the amyloid-forming domain in $PrP^{Sc}$ is believed to be a left-handed ß-helix (Govaerts et al., 2004). This ß-helix structure allows $PrP^{Sc}$ to form trimers through hydrophobic

interactions that can then stack vertically forming unbranched fibrils. The amyloid plaques in TSE are stained strongly by classical amyloid-staining dyes such as thioflavin T, and congo red (Ishikawa et al., 2004).

Despite the ability to form amyloid, mature amyloid plaque formation in TSE is a relatively rare occurrence. Only the rare familial mutations resulting in GSS, the isolated cases of kuru, and 5-10% of CJD cases are associated with amyloid plaque deposition (Ghetti et al., 1995; Hainfellner et al., 1997; Kovacs et al., 2002; Liberski and Brown, 2004). The vast majority of TSE cases in humans and animals are associated with little to no amyloid. This lack of amyloid accumulation in TSE indicates that cerebral amyloidosis is unlikely to cause the neuronal dysfunction and death found in TSE. Studies have shown that aggregations of non-fibrilliar PrP oligomers are neurotoxic (Soto and Satani, 2010), and can spread from cell to cell through direct cell to cell contact and by release into the intercellular media (Fevrier et al., 2004; Kanu et al., 2002). Transmission and propagation of aggregated $PrP^{Sc}$ through both synapses and actin-rich intercellular nanotubes has been observed (Gousset et al., 2009; Magalhaes et al., 2005). Small aggregated oligomers of $PrP^{Sc}$ were determined to be more infectious than monomeric or amyloid $PrP^{Sc}$ (Silveira et al., 2005). Formation of a transient oligomeric core may precede formation of amyloid fibrils when they do occur (Ohhashi et al., 2010). Accumulation of amyloid plaques may in fact be a neuroprotective strategy used by the CNS to deal with misfolded proteins that are resistant to normal degradation pathways.

Metal binding affinity of $PrP^C$

Octapeptide Repeat Domain: $PrP^C$ contains several octapeptide repeat sequences (PHGGSWGQ) toward the N-terminus, which have binding affinity for divalent metals such as copper, manganese, and zinc, with preferential binding for copper (Hornshaw et al., 1995; Viles et al., 1999). The number of octapeptide repeats differs from species to species. For example, humans, mice, sheep, and deer each have five octapeptide repeats in the wild type protein while bovine PrP has six (Mastrangelo and Westaway, 2001). Mutation of the prion protein gene including point mutations, deletions, or multiple insertions of the octapeptide repeats have been linked to inherited prion disease in humans (Mead et al., 2007; Yin et al., 2007) A higher number (up to 14) of repeats has been associated with the human form of the prion disease known as Gerstmann-Sträussler-Sheinker (GSS) syndrome (Krasemann et al., 1995; Palmer and Collinge, 1993). Binding of divalent cations to the octapeptide repeats has been speculated to facilitate the folding of the unstructured N-terminus, resulting in stabilization of the protein conformation (Cereghetti et al., 2003).

Recent studies have shown disease associated mutations in octapeptide repeats are critical for divalent metal-induced protein turnover and internalization by endocytosis, suggesting that octapeptide repeats in prion protein can alter the homeostasis of the divalent metal pool in the cell (Stevens et al., 2009). Studies using electron resonance imaging and X-ray crystallography on recombinant

octapeptide fragments have shown that a single copper is bound by each full octapeptide repeat segment in a pentacoordinate complex involving residues HGGGW (Aronoff-Spencer et al., 2000; Burns et al., 2002; Burns et al., 2003). Further studies on Cu coordination with the octapeptide repeat domain have shown that there are three distinct modes at physiological pH (Chattopadhyay et al., 2005). The antioxidant activity of $PrP^C$ requires Cu bound within the octapeptide repeat domain (Brown et al., 1999; Brown et al., 2001; Gaggelli et al., 2008; Treiber et al., 2007). Cu bound by the octapeptide repeat domain of $PrP^C$ is able to undergo full and reversible redox chemistry and can function to detoxify superoxide and reduce hydroxyl radicals (Nadal et al., 2007). Loss of this antioxidant activity may exascerbate neurodegeneration in TSE. Additionally, transgenic mice expressing $PrP^C$ devoid of the octapeptide repeat domain showed greater susceptibility to ischemic injury when compared to wild type mice (Mitteregger et al., 2007).

The endocytosis of the $PrP^C$ upon binding Cu was shown in a series of experiments in which the $PrP^C$ null mouse hybridoma cell line F14 was transfected with a variety of Prnp mutants fused with GFP (GFP-$PrP^C$) and their response to copper was measured. F14 cells transfected with normal GFP-$PrP^C$ showed a loss of cell surface fluorescence when exposed to copper, indicative of internalization, while cells expressing a form of PrP truncated from residues 38-231 did not. Conversely, chelation of divalent metals by the selective resin chelex caused an increase in surface fluorescence. Mutants in which the octapeptide repeats were knocked out (Δ51-90) and mutants in which there is one copy of the OR (Δ67-90)

showed no change in cell surface fluorescence upon Cu treatment while Δ67-90 showed a decrease less significant than GFP-$PrP^C$ but more significant than Δ51-90. These results showed that one octapeptide repeat was enough to rescue PrP internalization. Manganese and zinc were also tested but no statistical difference in cell surface fluorescence was seen (Haigh et al., 2005).

Interestingly, the N-terminal domain is not required for conversion from $PrP^C$ to $PrP^{Sc}$. Using a scrapie infected N2a mouse neuroblastoma cell model, the octapeptide repeat region was determined to have no effect on conversion from $PrP^C$ to $PrP^{Sc}$ in a chimeric mouse-Syrian hamster construct of the Prnp gene. All variations of the octapeptide repeat region tested showed persistent infection by $PrP^{Sc}$ (Rogers et al., 1993).

5th Site: As indicated above, $PrP^C$ is a putative metalloprotein since the octapeptide repeat sequences in the protein have high affinity for divalent cations including copper, manganese, and zinc, and the binding sites are suggested to play a role in the pathogenesis of prion diseases (Brown et al., 1997; Hesketh et al., 2007; Hornshaw et al., 1995; Moore et al., 2006). Initial studies on Cu occupancy indicated that while 5 atoms of Cu were bound to $PrP^C$, the octapeptide repeat domain only accounted for 4 atoms, arguing for a so called “5th site”. Additional higher affinity metal binding sites were identified at His 95 and 110 (mouse numbering) (Jackson et al., 2001; Jones et al., 2004). While His 110 appears to be the highest affinity site for Cu binding, His 95 was apparently required for the binding

of Mn (Brown, 2009).

Studies using recombinant $PrP^C$ have shown that Mn can irreversibly replace Cu bound to $PrP^C$, despite an apparent lower affinity, and this replacement causes conformational changes within the protein (Brazier et al., 2008; Zhu et al., 2008). Recombinant $PrP^C$ refolded in the presence of Mn was originally thought to bind up to four molecules of Mn at the octapeptide repeat domain, similar to Cu (Brown et al., 2000). However, isothermal titration calorimetry experiments have demonstrated that $PrP^C$ binds two molecules of Mn at each each at two different sites, with dissociation constants of 63 and 200 μM (Brazier et al., 2008). In comparison, divalent metal transporter 1 (DMT-1), a known transporter of Mn across the plasma membrane, was shown in kinetic studies of Mn uptake to transport Mn in mM concentrations (Garrick et al., 2006). Interestingly, the higher affinity binding site was not the octapeptide repeat domain, but the so called “5th site”. This study went on to show that Mn is able to replace Cu in Cu saturated PrP, even though PrP has a higher affinity for Cu at both binding sites (Brazier et al., 2008). The binding of Mn to $PrP^C$ was irreversible, as was the oxidation of Mn bound to $PrP^C$.

The biological consequence of Cu replacement by Mn on the prion protein is still unknown. However, molecular studies using circular dichroism and Raman optical activity indicate that upon PrP binding to Mn, the secondary structure becomes more organized, gaining greater α-helix and β-sheet content than Cu-bound PrP (Brazier et al., 2008; Zhu et al., 2008). Limited proteolytic digestion experiments using proteinase K have shown Mn-bound $PrP^C$ gains partial protease

resistance, similar to, but less profound than the diagnostic proteolytic resistance characteristic of $PrP^{Sc}$ (Brown et al., 2000; Kim et al., 2005). Once bound to Mn, PrP can also seed polymerization of soluble oligomers of metal free PrP (Abdelraheim et al., 2006; Giese et al., 2004). Most studies evaluating prion-Mn interactions were conducted in cell free systems using recombinant protein; however, the role of Mn in the pathogenesis of TSE has not been systematically studied and is currently unknown. Understanding the mechanisms of manganese interaction with prion protein may help to elucidate the pathophysiological mechanisms of prion diseases.

## Manganese and TSE

The essential elemental metal Manganese (Mn) is required by organisms as an enzymatic cofactor for normal functioning; however, Mn dyshomeostasis results in adverse neurological deficits (Aschner, 1999; Dobson et al., 2004; Levy and Nassetta, 2003; Pfeifer et al., 2004). Prolonged exposure to high concentrations of Mn results in an irreversible neurological disorder called manganism (Beuter et al., 1994; Gibbs et al., 1999; Myers et al., 2003). Early signs of manganism are associated with psychiatric disturbances, while later signs include rigidity, bradykinesia, dystonia, and ineffectiveness of levo-dopa therapy (Beuter et al., 1994; Dobson et al., 2004; McMillan, 1999). Several lines of evidence suggest that exposure to Mn or Mn-containing compounds induces a variety of cellular changes including mitochondrial dysfunction, increased oxidative stress, glutathione and

dopamine depletion, impairment of energy metabolism and antioxidant systems, and alterations in various cell signaling pathways (Erikson and Aschner, 2003; Kitazawa et al., 2002; Roth and Garrick, 2003).

Elevated Mn levels in the brain and blood of humans and animals afflicted with TSE have been observed. In particular, altered Mn content has been observed in the blood and brain of humans infected with Crueztfelt-Jacob Disease (CJD), mice infected with scrapie, and in cattle infected with bovine spongiform encephalopathy (BSE). Additionally, Mn-bound $PrP^{Sc}$ can be isolated from both humans and animals infected with TSE, again despite a lower affinity than copper (Hesketh et al., 2007; Hesketh et al., 2008; Thackray et al., 2002; Wong et al., 2001).

Our group has shown that $PrP^{C}$ interacts directly with the metal to protect cells from Mn toxicity, and Mn exposure increases $PrP^{C}$ protein levels independent of transcriptional upregulation. Our studies demonstrated that $PrP^{C}$ protects against Mn-induced neurotoxicity in mouse neural cells that do not express $PrP^{C}$ (PrPko). We found $PrP^{C}$ expressing cells are more resistant to Mn-induced cytotoxic and apoptotic cell death, and accumulated less Mn compared to PrPko. Also, Mn-induced increases in ROS production, caspase-3 and -9 activation, and DNA fragmentation were significantly lower in $PrP^{C}$ cells compared to PrPko cells. Further, the significantly reduced Mn uptake in $PrP^{C}$ cells suggested that $PrP^{C}$ might act as a metal sink, thereby preventing Mn from entering the cells and exerting its neurotoxic effect. Furthermore, we found Mn treatment significantly altered the turnover of $PrP^{C}$. Pulse chase experiments confirmed that the half-life of $PrP^{C}$ in Mn-

treated cells was significantly increased (Choi et al., 2007; Choi et al., 2010).

In addition, neuronal cells persistently infected with $PrP^{Sc}$ were found to be more susceptible to oxidative stress (Fernaeus et al., 2005; Milhavet et al., 2000). Therefore, it was believed that the loss of this protective mechanism upon conversion from $PrP^{C}$ to $PrP^{Sc}$ may contribute to the neurodegeneration associated with spongiform encephalopathy. However, information uncovered by the author and presented in the first research chapter showed that infection by $PrP^{Sc}$ actually conferred protection from Mn neurotoxicity. The octapeptide domain of $PrP^{C}$ may be required for the Mn-induced increase in stability and accumulation of the protein. Studies using *in vitro* neuronal cells expressing N-terminally truncated forms of $PrP^{C}$ show increased toxicity with Cu and Mn treatments (Haigh and Brown, 2006). Zinc, iron, and nickel were also tested in these studies, but no significant difference was found. Since $PrP^{C}$ serves as a template for propagation of TSE upon scrapie infection, Mn-induced stabilization of $PrP^{C}$ may accelerate conformational conversion of $PrP^{C}$ to $PrP^{Sc}$. Whether the increase in Mn concentration observed in the brain during the progression of TSE in humans and animals is a key step in the pathogenesis of TSE or is a result of impaired homeostatic regulatory systems, including altered metal binding upon conversion to $PrP^{Sc}$, remains to be determined. Further studies are underway to elucidate the role of the octapeptide repeat domain and $5^{th}$ site in Mn-induced changes in $PrP^{C}$ and the role Mn binding plays in the pathogenesis of the disease.

Environmental contributions to TSE etiology and pathogenesis

Environmental exposure to transition metals has been linked to the pathogenesis of various neurodegenerative disorders (Migliore and Coppede, 2009). Metal neurotoxicity often exacerbates the degenerative changes that occur during these diseases, including ionic imbalance, oxidative stress, and protein aggregation (Bowman et al., 2011; Brown, 2004; Perl and Good, 1991). The amyloidogenic proteins implicated in the pathology of PD, AD, ALS, and TSE have all been shown to bind divalent metals (Brown, 2009). Additionally, these proteins are believed to have a role in maintaining metal homeostasis within the cell. The dysregulation of metal homeostasis observed in the terminal stages of neurodegenerative disorders highlights the involvement of metals in the molecular pathways of neurodegeration. To date, the vast majority of work done to elucidate the mechanisms of TSE pathogenesis has focused on the genetic determinants and biophysical kinetics of protein aggregation. A more detailed understanding of the environmental contributions, including the role of metals, will enable the development of effective treatment strategies for these debilitating diseases.

Sporadic cases of TSE in humans and animals are thought to arise from "thermodynamically unlucky" folding of $PrP^{C}$ to a pathogenic isoform. However, the environmental contribution to TSE etiology has received less attention than the genetic and molecular determinants of pathogenesis. Exposure to organophosphate pesticides has been hypothesized to induce structural changes within PrP leading to

TSE pathogenesis (Purdey, 1996). However, studies using cell culture and mouse models of TSE using the organophosphate compounds phosmet and dimethoate have failed to find any increase in ß-sheet content or PrP aggregation, nor was the course of TSE changed as a result of treatment with these compounds (Shaw et al., 2002). Interestingly, phosmet exposure did increase the level of cell surface $PrP^{C}$ in human neuroblastoma cells independent of transcription (Gordon et al., 1998).

Studies have identified a correlation with low levels of Cu and high levels of Mn as potential environmental risk factors leading to the onset of sporadic TSE in animals (Davies and Brown, 2009; Purdey, 2000). A study of monozygotic twins with a pathogenic hereditary mutation to PrP developed TSE pathology seven years apart from each other (Bowman et al., 2011). These findings argue strongly for the possibility of an environmental determinant to the onset of TSE. The recurrence of TSE in livestock despite multiple governmental programs designed to eradicate the disease argues for the persistence of the pathogen in the environment. A correlation between soil clay content and incidence of chronic wasting disease in elk has been discovered indicating that soil constituents may affect the persistence of $PrP^{Sc}$ in the environment (Johnson et al., 2007). A recent study found that infectious $PrP^{Sc}$ can persist in soils for at least two years (Davies and Brown, 2009). Additionally, the presence of high levels of Mn in soils not only protects the protein from degradation, but may actually increase infectivity by up to 100-fold. These studies provide a route whereby $PrP^{Sc}$ derived from carcasses or farm runoff can enter into the environment. Then oral inoculation of ruminants can occur through ingestion of soil microparticles

while grazing. The retention of infectivity in the environment seems to depend heavily on the composition of the soil and a greater understanding of these determinants would greatly help in assessing the risk factors of TSE.

It seems clear that exogenous environmental variables are determinants that contribute to the spread of sporadic TSE and other neurodegenerative disorders including Parkinson's disease, Alzheimer's disease, and amyotrophic lateral sclerosis. Without a greater understanding of these variables, the risk factors and appropriate countermeasures cannot be accurately predicted. The contribution of divalent metals to pathogenesis remains an important area of study for all neurodegenerative diseases. Therefore the environmental contributors to the etiology of one neurodegenerative disorder may have implications for each.

## The ubiquitin proteosome system

Ubiquitination is a tightly controlled cellular process that is involved in degradation of proteins, protein trafficking, and signaling. The first step in the addition of the 76 amino acid-long ubiquitin peptide to a substrate is the activation of ubiquitin by an E1 enzyme by adenylation of the C-terminus in an ATP dependent manner and the formation of a thioester bond to a catalytic Cys residue. The activated ubiquitin is then transferred to an E2 conjugating enzyme through a second thioester bond. The E2 enzyme then binds an E3 ubiquitin ligase that will attach the activated ubiquitin or ubiquitin-like peptide to a lysine residue on the

protein substrate. The E3 enzyme can then covalently attach subsequent ubiquitin molecules to any of the seven internal lysines (Lys-6, Lys-11, Lys-27, Lys-29, Lys-33, Lys-48 and Lys-63) on the first forming a poly ubiquitin chain. (Clague and Urbe, 2010; Mukhopadhyay et al., 2007; Tyedmers et al., 2010; Whatley et al., 2008).

Poly ubiquitin chains are classically associated with marking proteins for degradation by the 26S proteosome; however monoubiquitination of proteins and some specific polyubiquitination motifs are involved in DNA repair, protein localization, endosomal trafficking, and autophagic protein degradation (Mukhopadhyay et al., 2007; Sarge and Park-Sarge, 2011). Specificity between substrates appears to be encoded in the specific pairing of E2-E3 enzymes since only two human E1s have been identified, whereas 40 different E2 and over 600 E3 enzymes have been found (Deshaies and Joazeiro, 2009). The fate of the target protein is largely determined by which lysine residue subsequent ubiquitins are attached to within the polyubiquitin chain, although the exact signals and E1-E2-E3 proteins involved in each process are still a subject of ongoing research.

UPS dysfunction in proteinopathies

Although the etiology and pathogenesis of AD, PD, ALS, HD, and TSE differ, one of the pathological similarities shared between all proteinacious neurodegenerative disorders is accumulation of insoluble protein aggregates in intra- or extracellular inclusion bodies. These inclusions are largely formed by a single

protein constituent that is associated with the pathogenesis of the specific disease. The constituents of the disease-associated inclusions are often ubiquitinated, yet are not degraded by the UPS (Ardley and Robinson, 2004; Kang et al., 2004; Sarge and Park-Sarge, 2011). Monoubiquitination of proteins has been determined to act as a signal for protein sorting to intracellular vesicles (Mukhopadhyay et al., 2007; Sarge and Park-Sarge, 2011); however, a detailed understanding of the trafficking and quality control of amyloidogenic proteins through the UPS remains recondite. Intracellular protein aggregates have been shown to directly inhibit UPS function, causing a feedback loop that may exacerbate UPS dysfunction during the course of disease pathogenesis (Bence et al., 2001; Bennett et al., 2005; Holmberg et al., 2004) .

Mahogunin RING-finger 1 is an E3 ubiquitin ligase

The E3 ubiquitin ligase mahogunin RING-finger 1 (Mgrn1) contains a C3HC4 RING-finger Zn-binding domain, similar to other zinc finger ubiquitin ligases (He et al., 2003b; Phan et al., 2002). The gene sequence has two alternative exons that produce four alternate splice variations of 532, 554, 556, and Mgrn1 has displayed both mono- and polyubiquitination activity in both *in vitro* and *in vivo* models (Jiao et al., 2009; Phan et al., 2002). Although E3 ubiquitin ligases encode specificity for specific substrates, Mgrn1 has been implicated in a vast array of functions outlined below.

Mgrn1 was first identified as a downstream accessory protein involved in pigment type switching through the G-protein coupled receptor, melanocortin-1 (Mc1r), in hair follicle melanocytes (He et al., 2003a; Miller et al., 1997). First dubbed *mahoganoid* (*md/md*), this spontaneous mutation produced animals with a black coat even in the presence of the normally yellow gain of function mutations of the agouti gene (Miller et al., 1997). Discovered in conjunction with *mahogany*, which was later identified as the mouse ortholog for the human gene attractin (Atrn), both are downstream modulators for the production of the pigments eumelanin (black) or pheomelanin (red/yellow) through Mc1r signaling. Agouti binding functions as a competitive inhibitor to reduce Mc1r activity, resulting in the production of pheomelanin, while activation of Mc1r by α-melanocyte signaling hormone (α-MCH) binding causes melanocytes to produce eumalanin (Ollmann et al., 1997; Sakai et al., 1997). Both Mrgn1 and Atrn loss of function phenotypes require the presence of Mc1r for the expression of eumelanin since Mc1r(-/-) animals are yellow regardless of the Mgrn1 or Atrn genotype (Miller et al., 1997). While Mc1r was determined to be a substrate for Mgrn1 binding, Mgrn1 does not ubiquitinate Mc1r or melanocortin-4 receptor (Mc4r), but does ubiquitinate Mc2r, highlighting the specificity of the E3 ubiquitin ligase activity (Cooray et al., 2011; Perez-Oliva et al., 2009). Perez-Oliva and colleagues found that Mgrn1 reduced Mc1r and Mc4r signaling and production of cAMP without altering its cell surface expression or rate of turnover by inhibiting the interaction of Mc1r and Mc4r with Gα, thus preventing the activation of adenylate cyclase. This competitive inhibition of GPCR function without ubiquitination appears

to be a novel role for E3 ubiquitin ligases. However, a recent study has shown that Mgrn1 controls the sorting of Mc4r to the lysosome for degradation through monoubiquitination of tumor susceptibility gene 101 (TSG101) and that knockdown of Mgrn1 with siRNA did not restore cAMP levels, thus contradicting the results of Perez-Oliva, *et al.* with regard to Mc4r (Overton and Leibel, 2011). TSG101 is a key component of the endosome sorting complex required for trafficking (ESCRT-1) pathway that is responsible for trafficking vesicles to the lysosome for degradation (Babst et al., 2000). Depletion of Mgrn1 in HeLa cells produced enlarged early and late endosomal vesicles, and inhibited the lysosomal degradation of activated epidermal growth factor receptor (EGFR) (Kim et al., 2007). Additionally, Mgrn1 may play some role in the regulation of metabolism since Mgrn1 loss of function caused reduced food intake and subsequent body mass reduction in normally obese Agouti overexpressing Yellow mice, and resulted in an 80% reduction in plasma insulin in Mc4r null mice (Overton and Leibel, 2011; Phan et al., 2006). Finally, Mgrn1 knockout pups have altered expression of the patterning genes Nodal1, Lefty1, and Lefty2 leading to a high instance of congenital heart defects and greatly decreased survivability associated with abnormal L/R patterning (Cota et al., 2006). Clearly, Mgrn1 is involved in a diverse and critical number of cellular processes and should continue to be the target of dedicated investigation.

Mahogunin and TSE

Mgrn1 has emerged as a molecule of marked importance with regard to TSE pathogenesis since Mgrn1 knockout mice also display progressive spongiform vacuolation of the CNS similar to TSE but without the presence of pathogenic $PrP^{Sc}$ (He et al., 2003b). Specifically, the non-agouti curly ($md^{nc}/md^{nc}$) mutation of Mahogunin caused progressive spongiform changes and degeneration in the cerebral cortex, striatum, thalamus, hippocampus, and brain stem, and cerebellum. By one year of age, mice had widespread astrogliosis associated with neuronal loss. Further studies on the role of Mgrn1 in spongiform degeneration discovered that $PrP^{C}$ exposed to the cytosol allosterically inhibits Mgrn1 E3 ubiquitin ligase function (Chakrabarti and Hegde, 2009). Therefore, it is possible that the interaction of Mgrn1 with intercellular $PrP^{Sc}$ may be a key contributor to spongiform degeneration indicative of TSE. However, recent evidence has indicated that neither overexpression nor knockout of Mgrn1 affects the progression of mouse adapted scrapie (Silvius et al., 2013). Although Mgrn1 binds with $PrP^{C}$ at the octapeptide repeat domain, $PrP^{C}$ is not a substrate for Mgrn1-catalyzed ubiquitination (Chakrabarti and Hegde, 2009; He et al., 2003b). However, since $PrP^{Sc}$ accumulates in early endosomal vesicles, inhibition of Mgrn1 activity during TSE pathogenesis may alter vesicle trafficking and prevent lysosomal degradation of $PrP^{Sc}$ aggregates. A possible mechanism for the interaction of Mn induced cytosolic PrP and Mgrn1 is proposed in research chapter 3.

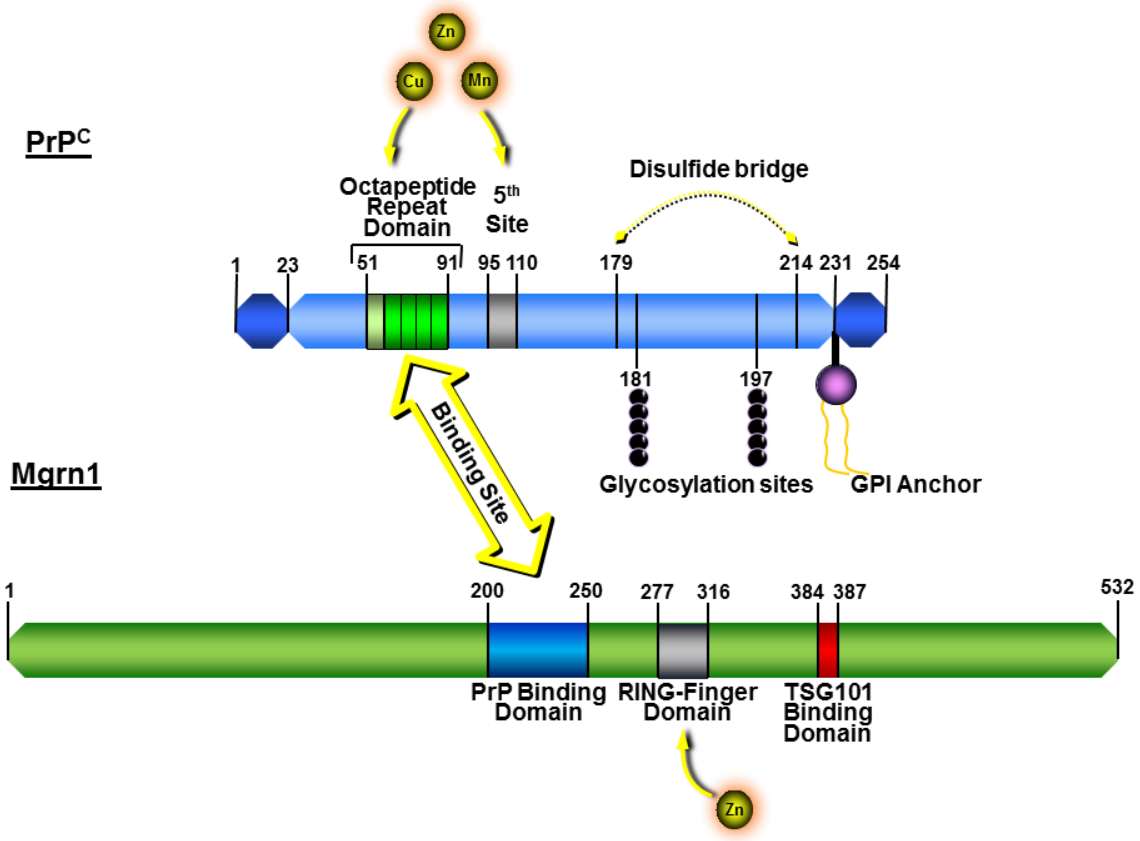


Figure 3 Interaction of $PrP^C$ and Mgrn1

Apoptotic cell death in TSE

Activation of caspases and fragmentation of DNA, both hallmarks of apoptotic cell death, have been observed in both *in vitro* and *in vivo* models of TSE-related neurodegeneration (Bourteele et al., 2007; Carimalo et al., 2005; Fairbairn et al., 1994; Hetz et al., 2003; Offen et al., 2000). Caspase-3 belongs to a highly conserved group of cysteine proteases that are central in the execution of PCD in

response to apoptotic stimuli. Dependent upon the specific apoptotic stimuli, distinct initiator caspases are activated that in turn proteolytically cleave the full length procaspase-3 into a catalytically active form. In the extrinsic apoptotic pathway, extracellular death signals belonging to the tumor necrosis factor (TNF) family of proteins are transduced by TNF receptors which activate initiator caspases 8 and 10. In the intrinsic pathway, cellular damage by oxidative stress or cytotoxic agents causes depolarization of the mitochondrial membrane, release of cytochrome C from the mitochondria, and subsequent activation of initiator caspase-9 (Cain et al., 2002; Reed, 2004). After prolonged induction of the unfolded protein response during endoplasmic reticulum stress, initiator caspase-12 is activated which can lead to apoptotic cell death as well (Hetz et al., 2003). However, the apoptotic pathway involving ER stress is still under investigation as recent studies have found that ER induced PCD can occur independent of caspase-12 activation (Di Sano et al., 2006; Obeng and Boise, 2005; Steele et al., 2007).

A variety of potential apoptotic stimuli have been implicated in TSE related apoptosis, including oxidative and endoplasmic reticulum stress (Fairbairn et al., 1994; Ferreiro et al., 2006; Ferreiro et al., 2008; Hetz et al., 2003; Kim et al., 2001; Milhavet and Lehmann, 2002; Soto, 2008). Persistent infection by $PrP^{Sc}$ increases susceptibility to oxidative stress in neuroblastoma cells (Fernaeus et al., 2005; Milhavet et al., 2000). Our group has discovered that expression of $PrP^{C}$ exacerbates ER stress-related apoptosis induced by treatment with tunicamysin (Anantharam et al., 2008). Despite these discoveries, the signaling cascades leading

to prion-induced apoptosis are still unclear. A detailed understanding of the molecules involved in prion related cell death would not only expand the understanding of a unique neurodegenerative disease, but may also provide potential targets for pharmaceutical intervention.

The role of PKCδ in neurodegeneration

The delta isoform of protein kinase C (PKCδ) is a ubiquitously expressed, diacylglycerol (DAG) dependant, calcium independent serine/threonine kinase whose normal cellular functions include cellular differentiation, proliferation, secretion, and apoptosis (Benes and Soltoff, 2001; Kanthasamy et al., 2003; Kikkawa et al., 2002; Miyamoto et al., 2002; Orosco et al., 2006; Reyland, 2007). Under a variety of apoptotic stimuli, including agents of oxidative or endoplasmic reticulum stress, PKCδ is proteolytically cleaved by the effector caspase, caspase-3, into two subunits: regulatory and catalytic (Kanthasamy et al., 2003; Kikkawa et al., 2002; Kitazawa et al., 2005; Reyland, 2007; Yang et al., 2004). Separation of the regulatory domain from the catalytic domain by proteolytic cleavage produces a persistently active kinase that translocates to several different cellular organelles, including the nucleus, mitochondria, and plasma membrane, and induces apoptotic cell death (Kanthasamy et al., 2003; Kikkawa et al., 2002; Reyland, 2007; Yoshida, 2007). Expression of the catalytic domain alone was shown to be sufficient to induce apoptosis in cells (Denning et al., 2002). Inhibition of caspase-3 or PKCδ catalytic

activity protects cells from apoptosis induced by oxidative and endoplasmic reticulum stress (Anantharam et al., 2004; Choi et al., 2007; Hetz et al., 2003; Kaul et al., 2003; Kitazawa et al., 2003; Kitazawa et al., 2004; Latchoumycandane et al., 2005; Yang et al., 2004). A study done by our lab indicated that inhibition of PKCδ activity by rottlerin protects mice treated with theo xidative stress inducing Parkinsonian toxin MPTP (Zhang et al., 2007). Animals treated with rottlerin showed increased dopamine levels and subsequent locomotor function when compared to animals only treated with toxin. This study shows that inhibition of PKCδ proapoptotic activity may be a powerful tool in the treatment of neurodegenerative disorders.

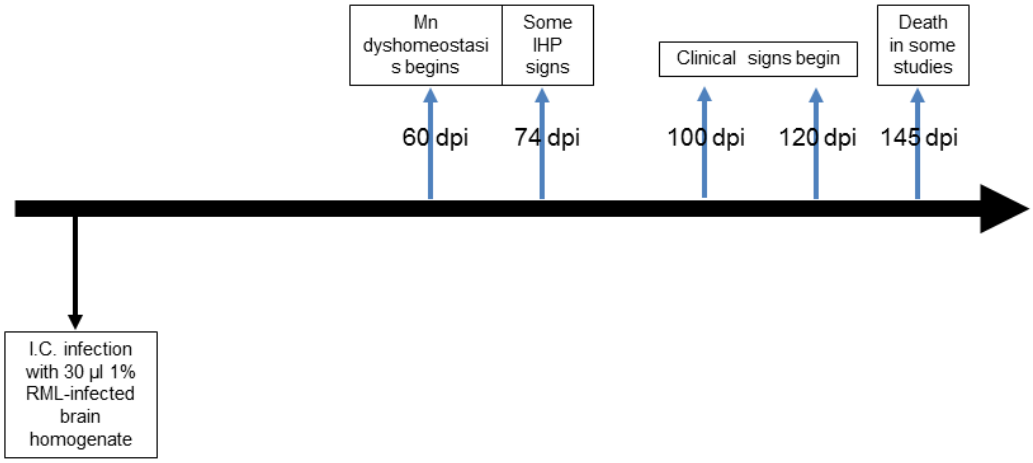


Figure 4 Progression of Murine RML Scrapie

Current and future therapies against prion disease

To date, there is only a single drug, quinacrine, currently undergoing clinical trials to treat TSE. Unfortunately, the vast majority of promising compounds that have shown anti-prion activity in *in vitro* cell culture models fail to show any impact on the course of the disease in *in vivo* animal models or during clinical trials. The focus on inhibition of the prion mechanism may be premature since the mechanism of this phenomenon is still unknown. Due to the emerging interconnectivity of all proteinaceous neurodegenerative disorders, the pathways of neurodegeneration elucidated within PD, AD, and ALS models may help to establish new opportunities for pharmaceutical intervention in all prion diseases.

**References**

Abdelraheim, S.R., Kralovicova, S., Brown, D.R., 2006. Hydrogen peroxide cleavage of the prion protein generates a fragment able to initiate polymerisation of full length prion protein. Int J Biochem Cell Biol. 38**,** 1429-40.

Alpers, D.H., Isselbacher, K.J., 1967. Protein synthesis by rat intestinal mucosa. The role of ribonuclease. J Biol Chem. 242**,** 5617-22.

Anantharam, V., et al., 2004. Blockade of PKC{delta} Proteolytic Activation by Loss of Function Mutants Rescues Mesencephalic Dopaminergic Neurons from

Methylcyclopentadienyl Manganese Tricarbonyl (MMT)-Induced Apoptotic Cell Death. Ann N Y Acad Sci. 1035, 271-89.

Anantharam, V., et al., 2008. Opposing roles of prion protein in oxidative stress- and ER stress-induced apoptotic signaling. Free Radic Biol Med. 45, 1530-41.

Ardley, H.C., Robinson, P.A., 2004. The role of ubiquitin-protein ligases in neurodegenerative disease. Neurodegener Dis. 1, 71-87.

Aronoff-Spencer, E., et al., 2000. Identification of the Cu2+ binding sites in the N-terminal domain of the prion protein by EPR and CD spectroscopy. Biochemistry. 39, 13760-71.

Arsenault, R.J., et al., 2012. Induction of ligand-specific PrP (C) signaling in human neuronal cells. Prion. 6, 477-88.

Aschner, M., 1999. Manganese homeostasis in the CNS. Environ Res. 80, 105-9.

Babst, M., et al., 2000. Mammalian tumor susceptibility gene 101 (TSG101) and the yeast homologue, Vps23p, both function in late endosomal trafficking. Traffic. 1, 248-58.

Belay, E.D., Schonberger, L.B., 2005. The public health impact of prion diseases. Annu Rev Public Health. 26, 191-212.

Bellinger-Kawahara, C., et al., 1987. Purified scrapie prions resist inactivation by procedures that hydrolyze, modify, or shear nucleic acids. Virology. 160, 271-4.

Bence, N.F., Sampat, R.M., Kopito, R.R., 2001. Impairment of the ubiquitin-proteasome system by protein aggregation. Science. 292, 1552-5.

Benes, C., Soltoff, S.P., 2001. Modulation of PKCdelta tyrosine phosphorylation and activity in salivary and PC-12 cells by Src kinases. Am J Physiol Cell Physiol. 280, C1498-510.

Bennett, E.J., et al., 2005. Global impairment of the ubiquitin-proteasome system by nuclear or cytoplasmic protein aggregates precedes inclusion body formation. Mol Cell. 17, 351-65.

Beraldo, F.H., et al., 2011. Metabotropic glutamate receptors transduce signals for neurite outgrowth after binding of the prion protein to laminin gamma1 chain. FASEB J. 25, 265-79.

Beuter, A., et al., 1994. Diadochokinesimetry: a study of patients with Parkinson's disease and manganese exposed workers. Neurotoxicology. 15, 655-64.

Bishop, G.M., et al., 2002. Iron: a pathological mediator of Alzheimer disease? Dev Neurosci. 24, 184-7.

Bolton, D.C., Meyer, R.K., Prusiner, S.B., 1985. Scrapie PrP 27-30 is a sialoglycoprotein. J Virol. 53, 596-606.

Bossy-Wetzel, E., Schwarzenbacher, R., Lipton, S.A., 2004. Molecular pathways to neurodegeneration. Nat Med. 10 Suppl, S2-9.

Bourteele, S., et al., 2007. Alteration of NF-kappaB activity leads to mitochondrial apoptosis after infection with pathological prion protein. Cell Microbiol. 9, 2202-17.

Bowman, A.B., et al., 2011. Role of manganese in neurodegenerative diseases. J Trace Elem Med Biol. 25, 191-203.

Braak, H., Del Tredici, K., 2011. Alzheimer's pathogenesis: is there neuron-to-neuron propagation? Acta Neuropathol. 121, 589-95.

Brazier, M.W., et al., 2008. Manganese binding to the prion protein. J Biol Chem. 283, 12831-9.

Brown, D.R., et al., 1997. The cellular prion protein binds copper in vivo. Nature. 390, 684-7.

Brown, D.R., et al., 1999. Normal prion protein has an activity like that of superoxide dismutase. Biochem J. 344 Pt 1, 1-5.

Brown, D.R., et al., 2000. Consequences of manganese replacement of copper for prion protein function and proteinase resistance. Embo J. 19, 1180-6.

Brown, D.R., Clive, C., Haswell, S.J., 2001. Antioxidant activity related to copper binding of native prion protein. J Neurochem. 76, 69-76.

Brown, D.R., 2004. Metallic prions. Biochem Soc Symp. 193-202.

Brown, D.R., 2009. Brain proteins that mind metals: a neurodegenerative perspective. Dalton Trans. 4069-76.

Burns, C.S., et al., 2002. Molecular features of the copper binding sites in the octarepeat domain of the prion protein. Biochemistry. 41, 3991-4001.

Burns, C.S., et al., 2003. Copper coordination in the full-length, recombinant prion protein. Biochemistry. 42, 6794-803.

Bush, A.I., Curtain, C.C., 2008. Twenty years of metallo-neurobiology: where to now? Eur Biophys J. 37, 241-5.

Cahill, C.M., et al., 2009. Amyloid precursor protein and alpha synuclein translation, implications for iron and inflammation in neurodegenerative diseases. Biochim Biophys Acta. 1790, 615-28.

Cain, K., Bratton, S.B., Cohen, G.M., 2002. The Apaf-1 apoptosome: a large caspase-activating complex. Biochimie. 84, 203-14.

Carimalo, J., et al., 2005. Activation of the JNK-c-Jun pathway during the early phase of neuronal apoptosis induced by PrP106-126 and prion infection. Eur J Neurosci. 21, 2311-9.

Cereghetti, G.M., et al., 2003. Stability and Cu(II) binding of prion protein variants related to inherited human prion diseases. Biophys J. 84, 1985-97.

Chakrabarti, O., Hegde, R.S., 2009. Functional depletion of mahogunin by cytosolically exposed prion protein contributes to neurodegeneration. Cell. 137, 1136-47.

Chattopadhyay, M., et al., 2005. The octarepeat domain of the prion protein binds Cu(II) with three distinct coordination modes at pH 7.4. J Am Chem Soc. 127, 12647-56.

Chen, S., et al., 2003. Prion protein as trans-interacting partner for neurons is involved in neurite outgrowth and neuronal survival. Mol Cell Neurosci. 22, 227-33.

Chiarini, L.B., et al., 2002. Cellular prion protein transduces neuroprotective signals. Embo J. 21, 3317-26.

Choi, C.J., et al., 2007. Normal Cellular Prion Protein Protects against Manganese-Induced Oxidative Stress and Apoptotic Cell Death. Toxicol Sci. 98, 495-509.

Choi, C.J., et al., 2010. Manganese upregulates cellular prion protein and contributes to altered stabilization and proteolysis: relevance to role of metals in pathogenesis of prion disease. Toxicol Sci. 115, 535-46.

Ciechanover, A., Brundin, P., 2003. The ubiquitin proteasome system in neurodegenerative diseases: sometimes the chicken, sometimes the egg. Neuron. 40, 427-46.

Clague, M.J., Urbe, S., 2010. Ubiquitin: same molecule, different degradation pathways. Cell. 143, 682-5.

Coitinho, A.S., et al., 2007. Short-term memory formation and long-term memory consolidation are enhanced by cellular prion association to stress-inducible protein 1. Neurobiol Dis. 26, 282-90.

Collinge, J., 2005. Molecular neurology of prion disease. J Neurol Neurosurg Psychiatry. 76, 906-19.

Cooray, S.N., Guasti, L., Clark, A.J., 2011. The E3 ubiquitin ligase Mahogunin ubiquitinates the melanocortin 2 receptor. Endocrinology. 152, 4224-31.

Cota, C.D., et al., 2006. Mice with mutations in Mahogunin ring finger-1 (Mgrn1) exhibit abnormal patterning of the left-right axis. Dev Dyn. 235, 3438-47.

Davies, P., Brown, D.R., 2009. Manganese enhances prion protein survival in model soils and increases prion infectivity to cells. PLoS One. 4, e7518.

DeArmond, S.J., et al., 1987. Changes in the localization of brain prion proteins during scrapie infection. Neurology. 37, 1271-80.

Denning, M.F., et al., 2002. Caspase activation and disruption of mitochondrial membrane potential during UV radiation-induced apoptosis of human keratinocytes requires activation of protein kinase C. Cell Death Differ. 9, 40-52.

Deshaies, R.J., Joazeiro, C.A., 2009. RING domain E3 ubiquitin ligases. Annu Rev Biochem. 78, 399-434.

Desplats, P., et al., 2009. Inclusion formation and neuronal cell death through neuron-to-neuron transmission of alpha-synuclein. Proc Natl Acad Sci U S A. 106, 13010-5.

Di Natale, G., et al., 2005. Copper(II) interaction with unstructured prion domain outside the octarepeat region: speciation, stability, and binding details of copper(II) complexes with PrP106-126 peptides. Inorg Chem. 44, 7214-25.

Di Sano, F., et al., 2006. Endoplasmic reticulum stress induces apoptosis by an apoptosome-dependent but caspase 12-independent mechanism. J Biol Chem. 281, 2693-700.

Dobson, A.W., Erikson, K.M., Aschner, M., 2004. Manganese neurotoxicity. Ann N Y Acad Sci. 1012, 115-28.

Edgeworth, J.A., et al., 2010. Spontaneous generation of mammalian prions. Proc Natl Acad Sci U S A. 107, 14402-6.

Erikson, K.M., Aschner, M., 2003. Manganese neurotoxicity and glutamate-GABA interaction. Neurochem Int. 43, 475-80.

Fairbairn, D.W., et al., 1994. Detection of apoptosis induced DNA cleavage in scrapie-infected sheep brain. FEMS Microbiol Lett. 115, 341-6.

Fernaeus, S., et al., 2005. Increased susceptibility to oxidative stress in scrapie-infected neuroblastoma cells is associated with intracellular iron status. Neurosci Lett. 389, 133-6.

Ferreiro, E., et al., 2006. An endoplasmic-reticulum-specific apoptotic pathway is involved in prion and amyloid-beta peptides neurotoxicity. Neurobiol Dis. 23, 669-78.

Ferreiro, E., et al., 2008. Involvement of mitochondria in endoplasmic reticulum stress-induced apoptotic cell death pathway triggered by the prion peptide PrP(106-126). J Neurochem. 104, 766-76.

Fevrier, B., et al., 2004. Cells release prions in association with exosomes. Proc Natl Acad Sci U S A. 101, 9683-8.

Flechsig, E., et al., 2001. Transmission of scrapie by steel-surface-bound prions. Mol Med. 7, 679-84.

Gaeta, A., Hider, R.C., 2005. The crucial role of metal ions in neurodegeneration: the basis for a promising therapeutic strategy. Br J Pharmacol. 146, 1041-59.

Gaggelli, E., et al., 2008. Structural characterization of the intra- and inter-repeat copper binding modes within the N-terminal region of "prion related protein" (PrP-rel-2) of zebrafish. J Phys Chem B. 112, 15140-50.

Gambetti, P., et al., 2011. Molecular biology and pathology of prion strains in sporadic human prion diseases. Acta Neuropathol. 121, 79-90.

Garrick, M.D., et al., 2006. Comparison of mammalian cell lines expressing distinct isoforms of divalent metal transporter 1 in a tetracycline-regulated fashion. Biochem J. 398, 539-46.

Ghetti, B., et al., 1995. Gerstmann-Straussler-Scheinker disease and the Indiana kindred. Brain Pathol. 5, 61-75.

Gibbs, C.J., Jr., Gajdusek, D.C., Latarjet, R., 1978. Unusual resistance to ionizing radiation of the viruses of kuru, Creutzfeldt-Jakob disease, and scrapie. Proc Natl Acad Sci U S A. 75, 6268-70.

Gibbs, J.P., et al., 1999. Focused medical surveillance: a search for subclinical movement disorders in a cohort of U.S. workers exposed to low levels of manganese dust. Neurotoxicology. 20, 299-313.

Giese, A., et al., 2004. Effect of metal ions on de novo aggregation of full-length prion protein. Biochem Biophys Res Commun. 320, 1240-6.

Gordon, I., et al., 1998. Phosmet induces up-regulation of surface levels of the cellular prion protein. Neuroreport. 9, 1391-5.

Gousset, K., et al., 2009. Prions hijack tunnelling nanotubes for intercellular spread. Nat Cell Biol. 11, 328-36.

Govaerts, C., et al., 2004. Evidence for assembly of prions with left-handed beta-helices into trimers. Proc Natl Acad Sci U S A. 101, 8342-7.

Guo, J.L., Lee, V.M., 2011. Seeding of normal Tau by pathological Tau conformers drives pathogenesis of Alzheimer-like tangles. J Biol Chem. 286, 15317-31.

Haigh, C.L., Edwards, K., Brown, D.R., 2005. Copper binding is the governing determinant of prion protein turnover. Mol Cell Neurosci. 30, 186-96.

Haigh, C.L., Brown, D.R., 2006. Prion protein reduces both oxidative and non-oxidative copper toxicity. J Neurochem. 98, 677-89.

Hainfellner, J.A., et al., 1997. Pathology and immunocytochemistry of a kuru brain. Brain Pathol. 7, 547-53.

He, L., et al., 2003a. Accessory proteins for melanocortin signaling: attractin and mahogunin. Ann N Y Acad Sci. 994, 288-98.

He, L., et al., 2003b. Spongiform degeneration in mahoganoid mutant mice. Science. 299, 710-2.

Hesketh, S., et al., 2007. Elevated manganese levels in blood and central nervous system occur before onset of clinical signs in scrapie and bovine spongiform encephalopathy. J Anim Sci. 85, 1596-609.

Hesketh, S., et al., 2008. Elevated manganese levels in blood and CNS in human prion disease. Mol Cell Neurosci. 37, 590-8.

Hetz, C., et al., 2003. Caspase-12 and endoplasmic reticulum stress mediate neurotoxicity of pathological prion protein. Embo J. 22, 5435-45.

Holmberg, C.I., et al., 2004. Inefficient degradation of truncated polyglutamine proteins by the proteasome. EMBO J. 23, 4307-18.

Hornshaw, M.P., McDermott, J.R., Candy, J.M., 1995. Copper binding to the N-terminal tandem repeat regions of mammalian and avian prion protein. Biochem Biophys Res Commun. 207, 621-9.

Ishikawa, K., et al., 2004. Amyloid imaging probes are useful for detection of prion plaques and treatment of transmissible spongiform encephalopathies. J Gen Virol. 85, 1785-90.

Jackson, G.S., et al., 2001. Location and properties of metal-binding sites on the human prion protein. Proc Natl Acad Sci U S A. 98, 8531-5.

Jellinger, K.A., 2009. Recent advances in our understanding of neurodegeneration. J Neural Transm. 116, 1111-62.

Jiao, J., et al., 2009. Abnormal regulation of TSG101 in mice with spongiform neurodegeneration. Biochim Biophys Acta. 1792, 1027-35.

Johnson, C.J., et al., 2007. Oral transmissibility of prion disease is enhanced by binding to soil particles. PLoS Pathog. 3, e93.

Jones, C.E., et al., 2004. Preferential Cu2+ coordination by His96 and His111 induces beta-sheet formation in the unstructured amyloidogenic region of the prion protein. J Biol Chem. 279, 32018-27.

Jones, C.E., et al., 2005. Probing copper2+ binding to the prion protein using diamagnetic nickel2+ and 1H NMR: the unstructured N terminus facilitates the coordination of six copper2+ ions at physiological concentrations. J Mol Biol. 346, 1393-407.

Jucker, M., Walker, L.C., 2011. Pathogenic protein seeding in Alzheimer disease and other neurodegenerative disorders. Ann Neurol. 70, 532-40.

Kang, S.C., et al., 2004. Prion protein is ubiquitinated after developing protease resistance in the brains of scrapie-infected mice. J Pathol. 203, 603-8.

Kanthasamy, A.G., et al., 2003. Role of proteolytic activation of protein kinase Cdelta in oxidative stress-induced apoptosis. Antioxid Redox Signal. 5, 609-20.

Kanu, N., et al., 2002. Transfer of scrapie prion infectivity by cell contact in culture. Curr Biol. 12, 523-30.

Kaul, S., et al., 2003. Caspase-3 dependent proteolytic activation of protein kinase C delta mediates and regulates 1-methyl-4-phenylpyridinium (MPP+)-induced apoptotic cell death in dopaminergic cells: relevance to oxidative stress in dopaminergic degeneration. Eur J Neurosci. 18, 1387-401.

Kikkawa, U., Matsuzaki, H., Yamamoto, T., 2002. Protein Kinase Cdelta (PKCdelta): Activation Mechanisms and Functions. J Biochem (Tokyo). 132, 831-9.

Kim, B.Y., et al., 2007. Spongiform neurodegeneration-associated E3 ligase Mahogunin ubiquitylates TSG101 and regulates endosomal trafficking. Mol Biol Cell. 18, 1129-42.

Kim, M.J., et al., 2001. Site-specific localization of protein kinase C isoforms in rat pancreas. Pancreatology. 1, 36-42.

Kim, N.H., et al., 2005. Effect of transition metals (Mn, Cu, Fe) and deoxycholic acid (DA) on the conversion of PrPC to PrPres. Faseb J. 19, 783-5.

Kitamoto, T., et al., 1991. N-terminal sequence of prion protein is also integrated into kuru plaques in patients with Gerstmann-Straussler syndrome. Brain Res. 545, 319-21.

Kitazawa, M., et al., 2002. Oxidative stress and mitochondrial-mediated apoptosis in dopaminergic cells exposed to methylcyclopentadienyl manganese tricarbonyl. J Pharmacol Exp Ther. 302, 26-35.

Kitazawa, M., Anantharam, V., Kanthasamy, A.G., 2003. Dieldrin induces apoptosis by promoting caspase-3-dependent proteolytic cleavage of protein kinase Cdelta in dopaminergic cells: relevance to oxidative stress and dopaminergic degeneration. Neuroscience. 119, 945-64.

Kitazawa, M., et al., 2004. Dieldrin Promotes Proteolytic Cleavage of Poly(ADP-Ribose) Polymerase and Apoptosis in Dopaminergic Cells: Protective Effect of Mitochondrial Anti-Apoptotic Protein Bcl-2. Neurotoxicology. 25, 589-98.

Kitazawa, M., et al., 2005. Activation of protein kinase C delta by proteolytic cleavage contributes to manganese-induced apoptosis in dopaminergic cells: protective role of Bcl-2. Biochem Pharmacol. 69, 133-46.

Kordower, J.H., et al., 2008. Lewy body-like pathology in long-term embryonic nigral transplants in Parkinson's disease. Nat Med. 14, 504-6.

Kovacs, G.G., et al., 2002. The prion protein in human neurodegenerative disorders. Neurosci Lett. 329, 269-72.

Krasemann, S., et al., 1995. Prion disease associated with a novel nine octapeptide repeat insertion in the PRNP gene. Brain Res Mol Brain Res. 34, 173-6.

Kretzschmar, H.A., et al., 1986. Molecular cloning of a human prion protein cDNA. DNA. 5, 315-24.

Kretzschmar, H.A., et al., 1992. Molecular cloning of a mink prion protein gene. J Gen Virol. 73 ( Pt 10), 2757-61.

Lakhan, S.E., Sabharanjak, S., De, A., 2009. Endocytosis of glycosylphosphatidylinositol-anchored proteins. J Biomed Sci. 16, 93.

Laszlo, L., et al., 1992. Lysosomes as key organelles in the pathogenesis of prion encephalopathies. J Pathol. 166, 333-41.

Latchoumycandane, C., et al., 2005. Protein kinase Cdelta is a key downstream mediator of manganese-induced apoptosis in dopaminergic neuronal cells. J Pharmacol Exp Ther. 313, 46-55.

Lee, S.J., et al., 2010. Cell-to-cell transmission of non-prion protein aggregates. Nat Rev Neurol. 6, 702-6.

Levy, B.S., Nassetta, W.J., 2003. Neurologic effects of manganese in humans: a review. Int J Occup Environ Health. 9, 153-63.

Liberski, P.P., Brown, P., 2004. Kuru: a half-opened window onto the landscape of neurodegenerative diseases. Folia Neuropathol. 42 Suppl A, 3-14.

Magalhaes, A.C., et al., 2005. Uptake and neuritic transport of scrapie prion protein coincident with infection of neuronal cells. J Neurosci. 25, 5207-16.

Mange, A., et al., 2002. PrP-dependent cell adhesion in N2a neuroblastoma cells. FEBS Lett. 514, 159-62.

Martins, V.R., Brentani, R.R., 2002. The biology of the cellular prion protein. Neurochem Int. 41, 353-5.

Mastrangelo, P., Westaway, D., 2001. Biology of the prion gene complex. Biochem Cell Biol. 79, 613-28.

McMillan, D.E., 1999. A brief history of the neurobehavioral toxicity of manganese: some unanswered questions. Neurotoxicology. 20, 499-507.

Mead, S., et al., 2007. Inherited prion disease with 5-OPRI: phenotype modification by repeat length and codon 129. Neurology. 69, 730-8.

Migliore, L., Coppede, F., 2009. Environmental-induced oxidative stress in neurodegenerative disorders and aging. Mutat Res. 674, 73-84.

Milhavet, O., et al., 2000. Prion infection impairs the cellular response to oxidative stress. Proc Natl Acad Sci U S A. 97, 13937-42.

Milhavet, O., Lehmann, S., 2002. Oxidative stress and the prion protein in transmissible spongiform encephalopathies. Brain Res Brain Res Rev. 38, 328-39.

Miller, K.A., et al., 1997. Genetic studies of the mouse mutations mahogany and mahoganoid. Genetics. 146, 1407-15.

Mitteregger, G., et al., 2007. The role of the octarepeat region in neuroprotective function of the cellular prion protein. Brain Pathol. 17, 174-83.

Miyamoto, A., et al., 2002. Increased proliferation of B cells and auto-immunity in mice lacking protein kinase Cdelta. Nature. 416, 865-9.

Molina-Holgado, F., et al., 2007. Metals ions and neurodegeneration. Biometals. 20, 639-54.

Moore, R.A., et al., 2006. Octapeptide repeat insertions increase the rate of protease-resistant prion protein formation. Protein Sci. 15, 609-19.

Moreno-Gonzalez, I., Soto, C., 2011. Misfolded protein aggregates: mechanisms, structures and potential for disease transmission. Semin Cell Dev Biol. 22, 482-7.

Mouillet-Richard, S., et al., 2000. Signal transduction through prion protein. Science. 289, 1925-8.

Mouillet-Richard, S., et al., 2005. Modulation of serotonergic receptor signaling and cross-talk by prion protein. J Biol Chem. 280, 4592-601.

Mukhopadhyay, S., et al., 2007. A natively unfolded yeast prion monomer adopts an ensemble of collapsed and rapidly fluctuating structures. Proc Natl Acad Sci U S A. 104, 2649-54.

Munch, C., O'Brien, J., Bertolotti, A., 2011. Prion-like propagation of mutant superoxide dismutase-1 misfolding in neuronal cells. Proc Natl Acad Sci U S A. 108, 3548-53.

Myers, J.E., et al., 2003. The nervous system effects of occupational exposure on workers in a South African manganese smelter. Neurotoxicology. 24, 885-94.

Nadal, R.C., et al., 2007. Prion protein does not redox-silence Cu2+, but is a sacrificial quencher of hydroxyl radicals. Free Radic Biol Med. 42, 79-89.

Naslavsky, N., et al., 1997. Characterization of detergent-insoluble complexes containing the cellular prion protein and its scrapie isoform. J Biol Chem. 272, 6324-31.

Nunziante, M., Gilch, S., Schatzl, H.M., 2003. Essential role of the prion protein N terminus in subcellular trafficking and half-life of cellular prion protein. J Biol Chem. 278, 3726-34.

Obeng, E.A., Boise, L.H., 2005. Caspase-12 and caspase-4 are not required for caspase-dependent endoplasmic reticulum stress-induced apoptosis. J Biol Chem. 280, 29578-87.

Offen, D., Elkon, H., Melamed, E., 2000. Apoptosis as a general cell death pathway in neurodegenerative diseases. J Neural Transm Suppl. 153-66.

Ohhashi, Y., et al., 2010. Differences in prion strain conformations result from non-native interactions in a nucleus. Nat Chem Biol. 6, 225-230.

Ollmann, M.M., et al., 1997. Antagonism of central melanocortin receptors in vitro and in vivo by agouti-related protein. Science. 278, 135-8.

Orosco, A., et al., 2006. Dual involvement of protein kinase C delta in apoptosis induced by syndecan-2 in osteoblasts. J Cell Biochem. 98, 838-50.

Overton, J.D., Leibel, R.L., 2011. Mahoganoid and mahogany mutations rectify the obesity of the yellow mouse by effects on endosomal traffic of MC4R protein. J Biol Chem. 286, 18914-29.

Palmer, M.S., Collinge, J., 1993. Mutations and polymorphisms in the prion protein gene. Hum Mutat. 2, 168-73.

Parchi, P., et al., 2010. Agent strain variation in human prion disease: insights from a molecular and pathological review of the National Institutes of Health series of experimentally transmitted disease. Brain. 133, 3030-42.

Perez-Oliva, A.B., et al., 2009. Mahogunin ring finger-1 (MGRN1) E3 ubiquitin ligase inhibits signaling from melanocortin receptor by competition with Galphas. J Biol Chem. 284, 31714-25.

Perl, D.P., Good, P.F., 1991. Aluminum, Alzheimer's disease, and the olfactory system. Ann N Y Acad Sci. 640, 8-13.

Peters, P.J., et al., 2003. Trafficking of prion proteins through a caveolae-mediated endosomal pathway. J Cell Biol. 162, 703-17.

Pfeifer, G.D., et al., 2004. Health and environmental testing of manganese exhaust products from use of methylcyclopentadienyl manganese tricarbonyl in gasoline. Sci Total Environ. 334-335, 397-408.

Phan, L.K., et al., 2002. The mouse mahoganoid coat color mutation disrupts a novel C3HC4 RING domain protein. J Clin Invest. 110, 1449-59.

Phan, L.K., Chung, W.K., Leibel, R.L., 2006. The mahoganoid mutation (Mgrn1md) improves insulin sensitivity in mice with mutations in the melanocortin signaling pathway independently of effects on adiposity. Am J Physiol Endocrinol Metab. 291, E611-20.

Piccardo, P., et al., 1996. Proteinase-K-resistant prion protein isoforms in Gerstmann-Straussler-Scheinker disease (Indiana kindred). J Neuropathol Exp Neurol. 55, 1157-63.

Prado, M.A., et al., 2004. PrPc on the road: trafficking of the cellular prion protein. J Neurochem. 88, 769-81.

Prusiner, S.B., et al., 1980. Molecular properties, partial purification, and assay by incubation period measurements of the hamster scrapie agent. Biochemistry. 19, 4883-91.

Prusiner, S.B., 1982. Novel proteinaceous infectious particles cause scrapie. Science. 216, 136-44.

Prusiner, S.B., DeArmond, S.J., 1990. Prion diseases of the central nervous system. Monogr Pathol. 86-122.

Prusiner, S.B., 1991a. Molecular biology and transgenetics of prion diseases. Crit Rev Biochem Mol Biol. 26, 397-438.

Prusiner, S.B., 1991b. Molecular biology of prion diseases. Science. 252, 1515-22.

Prusiner, S.B., 1991c. Molecular biology of prions causing infectious and genetic encephalopathies of humans as well as scrapie of sheep and BSE of cattle. Dev Biol Stand. 75, 55-74.

Purdey, M., 1996. The UK epidemic of BSE: slow virus or chronic pesticide-initiated modification of the prion protein? Part 1: Mechanisms for a chemically induced pathogenesis/transmissibility. Med Hypotheses. 46, 429-43.

Purdey, M., 2000. Ecosystems supporting clusters of sporadic TSEs demonstrate excesses of the radical-generating divalent cation manganese and deficiencies of antioxidant co factors Cu, Se, Fe, Zn. Does a foreign cation

substitution at prion protein's Cu domain initiate TSE? Med Hypotheses. 54, 278-306.

Reed, J.C., 2004. Apoptosis mechanisms: implications for cancer drug discovery. Oncology (Williston Park). 18, 11-20.

Renner, C., et al., 2004. Micellar environments induce structuring of the N-terminal tail of the prion protein. Biopolymers. 73, 421-33.

Reyland, M.E., 2007. Protein kinase Cdelta and apoptosis. Biochem Soc Trans. 35, 1001-4.

Rogers, M., et al., 1993. Conversion of truncated and elongated prion proteins into the scrapie isoform in cultured cells. Proc Natl Acad Sci U S A. 90, 3182-6.

Roth, J.A., Garrick, M.D., 2003. Iron interactions and other biological reactions mediating the physiological and toxic actions of manganese. Biochem Pharmacol. 66, 1-13.

Sakai, C., et al., 1997. Modulation of murine melanocyte function in vitro by agouti signal protein. EMBO J. 16, 3544-52.

Sakudo, A., et al., 2004. Prion protein suppresses perturbation of cellular copper homeostasis under oxidative conditions. Biochem Biophys Res Commun. 313, 850-5.

Santuccione, A., et al., 2005. Prion protein recruits its neuronal receptor NCAM to lipid rafts to activate p59fyn and to enhance neurite outgrowth. J Cell Biol. 169, 341-54.

Sarge, K.D., Park-Sarge, O.K., 2011. SUMO and its role in human diseases. Int Rev Cell Mol Biol. 288, 167-83.

Sayre, L.M., Perry, G., Smith, M.A., 1999. Redox metals and neurodegenerative disease. Curr Opin Chem Biol. 3, 220-5.

Shaw, I., et al., 2002. Studies on the putative interactions between the organophosphorus insecticide Phosmet and recombinant mouse PrP and its implication in the BSE epidemic. Vet Res Commun. 26, 263-71.

Silveira, J.R., et al., 2005. The most infectious prion protein particles. Nature. 437, 257-61.

Silvius, D., et al., 2013. Levels of the Mahogunin Ring Finger 1 E3 ubiquitin ligase do not influence prion disease. PLoS One. 8, e55575.

Soto, C., 2008. Endoplasmic reticulum stress, PrP trafficking, and neurodegeneration. Dev Cell. 15, 339-41.

Soto, C., Satani, N., 2010. The intricate mechanisms of neurodegeneration in prion diseases. Trends Mol Med.

Stahl, N., et al., 1987. Scrapie prion protein contains a phosphatidylinositol glycolipid. Cell. 51, 229-40.

Steele, A.D., et al., 2007. Prion pathogenesis is independent of caspase-12. Prion. 1, 243-7.

Stevens, D.J., et al., 2009. Early onset prion disease from octarepeat expansion correlates with copper binding properties. PLoS Pathog. 5, e1000390.

Thackray, A.M., et al., 2002. Metal imbalance and compromised antioxidant function are early changes in prion disease. Biochem J. 362, 253-8.

Treiber, C., et al., 2007. Copper is required for prion protein-associated superoxide dismutase-I activity in Pichia pastoris. Febs J. 274, 1304-11.

Tyedmers, J., Mogk, A., Bukau, B., 2010. Cellular strategies for controlling protein aggregation. Nat Rev Mol Cell Biol. 11, 777-88.

Um, J.W., et al., 2012. Alzheimer amyloid-beta oligomer bound to postsynaptic prion protein activates Fyn to impair neurons. Nat Neurosci. 15, 1227-35.

Um, J.W., Strittmatter, S.M., 2012. Amyloid-ss induced signaling by cellular prion protein and Fyn kinase in Alzheimer disease. Prion. 6.

Viles, J.H., et al., 1999. Copper binding to the prion protein: structural implications of four identical cooperative binding sites. Proc Natl Acad Sci U S A. 96, 2042-7.

Viles, J.H., et al., 2001. Local structural plasticity of the prion protein. Analysis of NMR relaxation dynamics. Biochemistry. 40, 2743-53.

Wadsworth, J.D., Collinge, J., 2011. Molecular pathology of human prion disease. Acta Neuropathol. 121, 69-77.

Walker, L.C., LeVine, H., 3rd, 2012. Corruption and spread of pathogenic proteins in neurodegenerative diseases. J Biol Chem. 287, 33109-15.

Weissmann, C., et al., 2011. Prions on the move. EMBO Rep. 12, 1109-17.

Whatley, B.R., Li, L., Chin, L.S., 2008. The ubiquitin-proteasome system in spongiform degenerative disorders. Biochim Biophys Acta. 1782, 700-12.

Wong, B.S., et al., 2001. Oxidative impairment in scrapie-infected mice is associated with brain metals perturbations and altered antioxidant activities. J Neurochem. 79, 689-98.

Yang, Y., et al., 2004. Suppression of caspase-3-dependent proteolytic activation of protein kinase C delta by small interfering RNA prevents MPP+-induced dopaminergic degeneration. Mol Cell Neurosci. 25, 406-21.

Yin, S., et al., 2007. Human prion proteins with pathogenic mutations share common conformational changes resulting in enhanced binding to glycosaminoglycans. Proc Natl Acad Sci U S A. 104, 7546-51.

Yoshida, K., 2007. PKCdelta signaling: mechanisms of DNA damage response and apoptosis. Cell Signal. 19, 892-901.

Zanata, S.M., et al., 2002. Stress-inducible protein 1 is a cell surface ligand for cellular prion that triggers neuroprotection. Embo J. 21, 3307-16.

Zhang, D., et al., 2007. Neuroprotective effect of protein kinase C delta inhibitor rottlerin in cell culture and animal models of Parkinson's disease. J Pharmacol Exp Ther. 322, 913-22.

Zhu, F., et al., 2008. Raman optical activity and circular dichroism reveal dramatic differences in the influence of divalent copper and manganese ions on prion protein folding. Biochemistry. 47, 2510-7.

Zobeley, E., et al., 1999. Infectivity of scrapie prions bound to a stainless steel surface. Mol Med. 5, 240-3.

# CHAPTER 2: INFECTIOUS PRION PROTEIN ALTERS MANGANESE TRANSPORT AND NEUROTOXICITY IN A CELL CULTURE MODEL OF PRION DISEASE

An article published in the journal Neurotoxicology

Dustin P. Martin[1], Vellareddy Anantharam[1], Huajun Jin[1], Travis Witte[2], Robert Houk[2], Arthi Kanthasamy [1], Anumantha G. Kanthasamy[1*]

**[1]Department of Biomedical Sciences, Iowa Center for Advanced Neurotoxicity, [2]Department of Chemistry, Iowa State University, Ames, IA 50011**

***Corresponding Author**

Dr. Anumantha G. Kanthasamy, Distinguished Professor and Lloyd Chair, Parkinson's Disorder Research Laboratory, Iowa Center for Advanced Neurotoxicology, Department of Biomedical Sciences, 2062 Veterinary Medicine Building, Iowa State University, Ames, IA 50011, USA Phone: 01-515-294-2516; Fax: 01-515-294-2315; Email: akanthas@iastate.edu

**Abstract**

Protein misfolding and aggregation are considered key features of many neurodegenerative diseases, but biochemical mechanisms underlying protein misfolding and the propagation of protein aggregates are not well understood. Prion disease is a classical neurodegenerative disorder resulting from the misfolding of endogenously expressed normal cellular prion protein ($PrP^C$). Although the exact function of $PrP^C$ has not been fully elucidated, studies have suggested that it can function as a metal binding protein. Interestingly, increased brain manganese (Mn) levels have been reported in various prion diseases indicating divalent metals also may play a role in the disease process. Recently, we reported that $PrP^C$ protects against Mn-induced cytotoxicity in a neural cell culture model. To further understand the role of Mn in prion diseases, we examined Mn neurotoxicity in an infectious cell culture model of prion disease. Our results show CAD5 scrapie-infected cells were more resistant to Mn neurotoxicity as compared to uninfected cells ($EC_{50}$ = 428.8 μM for CAD5 infected cells vs. 211.6 μM for uninfected cells). Additionally, treatment with 300 μM Mn in persistently infected CAD5 cells showed a reduction in mitochondrial impairment, caspase-3 activation, and DNA fragmentation when compared to uninfected cells. Scrapie-infected cells also showed significantly reduced Mn uptake as measured by inductively coupled plasma-mass spectrometry (ICP-MS), and altered expression of metal transporting proteins DMT1 and transferrin. Together, our data indicate that conversion of PrP to the pathogenic isoform

enhances its ability to regulate Mn homeostasis, and suggest that understanding the interaction of metals with disease-specific proteins may provide further insight to protein aggregation in neurodegenerative diseases.

## 1. Introduction

A conformational isomer of the endogenously expressed prion protein is the putative pathogenic agent in transmissible spongiform encephalopathy (TSE) or prion disease (Prusiner, 1991) . Normal cellular prion protein ($PrP^{C}$) is converted to the pathogenic β-sheet-rich conformation of scrapie prion ($PrP^{Sc}$) through a still unclear mechanism (Bolton et al., 1985; Collinge, 2005; Prusiner and DeArmond, 1990). Prion diseases are fatal neurodegenerative disorders that affect both humans and animals (Prusiner, 1991). The regions of the brain that control motor function, including the basal ganglia, cerebral cortex, thalamus, brain stem, and cerebellum, are severely affected in TSE. The major neurological symptoms of TSE are extrapyramidal motor signs, including tremors, postural instability, ataxia, and myoclonus (Aguzzi and Heikenwalder, 2006; Brandner, 2003; Brown, 2002; Tatzelt and Schatzl, 2007). The neuropathological characterization of prion disease involves massive neuronal degeneration and vacuolization associated with accumulation of $PrP^{Sc}$ giving neural tissue the diagnostic spongiform appearance when examined histologically (Collinge, 2001; Owen et al., 1989; Palmer and Collinge, 1992). Increased oxidative stress markers, such as malondialdehyde, 3-nitrotyrosine, 8-hydroxyguanosine, protein carbonyls, and dysregulation of iron homeostasis were observed in the brain tissues of both animal and human prion diseases, suggesting that oxidative damage plays an important role in the pathogenesis of TSE (Freixes et al., 2006; Lee et al., 1999; Petersen et al., 2005; Yun et al., 2006).

Although normal cellular $PrP^C$ is abundantly expressed in the central nervous system (CNS), its biological function still remains unclear. $PrP^C$ is a glycosylphosphatidylinositol (GPI)-anchored cell surface protein that is believed to function as an antioxidant, a cellular adhesion molecule, a signal transducer, and a metal binding protein (Brown, 2004; Chen et al., 2003; Chiarini et al., 2002; Collinge, 2005; Mange et al., 2002; Prusiner and Kingsbury, 1985; Prusiner et al., 1990; Sakudo et al., 2004). Properly folded prion protein is present on lipid membrane rafts, and is believed to be internalized via clathrin-mediated endocytosis (Nunziante et al., 2003; Peters et al., 2003; Prado et al., 2004). Recent evidence indicates that $PrP^C$ is an important metal binding protein for divalent metals, such as copper (Cu), manganese (Mn), and zinc (Zn) (Brazier et al., 2008; Brown, 2009; Choi et al., 2007; Hornshaw et al., 1995; Viles et al., 1999). $PrP^C$ contains several octapeptide repeat sequences (PHGGSWGQ) toward the N-terminus, which have binding affinity for divalent metals with preferential binding for Cu (Hornshaw et al., 1995; Viles et al., 1999). Additional higher affinity metal binding sites have been identified at His 95 and 110 (mouse numbering) (Jackson et al., 2001; Jones et al., 2004), but the exact role of these higher affinity metal binding sites remains elusive.

Interestingly, increased Mn content has been observed in the blood and brain of humans infected with Crueztfelt-Jacob Disease (CJD), mice infected with scrapie, and cattle infected with bovine spongiform encephalopathy (BSE)

(Hesketh et al., 2008; Hesketh et al., 2007; Thackray et al., 2002; Wong et al., 2001b). Additionally, Mn-bound $PrP^{Sc}$ can be isolated from both humans and animals infected with prion disease. Despite these findings, the role of Mn in the pathogenesis of prion disease is currently unknown. Recent studies using recombinant PrP have shown that Mn can irreversibly displace Cu bound to PrP, despite an apparent lower affinity, and this displacement causes conformational changes within the protein (Brazier et al., 2008; Zhu et al., 2008). The biological consequence of Cu replacement by Mn on the prion protein is yet to be established. Recently, we observed that divalent Mn binds to PrP resulting in a reduced neurotoxic response during the early acute phase of the Mn toxicity in an uninfected model of prion disease (Choi et al., 2007). However, prolonged exposure to Mn upregulates $PrP^{C}$ by stabilizing the protein without any change in gene transcription (Choi et al., 2010). In order to determine whether Mn plays a role in the infectious nature of PrP, in the present study we characterized the neurotoxic effect of Mn in a cell culture model of infectious prion disease.

## 2. Materials and Methods

### *2.1 Chemicals*

Manganese chloride ($MnCl_2$), 3-(4,5-dimethylthiazol-3-yl)-2,5-diphenyltetrazolium bromide (MTT), ethylenediaminetetraacetic acid (EDTA), phenylmethylsulfonyl fluoride (PMSF), sodium chloride (NaCl), Tris HCl, Triton-X, sodium

deoxycholate, dithiothreitol (DTT), proteinase K (PK), were purchased from Sigma (St. Louis, MO); Sytox green nucleic dye was purchased from Molecular Probes (Eugene, OR). Cell Death Detection ELISA plus Assay Kit was purchased from Roche Molecular Biochemicals (Indianapolis, IN). Bradford protein assay kit and acrylamide stock solution were purchased from Bio-Rad Laboratories (Hercules, CA). Opti-MEM, fetal bovine serum, penicillin, and streptomycin were purchased from Invitrogen (Carlsbad, CA). 6H4 anti-PrP monoclonal antibody was purchased from Prionics (Schlieren, Switzerland). Anti-4-hydroxynonenal (4-HNE) antibody was purchased from R&D Systems (Minneapolis, MN). Anti-mouse divalent metal transporter (DMT-1) was purchased from Alpha Diagnostic International (San Antonio, TX). Anti-mouse transferrin (Tf) was purchased from Santa Cruz Biotechnology (Santa Cruz, CA). Anti-β-actin antibody was purchased from Sigma-Aldrich (St. Louis, MO). Alexa Flour 680 conjugated goat anti-mouse IgG was purchased from Invitrogen (Carlsbad, CA). Goat anti-rabbit IgG IR800 Conjugate was purchased from Rockland Immunochemicals (Gilbertsville, PA)

*2.2 Cell culture model of prion disease*

The CAD-2A2D5 subclone of uninfected and infected Cath.a-differentiated cells (CAD5) were a generous gift from Dr. Charles Weissmann of the Scripps Institute (Jupiter, FL). Lack of suitable cell culture models for prion disease has hindered in vitro mechanistic investigations over the past few decades. Recently,

Dr. Weissmann's laboratory has successfully created CAD cells with remarkable susceptibility for infection by the Rocky Mountain Lab (RML) mouse scrapie strain. The development and characterization of CAD5 infectious prion cell culture model is described elsewhere (Mahal et al., 2007). Both uninfected and RML scrapie-infected cells were grown in Opti-MEM media supplemented with 50 units penicillin, 50 µg/ml streptomycin, and 10% qualified fetal bovine serum (Invitrogen) and screened for retention of RML scrapie infection in CAD5 cells over five subsequent passages. Cells were maintained in a humidified atmosphere of 5% $CO_2$ at 37ºC.

*2.3 Limited proteolysis*

Control and RML-infected CAD5 cells were seeded in a T175 flask and allowed to grow to ~90% confluence. Cells were washed once with ice cold phosphate buffered saline (PBS) and then lysed in the flask by adding 2 ml of lysis buffer (150 mM NaCl, 50 mM Tris-HCl pH 7.4, 5 mM EDTA, 2% Triton X, and 2% sodium deoxycholate) and incubated at 4ºC for 30 mins. Protein concentrations were determined by Bradford assay, and 2 mg of protein from each sample were brought to equal volume with addition of excess lysis buffer. Limited proteolysis was begun by addition of PK to each sample at a concentration of 20 µg/ml and incubated at 37°C for 1 h. Reaction was quenched by the addition of 2 mM PMSF (final concentration). After PK digestion, samples were ultracentrifuged at 120,000 X g for 2 h using an Optima

Max Ultracentrifuge (Beckman-Coulter, Brea, CA) to pellet the PK-resistant fraction. The supernatant was discarded and 30 µl of PAGE loading buffer and DTT was added directly to the pellet. The samples were then sonicated for 5 mins in a cup horn sonicator, boiled for 10 mins, and separated by SDS-PAGE on a 15% polyacrylamide gel and transferred to nitrocellulose membrane. The membranes were treated with 6H4 anti-PrP monoclonal antibody for 2 h at room temperature. Detection was done with an electrochemiluminescence (ECL) detection kit (GE Healthcare, Piscataway, NJ).

*2.4 SDS-PAGE and Western blot*

Western blot analysis was performed as described previously (Anantharam et al., 2002; Kitazawa et al., 2005; Latchoumycandane et al., 2005). Following Mn treatment, cells were collected by scraping and washed once with ice cold PBS, and then lysed in RIPA (Radio-Immunoprecipitation Assay) buffer with phosphatase and protease inhibitor cocktail (Thermo Scientific, Rockfort, IL). Protein concentrations of samples were determined using Bradford assay. Samples were then separated by SDS-PAGE using a 12% polyacrylamide gel and transferred onto nitrocellulose membrane. After 1 h in blocking buffer, the membranes were treated with either anti-4-hydroxynonenal antibody, anti-transferrin antibody, or anti-divalent metal transporter 1 at 4ºC overnight. Membranes were co-treated with anti-β-actin antibody in blocking buffer to ensure equal protein loading. Membranes were then treated with anti-mouse

and anti-rabbit fluorescent secondary antibodies for 1 h at room temperature. Visualization and band quantification was done using an Odyssey scanner (Licor, Lincoln, NE).

*2.5 MTT Assay*

The MTT cell viability assay was performed as described previously (Choi et al., 2007; Latchoumycandane et al., 2005). 100,000 uninfected and RML scrapie-infected CAD5 cells were seeded on a 96-well microplate, allowed to adhere for 12 h, and then treated for 16 h with manganese chloride ($MnCl_2$) in Opti-MEM in the following concentrations: 0, 10μM, 30μM, 50μM, 100μM, 300μM, 500μM, 1mM, 2mM, 3mM, and 5mM. Following the treatment, the cells were washed with warm PBS and then incubated with 200 μl 0.25% (w/v) MTT in serum free Opti-MEM for 30 mins at 37°C. MTT treatment was removed, cells were washed with warm PBS, and 200 μl of 100% dimethyl sulfoxide (DMSO) was added to each well and pipetted up and down to dissolve the contents of the wells. Yellow MTT is reduced by a mitochondrial dehydrogenase in living cells to dark blue formazan crystals that accumulate in the mitochondria. Absorbance was read at 570 and 630 nm using a SpectroMax microplate reader (model 190; Molecular Devices, Sunnyvale, CA).

*2.6 Sytox Staining*

One million uninfected and RML scrapie-infected CAD5 cells were plated in a 6-well plate, allowed to adhere to the plate for 12 h, and then were treated with 300 μM and 500 μM $MnCl_2$ in Opti-MEM supplemented with 1 μM Sytox green dye for 24 h. Sytox green is a cell-impermeable nucleic acid dye that intercalates with DNA and produces green fluorescence in dead or dying cells. Pictures were taken with a Nikon inverted fluorescence microscope (model TE-2000U; Nikon, Tokyo, Japan); images were captured with a SPOT digital camera (Diagnostic Instruments, Sterling Heights, MI.)

*2.7 Caspase-3 Time Course*

Caspase-3 activity assay was performed as described previously (Anantharam et al., 2002; Kitazawa et al., 2005; Latchoumycandane et al., 2005). One million uninfected and RML scrapie-infected CAD5 cells were plated per well in a 6-well plate, allowed to adhere for 12 h, and were then treated with 300 μM $MnCl_2$ in Opti-MEM for 8, 12, 16, 20, and 24 h. Cells were collected with 0.25% trypsin-EDTA, spun down at 300 x g for 5 mins, and the cell pellet was washed with PBS. Cells were resuspended in caspase buffer (50 mM Tris-HCl (pH 7.4), 1 mM EDTA, and 10 mM EGTA) with 10 μM digitonin added and incubated for 30 mins on ice to lyse cells. The lysate was quickly spun down and supernatant was collected. 95 μl of the lysate was incubated with 5 μl of caspase-3 specific substrate Ac-DEVD-AFC for 1 h in a 96-well plate at 37ºC. AFC fluorescence was measured with excitation at 400 nm and emission at 505 nm with a

SpectraMax fluorescent plate reader (model GeminiXSE; Molecular Devices, Sunnyvale, CA). Protein concentration was determined by Bradford protein assay and data was expressed as fluorescent units per mg of protein per hour.

*2.8 DNA fragmentation ELISA on Mn treated CAD5 cells*

1 million uninfected and RML scrapie-infected CAD5 cells were plated per well in a 6-well plate, allowed to adhere for 12 h, and were then treated with 300 μM of $MnCl_2$ in Opti-MEM for 24 h. Cells were collected with 0.25% trypsin-EDTA and spun down at 300 x g for 5 mins and the cell pellet was washed with PBS. The amount of histone-associated low molecular weight DNA in the cytoplasm of the cells was determined with the Cell Death Detection ELISA PLUS Kit (Roche, Indianapolis, IN) as described previously (Anantharam et al., 2002; Choi et al., 2007; Kaul et al., 2003). Briefly, cells were lysed in provided lysis buffer for 30 mins at RT. Lysate was centrifuged for 10 mins at 200 X g and 20 μl of supernatant was incubated for 2 h with the mixture of HRP (horseradish peroxidase)-conjugated antibodies that recognize histones and single and double-stranded DNA. After washing away the unbound components, the final reaction product was measured colorimetrically with 2,2′-azino-di-[3-ethylbenz-thiazoline sulfonate] as an HRP substrate using a spectrophotometer at 405 nm and 490 nm. The difference in absorbance between 405 and 490 nm was used to determine the amount of DNA fragmentation in each sample. All sample

concentrations were normalized to protein concentration using the Bradford protein assay.

*2.9 Determination of intracellular manganese levels by IC-PMS*

Three million uninfected and RML scrapie-infected CAD5 cells were seeded in a T175, allowed to adhere for 12 h, and then were treated for 16 h with 300 μM $MnCl_2$ in Opti-MEM media. Cells were then collected by scraping and washed twice with PBS. Intracellular Mn concentration was measured at m/z 55 by inductively coupled plasma mass spectrometry (ICP-MS) as described in our previous publications (Afeseh Ngwa et al., 2009; Choi et al., 2007). A magnetic sector instrument (ELEMENT 1, Thermo Finnigan) was operated in medium resolution ($m/\Delta m$ = 4,000) to resolve the isotope of interest from possible interferences (Shum et al., 1992). Each sample was placed in an acid-washed 5 ml Teflon vial and digested in 200 μl triply distilled high purity nitric acid (TraceMetal Grade, Fisher Scientific, Pittsburg, PA). The digested samples were then diluted to a final volume of 5 ml with 18.2 MΩ deionized water (Elix and Milli-Q Gradient, Millipore, Billerica, MA) resulting in a final acid concentration of 4%. An internal standard method was used for quantification. Gallium (Ga) at m/z 69 was chosen as the internal standard because its m/z ratio is similar to that of Mn, and it has no major spectroscopic interferences. A small spike of Ga standard solution was added to each sample for a final Ga concentration of 10 ppb. A 10 ppb multi-element standard (Mn and Ga) was prepared. The nitric acid blank, the

multi-element standard, and each of the samples were introduced into the ICP-MS via a 100 µl/min self-aspirating perfluoroalkoxy (PFA) nebulizer (Elemental Scientific, Inc., Appleton, WI). The nitric acid blank was used to rinse the nebulizer between each sample. The results for each sample were calculated using the integrated average background-subtracted peak intensities from 70 consecutive scans. A normalization factor for Mn was derived from the multi-element standard to account for differences in the ionization efficiency of each element. The Mn concentration was then calculated for each sample.

*2.10 Data Analysis*

Statistical analysis was performed with Prism 4.0 software (GraphPad Software, San Diego, CA). Statistical significance among treatments was determined by one-way ANOVA analysis with Tukey's multiple comparison testing and is indicated by asterisks with *$p<0.05$, **$p<0.01$, and ***$p<0.001$. Analyses between two data sets were done using Student's t-test. $EC_{50}$ values were determined by the fitting of a nonlinear regression curve to the data from the MTT assay. Data typically represent three separate experiments and are expressed as mean ± S.E.M.

**3. Results**

*3.1 CAD5 characterization and limited proteolysis*

First, we examined the morphological features and prion infection of CAD5 cell model used in our experiments. Fig. 1A details the tendency for the RML scrapie-infected CAD5 cells to grow as aggregate colonies, while the uninfected cells form a more uniform monolayer. Additionally, the RML scrapie-infected cells have an increased doubling time compared to the uninfected cells when cultured over several days (data not shown). We do not see any differences in the growth characteristics such as doubling time, morphology, etc. between infected and uninfected cells because entire treatment is less than 36 hrs. Importantly, the CAD5 strain was able to retain persistent RML scrapie infection over multiple passages as determined by limited proteolytic digestion with PK and subsequent immunoblot using the 6H4 anti-PrP MAb (Fig. 1B). An abundant proteolytically resistant $PrP^{Sc}$ was detected in scrapie-infected cells as compared to uninfected cells (Fig. 1B).

*3.2 RML scrapie-infected CAD5 cells are more resistant to Mn-induced toxicity*

Several lines of evidence from our lab and others have shown that Mn-induced toxicity in neuronal cell models is associated with mitochondrial dysfunction and subsequent generation of reactive oxygen species (ROS) leading to cell death (Aschner et al., 2009; Kitazawa et al., 2005; Latchoumycandane et al., 2005; Roth et al., 2002; Worley et al., 2002). In an effort to establish a cytotoxic dose of Mn for further cell viability studies in the

CAD5 cell culture model of prion disease, both uninfected and RML scrapie-infected CAD5 cells were exposed to a full dose range of 10-5000 μM Mn for 16 h and viability was measured by MTT assay. As shown in Fig. 2A, a concentration-dependent decrease in cell viability for both uninfected and RML scrapie-infected cells was observed. A statistically significant difference ($p<0.05$) was observed between the $EC_{50}$ values for uninfected and RML-infected cells, as calculated by a three-parameter nonlinear regression of dose response curves. Unexpectedly, the RML scrapie-infected cells showed increased resistance to Mn treatment with a calculated $EC_{50}$ value of 428.8 μM, greater than double the $EC_{50}$ value of the uninfected cells, 211.6 μM. The cytotoxicity results were further confirmed by qualitative analysis using Sytox green staining. Uninfected and RML-infected cells were exposed to 300 and 500 μM Mn for 24 h and pictures were taken using a Nikon inverted fluorescent microscope. The difference in the number of Sytox positive cells is evident at both concentrations of Mn, with uninfected CAD5 cells showing a much greater number of Sytox stained cells (Fig. 2B). These studies led us to further examine this disparity in the cytotoxic doses of Mn on the uninfected and RML scrapie-infected CAD5 cell line. Based upon these data, we selected 300 μM Mn as an optimal dose for comparative studies of Mn-induced cytotoxicity.

*3.3 RML scrapie-infected CAD5 cells are more resistant to Mn-induced apoptotic cell death*

Mn-induced neurotoxicity is a known activator of proapoptotic signaling cascades in neuronal cells (Aschner et al., 2009; Kitazawa et al., 2005; Latchoumycandane et al., 2005; Stredrick et al., 2004). In order to explore the activation of proapoptotic caspases by Mn-induced neurotoxicity in uninfected and RML scrapie-infected CAD5 cells, we assayed the activity of the effector caspase, caspase-3, at 8, 12, 16, 20, and 24 h treatments with 300 μM of Mn. At 24 h treatment, a statistically significant increase in the activation of caspase-3 in uninfected cells ($p<0.001$) was observed, but no such increase was noted in RML-infected cells (Fig. 3A). Furthermore, we quantitatively assessed the level of DNA fragmentation on cells treated for 24 h with 300 μM Mn using a Cell Death Detection ELISA Kit. We found a statistically significant increase in the level of histone-associated low molecular weight DNA in uninfected cells at this time point ($p<0.001$), while the RML-infected cells showed no significant increase (Fig. 3B). These results indicate that RML scrapie-infected CAD5 cells are more resistant to Mn-induced apoptotic cell death than uninfected cells.

*3.4 RML scrapie infection attenuates Mn-induced oxidative damage*

To further probe the decreased susceptibility of RML-infected CAD5 cells to Mn-induced toxicity, we evaluated the incidence of Mn-induced oxidative stress by examining a product of lipid peroxidation, 4-hydroxynonenal (4-HNE), in Mn-treated CAD5 cells (Alikunju et al., 2011; Sango et al., 2008). Multiple studies have shown that neuronal cell lines persistently infected with $PrP^{Sc}$ show

increased susceptibility to oxidative stress (Fernaeus et al., 2005; Milhavet et al., 2000). As shown in Fig. 4A, uninfected CAD5 cells showed a time-dependent increase in the levels of 4-HNE in response to treatment with 300 μM of Mn. Surprisingly, scrapie-infected CAD5 cells treated with Mn showed reduced levels of 4-HNE when compared to uninfected cells (Fig. 4A). Densitometric analysis revealed a statistically significant ($p<0.05$) decrease in the 4-HNE band intensity of RML scrapie-infected cells at 24 h (Fig. 4B).

*3.5 RML Infected CAD5 Cells Have Reduced Manganese Accumulation*

The binding of divalent cations to $PrP^C$ induces clathrin-mediated endocytosis of lipid raft domains and this process is dependent upon the metal binding sites of $PrP^C$ (Brown and Harris, 2003; Hooper et al., 2008; Pauly and Harris, 1998; Perera and Hooper, 2001). A recent study from our group showed that knockout of $PrP^C$ alters Cu and Mn levels in a neuronal cell culture model (Choi et al., 2007). Also, other studies have shown altered divalent metal content in the brains of $PrP^C$ null and TSE-infected animals. These results indicate that $PrP^C$ may have a role in divalent metal homeostasis, and that conversion to the disease isoform alters the ability of $PrP^C$ to regulate intracellular concentrations. In order to examine the consequence of RML scrapie infection on Mn homeostasis, we treated uninfected and RML scrapie-infected CAD5 cells with 300 μM Mn for 16 h and determined the intracellular Mn concentration by inductively coupled plasma mass spectrometry (ICP-MS). Uninfected and RML

cells had similar basal levels of cytoplasmic Mn; however, Mn treatment increased intracellular Mn levels 187-fold in uninfected CAD5 cells and 130-fold in RML infected cells (Fig. 5A). This difference was statistically significant $p<0.01$.

In order to determine a mechanism for the difference in intracellular Mn concentration, we assessed the levels of DMT1 and transferrin in control and Mn-treated CAD5 cells. As seen in Fig. 5B-C, the basal level of DMT1 was increased in RML scrapie-infected CAD5 cells as compared to uninfected cells. However, Mn treatment did not cause any significant change in DMT1 levels in either cell types (Fig. 5B and 5D). Also, the basal level of expression of TF in uninfected and RML scrapie-infected cells is not significantly different (Fig. 5E-F). However, upon Mn treatment, there is a statistically significant, time-dependent increase in the level of TF in RML scrapie-infected cells. There was a slight but not significant increase in the levels of TF in uninfected cells at 24 h (Fig. 5E and 5G). These results show some differences existing in metal transporter protein between uninfected and RML scrapie-infected cells. However, the altered expression of these proteins between the uninfected and infected CAD5 cells are contradictory to the expected intracellular Mn concentrations since both DMT1 and TF are involved in Mn influx yet are increased in the infected cells that have a decreased Mn content. These results indicate that there are other factors influencing the intracellular level of Mn. Altered expression of proteins that are involved in Mn efflux may also play role in Mn-homeostasis. The mechanisms of

regulation that are affected by conversion from $PrP^{C}$ to $PrP^{Sc}$ remain an interesting target for further study.

**4. Discussion**

In this study we have shown that RML scrapie-infected catecholaminergic cells are more resistant to Mn-induced neurotoxicity than uninfected cells. Consistent with cytotoxicity, caspase-3 activation, DNA fragmentation, and ROS generation are attenuated in Mn-treated RML scrapie-infected CAD5 cells. Another notable finding of our study was that metal transport proteins DMT and transferrin are altered in scrapie-infected cells as compared to uninfected cells. To our knowledge, this is the first report demonstrating reduced metal neurotoxicity in an infectious model of prion disease.

Our understanding of the role of metals in key neurobiological processes, as well as in the pathogenesis of various neurodegenerative diseases, has greatly expanded over the last two decades. Studies overwhelmingly demonstrate that metal dyshomeostasis, protein aggregation, and oxidative stress are interconnected pathophysiological mechanisms of all neurodegenerative diseases associated with proteinopathies. Significant imbalances in major transition metals such as iron, copper, and zinc are implicated in other major neurodegenerative conditions such as Parkinson's disease (PD), Alzheimer's disease (AD), Amyotrophic lateral sclerosis (ALS) and

Huntington Disease (HD) (Bishop et al., 2002; Bossy-Wetzel et al., 2004; Brown, 2009; Bush and Curtain, 2008; Cahill et al., 2009; Gaeta and Hider, 2005; Molina-Holgado et al., 2007; Sayre et al., 1999). Another common pathological feature of these neurodegenerative disorders is the aggregation of β-sheet-rich synaptic proteins associated with each disease (e.g., α-synuclein in PD, a-beta in AD, and huntingtin in HD). Environmental exposure to transition metals is linked to pathological processes of various neurodegenerative conditions since metal exposure is known to augment key degenerative changes including ionic imbalance, oxidative stress, and protein aggregation (Afeseh Ngwa et al., 2009; Anantharam et al., 2002; Aschner et al., 2009; Crossgrove and Zheng, 2004; Kitazawa et al., 2001; Park et al., 2005; Wu et al., 2008).

Emerging evidence indicates that dysregulation of divalent cation homeostasis may play a role in the pathogenesis of prion diseases (Basu et al., 2007; Brown, 2009; Choi et al., 2006; Singh et al., 2009). $PrP^{C}$ contains multiple octapeptide repeat sequences (PHGGSWGQ) toward the N-terminus that have binding affinity for various divalent metals including copper and manganese (Hornshaw et al., 1995; Viles et al., 1999). The number of octapeptide repeats differs from species to species; however, point mutations, deletions or multiple insertions of the octapeptide repeats in the prion protein gene have been linked to inherited prion disease in humans (Krasemann et al., 1995; Mead et al., 2007; Palmer and Collinge, 1993; Yin et al., 2007). Structural studies have suggested that most of the N-terminus of prion protein is rather unstructured, while the C-

terminus is highly structured (Di Natale et al., 2005; Jones et al., 2005; Renner et al., 2004; Viles et al., 2001). Binding of divalent cations to $PrP^C$ has been speculated to facilitate the folding of the largely unstructured N-terminus, thereby stabilizing the protein conformation (Cereghetti et al., 2003). The antioxidant properties of $PrP^C$ have been linked to Cu residency in the octapeptide repeat domain (Brown et al., 2001; Brown et al., 1999; Gaggelli et al., 2008; Treiber et al., 2007). Cu bound by $PrP^C$ is able to undergo full and reversible redox chemistry, allowing for the detoxification of superoxide and the reduction of hydroxyl radicals (Nadal et al., 2007). Recently, we showed that prion protein expressing cells are more resistant to oxidative damage as compared to prion knockout cells (Anantharam et al., 2008).

Mn is an important trace elemental metal that is required by most organisms for normal functioning; however, continued exposure to high concentrations of Mn results in adverse neurological deficits commonly referred to manganism. Interestingly, elevated Mn levels have been observed in the brain and blood of humans and animals afflicted with prion diseases and Mn-bound $PrP^{Sc}$ has been isolated from TSE-infected neural tissue (Hesketh et al., 2008; Hesketh et al., 2007; Thackray et al., 2002; Wong et al., 2001a). In vitro titration calorimetry studies done using recombinant PrP have shown that Mn can replace Cu residency in the metal binding sites despite a calculated lower affinity (Brazier et al., 2008; Zhu et al., 2008). Mn binding to $PrP^C$ induces biophysical properties similar to $PrP^{Sc}$, including increased β-sheet content, proteolytic resistance, and

the ability to seed aggregation of soluble oligomers, yet the role of metals in the disease is not very well understood (Abdelraheim et al., 2006; Brazier et al., 2008; Brown et al., 2000; Giese et al., 2004; Kim et al., 2005). Recently, we demonstrated that $PrP^{C}$ effectively attenuates Mn transport into neuronal cells and protects against Mn-induced oxidative stress, mitochondrial dysfunction, cellular antioxidant depletion, and apoptosis (Choi et al., 2007). In addition, we found that Mn treatment upregulates $PrP^{C}$ levels independently of transcription (Choi et al., 2010). Further mechanistic studies revealed that Mn increases stability of prion protein, suggesting that Mn may promote the conversion of $PrP^{C}$ to $PrP^{Sc}$. Our present study shows that the scrapie-infected cells are more resistant to Mn neurotoxicity and the infected cells have altered metal transport as compared to uninfected cells. Taken together, these results suggest that conversion to $PrP^{Sc}$ may result in greater affinity for Mn and increased ability for $PrP^{Sc}$ to sequester and export excess Mn through the exosomal pathway in neuronal cells (Fevrier et al., 2005). Additionally, the resistance of prion-infected cells to Mn neurotoxicity may aid the propagation of prion protein aggregation from infected cells to healthy cells. Further studies are on-going in our laboratory to address these possibilities. However, the possibility of other factors such as altered expression of Mn efflux proteins or the increase or activation of other survival factors influencing Mn toxicity in infected cells cannot be completely ruled out.

In this study we focused on the CAD cell line, which is derived from catecholaminergic neurons; whereas in humans and animals with prion disease,

higher Mn levels in brain tissue may be attributed to an increase in Mn-levels in microglia and astrocytes which constitute at least 90% of the total brain cell population. Consequence of prion infection on glial cells remains an interesting area of study. Unfortunately, the mechanisms involved in the regulation of cellular Mn homeostasis are still not well understood. Influx of Mn across the plasma membrane is believed to be mediated by divalent metal transporter 1 (DMT1) and transferrin (TF), despite dissociation constants in the millimolar range (Aschner et al., 1999; Erikson and Aschner, 2006; Fitsanakis et al., 2007; Garrick et al., 2006; Yokel, 2009). It is possible that ferroportin and ion channels are involved in Mn efflux (Yin et al., 2010). Increased resistance to oxidative stress in RML scrapie-infected cells is not likely to be a contributing factor in reducing the Mn toxicity observed in this work since prion infection has been shown to increase susceptibility of neuronal cells to oxidative stress (Fernaeus and Land, 2005; Fernaeus et al., 2005). Finally, a large body of evidence indicates that presence of dopamine in SH-SY5Y and other dopaminergic cell lines may directly influence the degree of Mn toxicity (For review see (Aschner et al., 2009; Smargiassi and Mutti, 1999.). However, in Cath.a cells, suppression of dopamine production with alpha-methyl-para-tyrosine offered no significant protection from Mn exposure suggesting that dopamine content was not responsible for the enhanced sensitivity to Mn toxicity which rules out the utilization of Mn as a co-factor (Stredrick et al., 2004). Further work is clearly needed to elucidate the interconnectivity of metal dyshomeostasis and protein aggregation in neurodegenerative disorders.

**Conflict of interest**

There are no conflicts of interest to declare.

**Acknowledgements**

This work was supported by National Institutes of Health Grants ES019276 and ES10586. We thank Dr. Charles Weissmann and his colleagues from the Scripps Institute (Jupiter, FL) for providing us the CAD5 cell model for our study. The ICP mass spectrometer was obtained with funds provided by the U. S. Department of Energy, Office of Nuclear Nonproliferation (NA-22), and the Office of Basic Energy Sciences, Division of Chemical Sciences, Geosciences, and Biosciences through the Ames Laboratory. The Ames Laboratory is operated for the U.S. Department of Energy by Iowa State University under Contract No. DE-AC02-07CH11358. The W. Eugene and Linda Lloyd Endowed Chair for AGK is also acknowledged. We thank Mary Ann deVries for assistance in the preparation of this manuscript.

**5. References**

Abdelraheim SR, Kralovicova S, Brown DR. Hydrogen peroxide cleavage of the prion protein generates a fragment able to initiate polymerisation of full length prion protein. Int J Biochem Cell Biol 2006; 38: 1429-40.

Afeseh Ngwa H, Kanthasamy A, Anantharam V, Song C, Witte T, Houk R, et al. Vanadium induces dopaminergic neurotoxicity via protein kinase Cdelta dependent oxidative signaling mechanisms: relevance to etiopathogenesis of Parkinson's disease. Toxicol Appl Pharmacol 2009; 240: 273-85.

Aguzzi A, Heikenwalder M. Pathogenesis of prion diseases: current status and future outlook. Nat Rev Microbiol 2006; 4: 765-75.

Alikunju S, Abdul Muneer PM, Zhang Y, Szlachetka AM, Haorah J. The inflammatory footprints of alcohol-induced oxidative damage in neurovascular components. Brain Behav Immun 2011; 25 Suppl 1: S129-36.

Anantharam V, Kanthasamy A, Choi CJ, Martin DP, Latchoumycandane C, Richt JA, et al. Opposing roles of prion protein in oxidative stress- and ER stress-induced apoptotic signaling. Free Radic Biol Med 2008; 45: 1530-41.

Anantharam V, Kitazawa M, Wagner J, Kaul S, Kanthasamy AG. Caspase-3-dependent proteolytic cleavage of protein kinase Cdelta is essential for

oxidative stress-mediated dopaminergic cell death after exposure to methylcyclopentadienyl manganese tricarbonyl. J Neurosci 2002; 22: 1738-51.

Aschner M, Erikson KM, Herrero Hernandez E, Tjalkens R. Manganese and its role in Parkinson's disease: from transport to neuropathology. Neuromolecular Med 2009; 11: 252-66.

Aschner M, Vrana KE, Zheng W. Manganese uptake and distribution in the central nervous system (CNS). Neurotoxicology 1999; 20: 173-80.

Basu S, Mohan ML, Luo X, Kundu B, Kong Q, Singh N. Modulation of proteinase K-resistant prion protein in cells and infectious brain homogenate by redox iron: implications for prion replication and disease pathogenesis. Mol Biol Cell 2007; 18: 3302-12.

Bishop GM, Robinson SR, Liu Q, Perry G, Atwood CS, Smith MA. Iron: a pathological mediator of Alzheimer disease? Dev Neurosci 2002; 24: 184-7.

Bolton DC, Meyer RK, Prusiner SB. Scrapie PrP 27-30 is a sialoglycoprotein. J Virol 1985; 53: 596-606.

Bossy-Wetzel E, Schwarzenbacher R, Lipton SA. Molecular pathways to neurodegeneration. Nat Med 2004; 10 Suppl: S2-9.

Brandner S. CNS pathogenesis of prion diseases. Br Med Bull 2003; 66: 131-9.

Brazier MW, Davies P, Player E, Marken F, Viles JH, Brown DR. Manganese binding to the prion protein. J Biol Chem 2008; 283: 12831-9.

Brown DR. Mayhem of the multiple mechanisms: modelling neurodegeneration in prion disease. J Neurochem 2002; 82: 209-15.

Brown DR. Metallic prions. Biochem Soc Symp 2004: 193-202.

Brown DR. Brain proteins that mind metals: a neurodegenerative perspective. Dalton Trans 2009: 4069-76.

Brown DR, Clive C, Haswell SJ. Antioxidant activity related to copper binding of native prion protein. J Neurochem 2001; 76: 69-76.

Brown DR, Hafiz F, Glasssmith LL, Wong BS, Jones IM, Clive C, et al. Consequences of manganese replacement of copper for prion protein function and proteinase resistance. Embo J 2000; 19: 1180-6.

Brown DR, Wong BS, Hafiz F, Clive C, Haswell SJ, Jones IM. Normal prion protein has an activity like that of superoxide dismutase. Biochem J 1999; 344 Pt 1: 1-5.

Brown LR, Harris DA. Copper and zinc cause delivery of the prion protein from the plasma membrane to a subset of early endosomes and the Golgi. J Neurochem 2003; 87: 353-63.

Bush AI, Curtain CC. Twenty years of metallo-neurobiology: where to now? Eur Biophys J 2008; 37: 241-5.

Cahill CM, Lahiri DK, Huang X, Rogers JT. Amyloid precursor protein and alpha synuclein translation, implications for iron and inflammation in neurodegenerative diseases. Biochim Biophys Acta 2009; 1790: 615-28.

Cereghetti GM, Schweiger A, Glockshuber R, Van Doorslaer S. Stability and Cu(II) binding of prion protein variants related to inherited human prion diseases. Biophys J 2003; 84: 1985-97.

Chen S, Mange A, Dong L, Lehmann S, Schachner M. Prion protein as trans-interacting partner for neurons is involved in neurite outgrowth and neuronal survival. Mol Cell Neurosci 2003; 22: 227-33.

Chiarini LB, Freitas AR, Zanata SM, Brentani RR, Martins VR, Linden R. Cellular prion protein transduces neuroprotective signals. Embo J 2002; 21: 3317-26.

Choi CJ, Anantharam V, Martin DP, Nicholson EM, Richt JA, Kanthasamy A, et al. Manganese upregulates cellular prion protein and contributes to altered stabilization and proteolysis: relevance to role of metals in pathogenesis of prion disease. Toxicol Sci 2010; 115: 535-46.

Choi CJ, Anantharam V, Saetveit NJ, Houk RS, Kanthasamy A, Kanthasamy AG. Normal Cellular Prion Protein Protects against Manganese-Induced Oxidative Stress and Apoptotic Cell Death. Toxicol Sci 2007; 98: 495-509.

Choi CJ, Kanthasamy A, Anantharam V, Kanthasamy AG. Interaction of metals with prion protein: possible role of divalent cations in the pathogenesis of prion diseases. Neurotoxicology 2006; 27: 777-87.

Collinge J. Prion diseases of humans and animals: their causes and molecular basis. Annu Rev Neurosci 2001; 24: 519-50.

Collinge J. Molecular neurology of prion disease. J Neurol Neurosurg Psychiatry 2005; 76: 906-19.

Crossgrove J, Zheng W. Manganese toxicity upon overexposure. NMR Biomed 2004; 17: 544-53.

Di Natale G, Grasso G, Impellizzeri G, La Mendola D, Micera G, Mihala N, et al. Copper(II) interaction with unstructured prion domain outside the octarepeat region: speciation, stability, and binding details of copper(II) complexes with PrP106-126 peptides. Inorg Chem 2005; 44: 7214-25.

Erikson KM, Aschner M. Increased manganese uptake by primary astrocyte cultures with altered iron status is mediated primarily by divalent metal transporter. Neurotoxicology 2006; 27: 125-30.

Fernaeus S, Land T. Increased iron-induced oxidative stress and toxicity in scrapie-infected neuroblastoma cells. Neurosci Lett 2005; 382: 217-20.

Fernaeus S, Reis K, Bedecs K, Land T. Increased susceptibility to oxidative stress in scrapie-infected neuroblastoma cells is associated with intracellular iron status. Neurosci Lett 2005; 389: 133-6.

Fevrier B, Vilette D, Laude H, Raposo G. Exosomes: a bubble ride for prions? Traffic 2005; 6: 10-7.

Fitsanakis VA, Piccola G, Marreilha dos Santos AP, Aschner JL, Aschner M. Putative proteins involved in manganese transport across the blood-brain barrier. Hum Exp Toxicol 2007; 26: 295-302.

Freixes M, Rodriguez A, Dalfo E, Ferrer I. Oxidation, glycoxidation, lipoxidation, nitration, and responses to oxidative stress in the cerebral cortex in Creutzfeldt-Jakob disease. Neurobiol Aging 2006; 27: 1807-15.

Gaeta A, Hider RC. The crucial role of metal ions in neurodegeneration: the basis for a promising therapeutic strategy. Br J Pharmacol 2005; 146: 1041-59.

Gaggelli E, Jankowska E, Kozlowski H, Marcinkowska A, Migliorini C, Stanczak P, et al. Structural characterization of the intra- and inter-repeat copper binding modes within the N-terminal region of "prion related protein" (PrP-rel-2) of zebrafish. J Phys Chem B 2008; 112: 15140-50.

Garrick MD, Kuo HC, Vargas F, Singleton S, Zhao L, Smith JJ, et al. Comparison of mammalian cell lines expressing distinct isoforms of divalent metal transporter 1 in a tetracycline-regulated fashion. Biochem J 2006; 398: 539-46.

Giese A, Levin J, Bertsch U, Kretzschmar H. Effect of metal ions on de novo aggregation of full-length prion protein. Biochem Biophys Res Commun 2004; 320: 1240-6.

Hesketh S, Sassoon J, Knight R, Brown DR. Elevated manganese levels in blood and CNS in human prion disease. Mol Cell Neurosci 2008; 37: 590-8.

Hesketh S, Sassoon J, Knight R, Hopkins J, Brown DR. Elevated manganese levels in blood and central nervous system occur before onset of clinical signs in scrapie and bovine spongiform encephalopathy. J Anim Sci 2007; 85: 1596-609.

Hooper NM, Taylor DR, Watt NT. Mechanism of the metal-mediated endocytosis of the prion protein. Biochem Soc Trans 2008; 36: 1272-6.

Hornshaw MP, McDermott JR, Candy JM. Copper binding to the N-terminal tandem repeat regions of mammalian and avian prion protein. Biochem Biophys Res Commun 1995; 207: 621-9.

Jackson GS, Murray I, Hosszu LL, Gibbs N, Waltho JP, Clarke AR, et al. Location and properties of metal-binding sites on the human prion protein. Proc Natl Acad Sci U S A 2001; 98: 8531-5.

Jones CE, Abdelraheim SR, Brown DR, Viles JH. Preferential Cu2+ coordination by His96 and His111 induces beta-sheet formation in the unstructured amyloidogenic region of the prion protein. J Biol Chem 2004; 279: 32018-27.

Jones CE, Klewpatinond M, Abdelraheim SR, Brown DR, Viles JH. Probing copper2+ binding to the prion protein using diamagnetic nickel2+ and 1H NMR: the unstructured N terminus facilitates the coordination of six

copper2+ ions at physiological concentrations. J Mol Biol 2005; 346: 1393-407.

Kaul S, Kanthasamy A, Kitazawa M, Anantharam V, Kanthasamy AG. Caspase-3 dependent proteolytic activation of protein kinase C delta mediates and regulates 1-methyl-4-phenylpyridinium (MPP+)-induced apoptotic cell death in dopaminergic cells: relevance to oxidative stress in dopaminergic degeneration. Eur J Neurosci 2003; 18: 1387-401.

Kim NH, Choi JK, Jeong BH, Kim JI, Kwon MS, Carp RI, et al. Effect of transition metals (Mn, Cu, Fe) and deoxycholic acid (DA) on the conversion of PrPC to PrPres. Faseb J 2005; 19: 783-5.

Kitazawa M, Anantharam V, Kanthasamy AG. Activation of oxidative stress-dependent cell signaling pathways in methylcyclopentadienyl manganese tricarbonyl (MMT)-induced apoptosis: Downstream events and regulatory mechanisms. 40th annual meeting of Society of Toxicology. San Francisco, CA, 2001.

Kitazawa M, Anantharam V, Yang Y, Hirata Y, Kanthasamy A, Kanthasamy AG. Activation of protein kinase C delta by proteolytic cleavage contributes to manganese-induced apoptosis in dopaminergic cells: protective role of Bcl-2. Biochem Pharmacol 2005; 69: 133-46.

Krasemann S, Zerr I, Weber T, Poser S, Kretzschmar H, Hunsmann G, et al. Prion disease associated with a novel nine octapeptide repeat insertion in the PRNP gene. Brain Res Mol Brain Res 1995; 34: 173-6.

Latchoumycandane C, Anantharam V, Kitazawa M, Yang Y, Kanthasamy A, Kanthasamy AG. Protein kinase Cdelta is a key downstream mediator of manganese-induced apoptosis in dopaminergic neuronal cells. J Pharmacol Exp Ther 2005; 313: 46-55.

Lee DW, Sohn HO, Lim HB, Lee YG, Kim YS, Carp RI, et al. Alteration of free radical metabolism in the brain of mice infected with scrapie agent. Free Radic Res 1999; 30: 499-507.

Mahal SP, Baker CA, Demczyk CA, Smith EW, Julius C, Weissmann C. Prion strain discrimination in cell culture: the cell panel assay. Proc Natl Acad Sci U S A 2007; 104: 20908-13.

Mange A, Milhavet O, Umlauf D, Harris D, Lehmann S. PrP-dependent cell adhesion in N2a neuroblastoma cells. FEBS Lett 2002; 514: 159-62.

Mead S, Webb TE, Campbell TA, Beck J, Linehan JM, Rutherfoord S, et al. Inherited prion disease with 5-OPRI: phenotype modification by repeat length and codon 129. Neurology 2007; 69: 730-8.

Milhavet O, McMahon HE, Rachidi W, Nishida N, Katamine S, Mange A, et al. Prion infection impairs the cellular response to oxidative stress. Proc Natl Acad Sci U S A 2000; 97: 13937-42.

Molina-Holgado F, Hider RC, Gaeta A, Williams R, Francis P. Metals ions and neurodegeneration. Biometals 2007; 20: 639-54.

Nadal RC, Abdelraheim SR, Brazier MW, Rigby SE, Brown DR, Viles JH. Prion protein does not redox-silence Cu2+, but is a sacrificial quencher of hydroxyl radicals. Free Radic Biol Med 2007; 42: 79-89.

Nunziante M, Gilch S, Schatzl HM. Essential role of the prion protein N terminus in subcellular trafficking and half-life of cellular prion protein. J Biol Chem 2003; 278: 3726-34.

Owen F, Poulter M, Lofthouse R, Collinge J, Crow TJ, Risby D, et al. Insertion in prion protein gene in familial Creutzfeldt-Jakob disease. Lancet 1989; 1: 51-2.

Palmer MS, Collinge J. Human prion diseases. Curr Opin Neurol Neurosurg 1992; 5: 895-901.

Palmer MS, Collinge J. Mutations and polymorphisms in the prion protein gene. Hum Mutat 1993; 2: 168-73.

Park RM, Schulte PA, Bowman JD, Walker JT, Bondy SC, Yost MG, et al. Potential occupational risks for neurodegenerative diseases. Am J Ind Med 2005; 48: 63-77.

Pauly PC, Harris DA. Copper stimulates endocytosis of the prion protein. J Biol Chem 1998; 273: 33107-10.

Perera WS, Hooper NM. Ablation of the metal ion-induced endocytosis of the prion protein by disease-associated mutation of the octarepeat region. Curr Biol 2001; 11: 519-23.

Peters PJ, Mironov A, Jr., Peretz D, van Donselaar E, Leclerc E, Erpel S, et al. Trafficking of prion proteins through a caveolae-mediated endosomal pathway. J Cell Biol 2003; 162: 703-17.

Petersen RB, Siedlak SL, Lee HG, Kim YS, Nunomura A, Tagliavini F, et al. Redox metals and oxidative abnormalities in human prion diseases. Acta Neuropathol 2005; 110: 232-8.

Prado MA, Alves-Silva J, Magalhaes AC, Prado VF, Linden R, Martins VR, et al. PrPc on the road: trafficking of the cellular prion protein. J Neurochem 2004; 88: 769-81.

Prusiner SB. Molecular biology of prion diseases. Science 1991; 252: 1515-22.

Prusiner SB, DeArmond SJ. Prion diseases of the central nervous system. Monogr Pathol 1990: 86-122.

Prusiner SB, Kingsbury DT. Prions--infectious pathogens causing the spongiform encephalopathies. CRC Crit Rev Clin Neurobiol 1985; 1: 181-200.

Prusiner SB, Scott M, Foster D, Pan KM, Groth D, Mirenda C, et al. Transgenetic studies implicate interactions between homologous PrP isoforms in scrapie prion replication. Cell 1990; 63: 673-86.

Renner C, Fiori S, Fiorino F, Landgraf D, Deluca D, Mentler M, et al. Micellar environments induce structuring of the N-terminal tail of the prion protein. Biopolymers 2004; 73: 421-33.

Roth JA, Horbinski C, Higgins D, Lein P, Garrick MD. Mechanisms of manganese-induced rat pheochromocytoma (PC12) cell death and cell differentiation. Neurotoxicology 2002; 23: 147-57.

Sakudo A, Lee DC, Yoshimura E, Nagasaka S, Nitta K, Saeki K, et al. Prion protein suppresses perturbation of cellular copper homeostasis under oxidative conditions. Biochem Biophys Res Commun 2004; 313: 850-5.

Sango K, Yanagisawa H, Kato K, Kato N, Hirooka H, Watabe K. Differential Effects of High Glucose and Methylglyoxal on Viability and

Polyol Metabolism in Immortalized Adult Mouse Schwann Cells. The Open Diabetes Journal 2008: 1-11.

Sayre LM, Perry G, Smith MA. Redox metals and neurodegenerative disease. Curr Opin Chem Biol 1999; 3: 220-5.

Shum SC, Neddersen R, Houk RS. Elemental speciation by liquid chromatography-inductively coupled plasma mass spectrometry with direct injection nebulization. Analyst 1992; 117: 577-82.

Singh A, Isaac AO, Luo X, Mohan ML, Cohen ML, Chen F, et al. Abnormal brain iron homeostasis in human and animal prion disorders. PLoS Pathog 2009; 5: e1000336.

Smargiassi A, Mutti A. Peripheral biomarkers and exposure to manganese. Neurotoxicology 1999; 20: 401-6.

Stredrick DL, Stokes AH, Worst TJ, Freeman WM, Johnson EA, Lash LH, et al. Manganese-induced cytotoxicity in dopamine-producing cells. Neurotoxicology 2004; 25: 543-53.

Tatzelt J, Schatzl HM. Molecular basis of cerebral neurodegeneration in prion diseases. Febs J 2007; 274: 606-11.

Thackray AM, Knight R, Haswell SJ, Bujdoso R, Brown DR. Metal imbalance and compromised antioxidant function are early changes in prion disease. Biochem J 2002; 362: 253-8.

Treiber C, Pipkorn R, Weise C, Holland G, Multhaup G. Copper is required for prion protein-associated superoxide dismutase-I activity in Pichia pastoris. Febs J 2007; 274: 1304-11.

Viles JH, Cohen FE, Prusiner SB, Goodin DB, Wright PE, Dyson HJ. Copper binding to the prion protein: structural implications of four identical cooperative binding sites. Proc Natl Acad Sci U S A 1999; 96: 2042-7.

Viles JH, Donne D, Kroon G, Prusiner SB, Cohen FE, Dyson HJ, et al. Local structural plasticity of the prion protein. Analysis of NMR relaxation dynamics. Biochemistry 2001; 40: 2743-53.

Wong BS, Brown DR, Pan T, Whiteman M, Liu T, Bu X, et al. Oxidative impairment in scrapie-infected mice is associated with brain metals perturbations and altered antioxidant activities. J Neurochem 2001a; 79: 689-98.

Wong BS, Chen SG, Colucci M, Xie Z, Pan T, Liu T, et al. Aberrant metal binding by prion protein in human prion disease. J Neurochem 2001b; 78: 1400-8.

Worley CG, Bombick D, Allen JW, Suber RL, Aschner M. Effects of manganese on oxidative stress in CATH.a cells. Neurotoxicology 2002; 23: 159-64.

Wu J, Basha MR, Zawia NH. The environment, epigenetics and amyloidogenesis. J Mol Neurosci 2008; 34: 1-7.

Yin S, Pham N, Yu S, Li C, Wong P, Chang B, et al. Human prion proteins with pathogenic mutations share common conformational changes resulting in enhanced binding to glycosaminoglycans. Proc Natl Acad Sci U S A 2007; 104: 7546-51.

Yin Z, Jiang H, Lee ES, Ni M, Erikson KM, Milatovic D, et al. Ferroportin is a manganese-responsive protein that decreases manganese cytotoxicity and accumulation. J Neurochem 2010; 112: 1190-8.

Yokel RA. Manganese flux across the blood-brain barrier. Neuromolecular Med 2009; 11: 297-310.

Yun SW, Gerlach M, Riederer P, Klein MA. Oxidative stress in the brain at early preclinical stages of mouse scrapie. Exp Neurol 2006; 201: 90-8.

Zhu F, Davies P, Thompsett AR, Kelly SM, Tranter GE, Hecht L, et al. Raman optical activity and circular dichroism reveal dramatic differences in the influence of divalent copper and manganese ions on prion protein folding. Biochemistry 2008; 47: 2510-7.

**Figures**

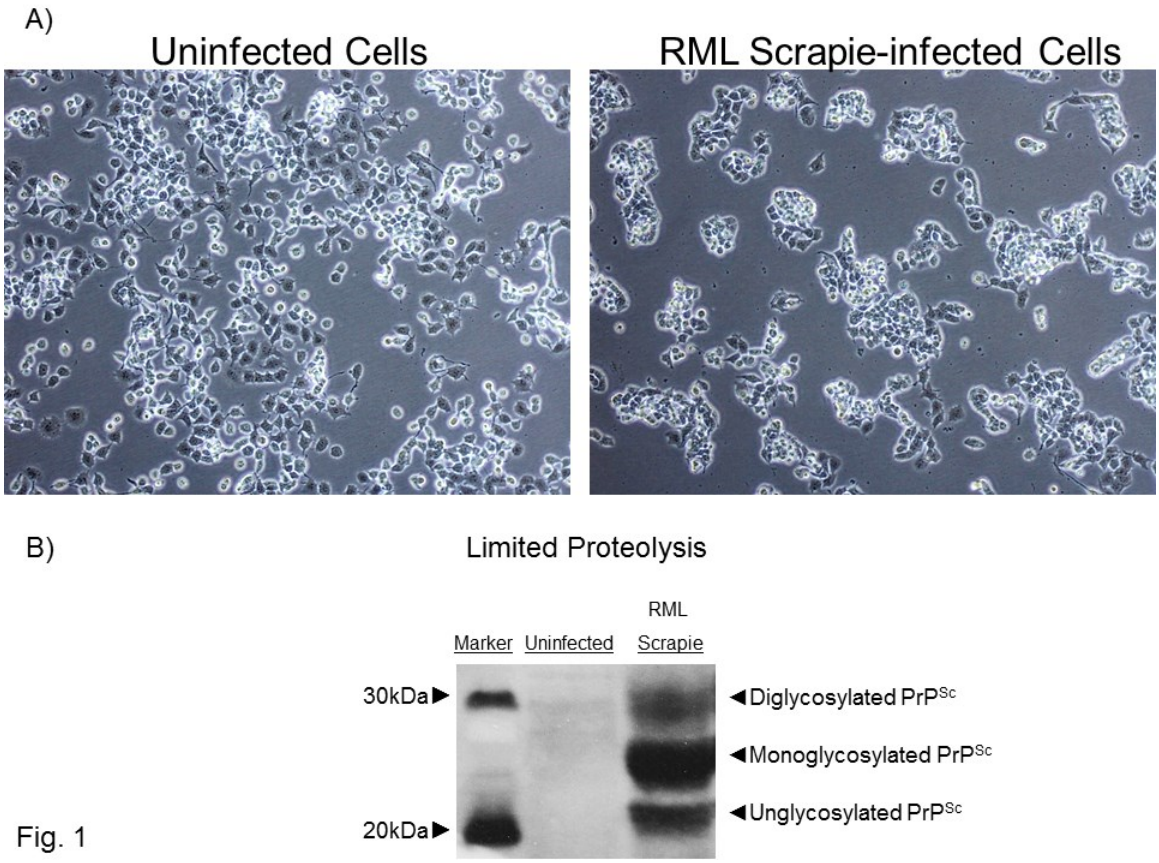


Fig. 1

**Fig. 1.** Characterization of CAD5 cells and RML scrapie infection. **A)** Phase contrast image of uninfected and RML scrapie-infected CAD5 cells. Scrapie-infected cells tend to grow in aggregated colonies and grow more slowly than uninfected cells. **B)** Lysate from uninfected and infected CAD5 cells was proteolytically digested by addition of 20 µg/ml PK for 1 h at 37ºC. Immunoblot with anti-PrP MAb showed complete digestion of $PrP^{C}$ in uninfected cells, and the presence of proteolytically resistant $PrP^{Sc}$ in infected cells. The multiple bands represent the three glycoforms of PrP.

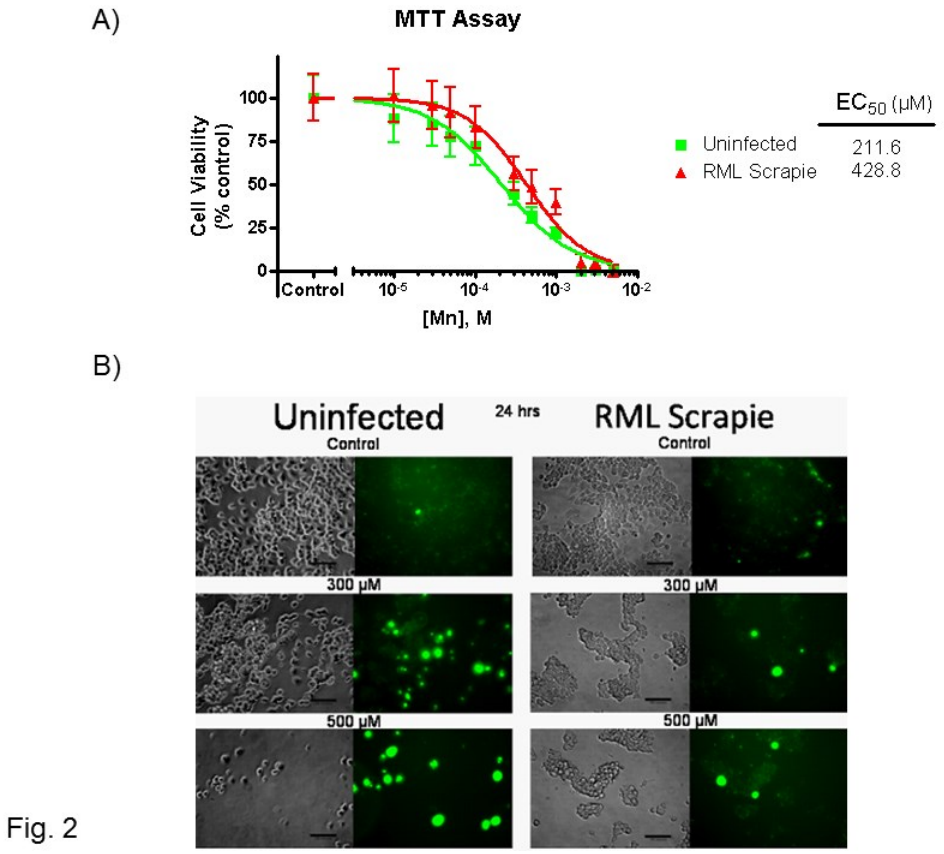


Fig. 2

**Fig. 2.** RML scrapie-infected CAD5 cells are more resistant to Mn-induced toxicity. **A)** Uninfected and RML scrapie-infected CAD5 cells were treated with 10, 30, 50, 100, 300, 500, 1000, and 5000 μM Mn for 16 h and cell viability was measured by MTT assay. The $LD_{50}$ value of the control cells was determined to be 211.6 μM (95% CI 136.8-304.8 μM, logEC50: -3.675±0.081) while in RML scrapie infected cells the $LD_{50}$ was calculated to be 428.8 μM (95% CI 290.9-632 μM, logEC50: -3.368±0.086). RML scrapie-infected cells showed reduced susceptibility to Mn-induced toxicity as evidenced by the statistically significant ($p<0.05$) increase in the $EC_{50}$ value. Data shown represent two repeats with a total of 16 individual data

points per concentration. **B)** Uninfected and RML scrapie-infected CAD5 cells were treated with 300 μM and 500 μM Mn for 24 h. Qualitative analysis of Mn-induced toxicity was done by Sytox green staining of dead and dying cells. We observed reduced staining by Sytox in RML scrapie-infected CAD5 cells when compared to uninfected cells.

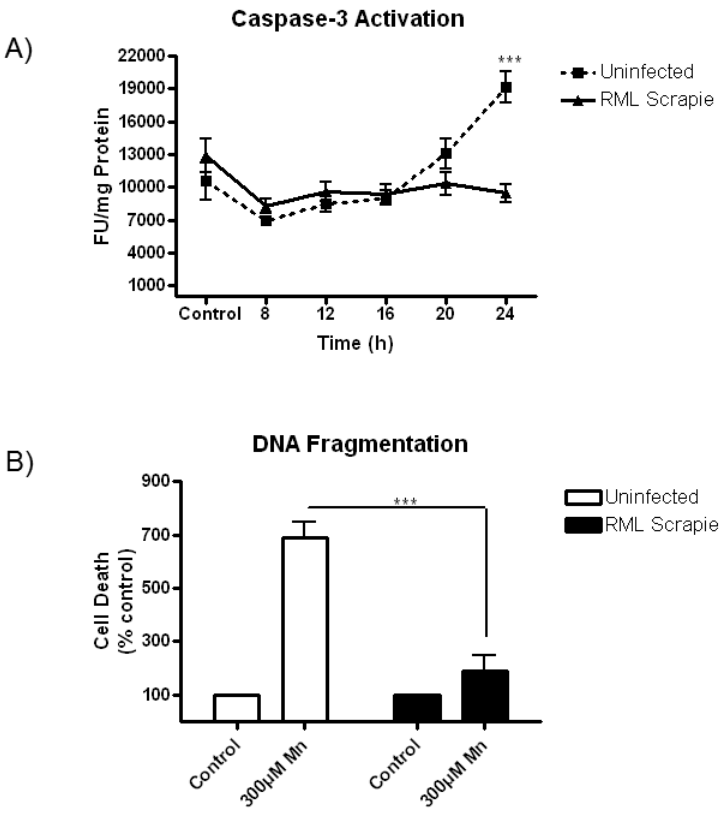


Fig. 3

**Fig. 3.** RML scrapie-infected CAD5 cells are more resistant to Mn-induced apoptotic cell death. Uninfected and RML scrapie-infected CAD5 cells were treated with 300 μM Mn and the activity of caspase-3 was determined by caspase-3 specific fluorogenic substrate over time. DNA fragmentation was assayed after 24 h of Mn treatment by ELISA. **A)**

Uninfected CAD5 cells showed a time-dependent increase in caspase-3 activity in response to Mn treatment ($p<0.001$), while RML scrapie-infected CAD5 cells showed no increase at 24 h. Data shown represents three repeats with a total n=7. **B)** DNA fragmentation was significantly increased ($p<0.001$) in uninfected cells treated with Mn when compared to RML scrapie-infected cells.

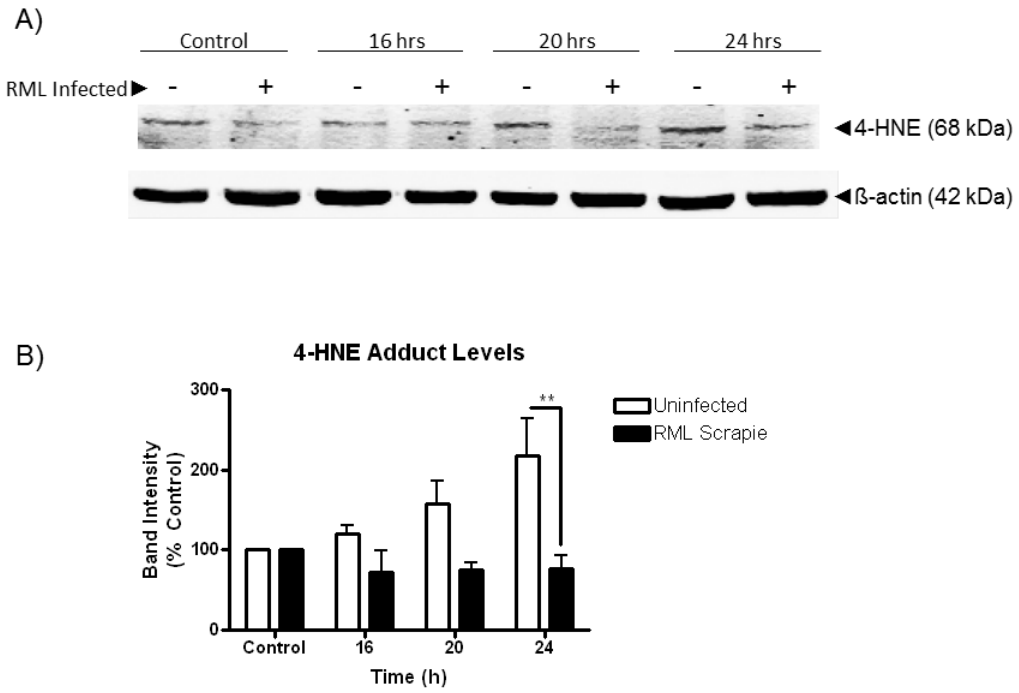


Fig. 4

**Fig. 4.** RML scrapie infection attenuates Mn-induced ROS generation. Uninfected and RML scrapie-infected CAD5 cells were treated with 300 μM Mn for 16, 20, and 24 h. **A)** Generation of Mn-induced ROS was

determined by the presence of lipid peroxidation product 4-HNE. Lysate from treated cells was probed after Western blot with anti-4-HNE antibody. To ensure equal protein loading, blots were co-treated with β-actin antibody. **B)** Uninfected CAD5 cells showed a time-dependent increase in 4-HNE levels as determined by densitometric analysis of three individual repeats. A statistically significantly difference in increases of 4-HNE levels is seen between uninfected and infected cells at 24 h ($p<0.01$).

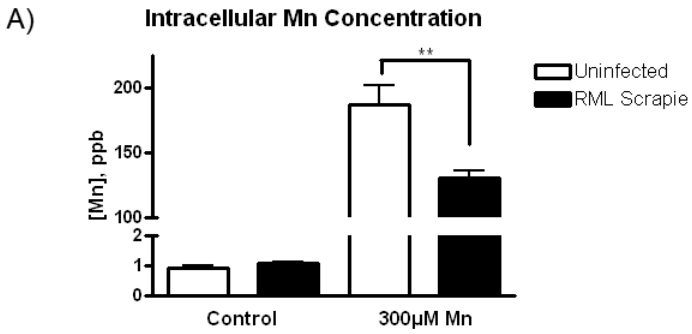


Fig. 5

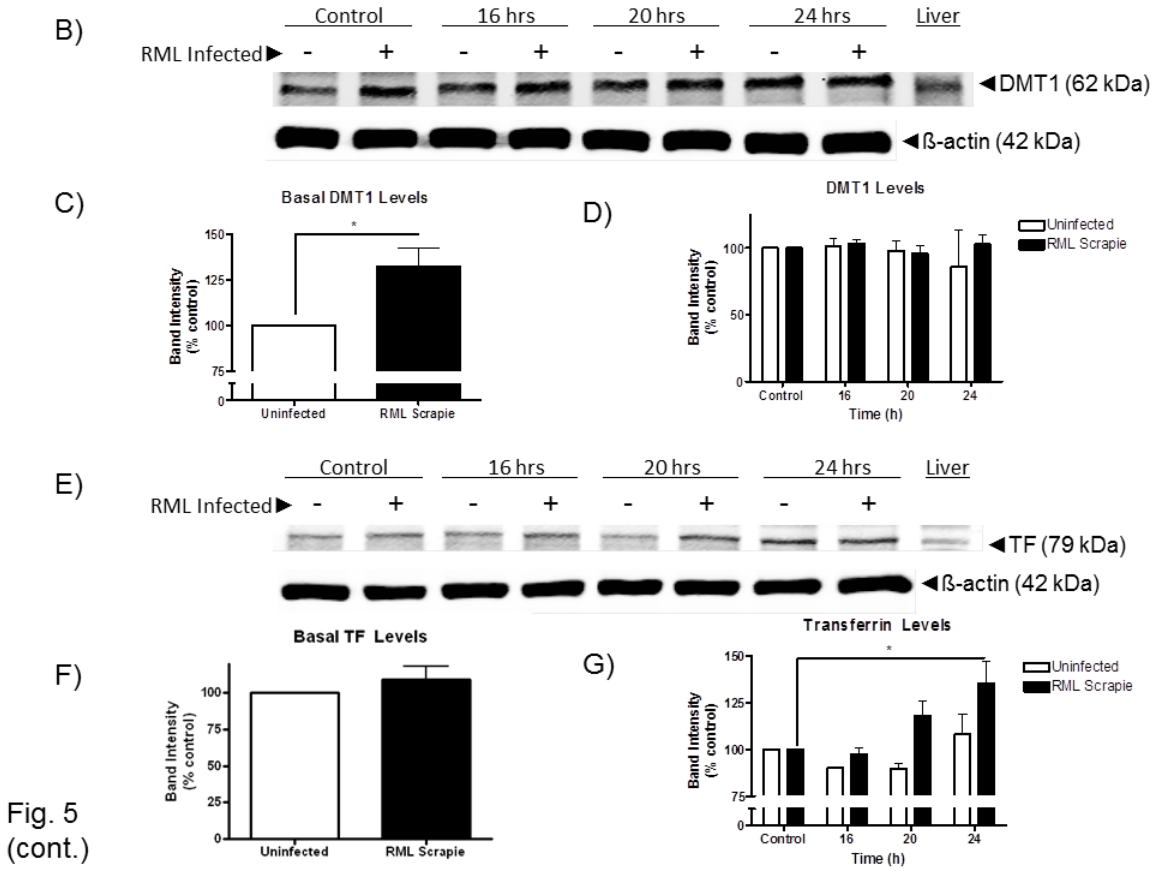


Fig. 5 (cont.)

**Fig. 5.** Mn-induced increases in intracellular Mn levels are reduced while the levels of metal uptake proteins are increased in RML-infected CAD5 cells. **A)** Uninfected and RML scrapie-infected CAD5 cells were treated with 300 μM Mn for 16 h and intracellular Mn levels were determined by ICP-MS. Basal levels of Mn in uninfected and infected CAD5 cells were not significantly different; however, a 187-fold increase was observed in uninfected CAD5 cells while RML infected cells saw a 130-fold increase. This difference was significantly different with $p<0.01$. **B-G)** The level of divalent metal regulator proteins, DMT1 and TF were determined by immunoblot. The basal level of DMT1 **(C)** was significantly increased in

RML scrapie-infected cells ($p<0.01$), while the basal level of TF **(E)** was unchanged between uninfected and infected cells. After 16, 20, and 24 h of treatment with 300 μM Mn, the level of TF was increased in a time-dependent manner in RML scrapie-infected cells ($p<0.01$) **(G)**. **D)** The level of DMT1 was not significantly increased with Mn treatment. These data represent a mean ± S.E.M. from quantification of three individual experiments.

# CHAPTER 3: MANGANESE ALTERS CELLULAR DISTRIBUTION OF PRION PROTEIN AND EXPRESSION OF MAHOGUNIN IN CELL AND ANIMAL MODELS OF TRANSMISSIBLE SPONGIFORM ENCEPHALOPATHY

A manuscript to be communicated to the journal Prion

Dustin Martin[1], Vellareddy Anantharam[1], Colleen Jeffrey[1], Arthi Kanthasamy[1] and Anumantha G. Kanthasamy*[1]

1Department of Biomedical Sciences, Iowa Center for Advanced Neurotoxicity, Iowa State University, Ames, IA 50011

*Corresponding Author

## Abstract

Despite considerable advances in our understanding of neurodegenerative processes associated with prion diseases in the last few decades, the cellular mechanisms responsible for the pathology of this devastating disease remain unknown. Impairment of the protein quality control systems and metal dyshomeostasis have been implicated in the pathogenesis of various proteinaceous neurodegenerative disorders. The loss of function of the

E3 ubiquitin ligase, Mahogunin RING finger 1 (Mgrn1), in knockout animals results in degenerative spongiform pathology within the CNS in the absence of pathogenically misfolded prion protein ($PrP^{Sc}$), indicating that impairment of Mgrn1 function may be a key determinant of spongiform degeneration observed in transmissible spongiform encephalopathy (TSE). Additionally, it has been determined that non-pathogenic prion protein ($PrP^{C}$) ectopically exposed to the cytosol is able to allosterically inhibit Mgrn1 E3 ubiquitin ligase function. However, the mechanism by which $PrP^{C}$, a glycophosphotidyl inositol-anchored membrane protein, would interact with cytosolically localized Mgrn1 during the course of TSE is unknown. In the present study, we report that $MnCl_2$ exposure of 200-300 μM results in increased total cytosolic PrP levels in the CAD5 cell culture model of murine RML scrapie. Additionally, the cellular distribution of $PrP^{C}$ is altered in the motor cortex of mice exposed to 10 mg/kg $MnCl_2$ by oral gavage for 10 days. Finally, we report that RML scrapie infection alters expression of Mgrn1 in response to $MnCl_2$ treatment independent of transcription in CAD5 cells. Since increased Mn has been observed in the brain and blood of humans and animals as a result of TSE infection, these findings provide a mechanism that integrates metal dyshomeostasis, inhibition of the ubiquitin proteasome system, and spongiform neurodegeneration.

## Introduction

Studies have demonstrated that prion protein undergoes a conversion from endogenous membrane-bound protein ($PrP^{C}$) to a misfolded transmissible neurodegenerative pathogen through changes to its secondary and tertiary structure by an as yet unidentified process (Prusiner, 1982). Misfolded prion protein ($PrP^{Sc}$) has been identified as the causative agent in transmissible spongiform encephalopathy (TSE), yet the various forms of this disease do not share a common etiology or pathology (Belay and Schonberger, 2005).

In most cases of TSE, upon conversion from the normal cellular isoform of prion protein ($PrP^{C}$) to $PrP^{Sc}$, the protein gains resistance to denaturation and proteolysis and forms aggregates (Prusiner et al., 1983; Prusiner, 1985 ). In some cases of TSE, amyloid plaques composed of $PrP^{Sc}$ accumulate in infected brain tissue (Bockman et al., 1985; Brown and Gajdusek, 1991; Prusiner et al., 1983; Prusiner, 1985). Although the etiology and pathogenesis of the various neurodegenerative disorders differ, one of the pathological similarities shared between all proteinacious neurological diseases is the accumulation of insoluble protein aggregates in intra- or extracellular inclusion bodies (Tai and Schuman, 2008). These inclusions are largely formed by a single protein constituent that is associated with the distinct pathology of the underlying disease state (Taylor et al., 2002). Disease-associated inclusions are often immunoreactive for ubiquitin, indicating that while the proteins constituents are ubiquitinated, they are not

degraded by the UPS (Ardley and Robinson, 2004; Kang et al., 2004; Sarge and Park-Sarge, 2011). Intracellular protein aggregations have been shown to greatly inhibit the UPS, providing a feedback loop that may exacerbate UPS dysfunction during disease pathogenesis (Bence et al., 2001; Bennett et al., 2005; Holmberg et al., 2004). The E3 ubiquitin ligase mahogunin RING-finger 1 (Mgrn1) has emerged as a molecule of marked importance with regard to TSE since Mgrn1 knockout mice display progressive spongiform degeneration in the absence of $PrP^{Sc}$ accumulation (He et al., 2003). Further studies on the role of Mgrn1 in spongiform degeneration discovered that prion protein exposed to the cytosol allosterically inhibits Mgrn1 E3 ubiquitin ligase function and that this interaction may cause the spongiform degeneration indicative of TSE (Chakrabarti and Hegde, 2009).

Although $PrP^{C}$ is highly expressed throughout the CNS, its endogenous function remains unknown. Evidence indicates that $PrP^{C}$ may function as an antioxidant, a cellular adhesion molecule, a signal transducer, or a metal binding protein (Brown, 2004; Chen et al., 2003; Chiarini et al., 2002; Mange et al., 2002; Sakudo et al., 2004). While the function of the $PrP^{C}$ is not well defined, the metal binding capacity of the protein has been well documented, and is believed to be required for its normal function (Brown and Sassoon, 2002; Brown, 2004; Brown, 2009). Although it is well known that elemental metals are required for normal functioning of cells, significant imbalances in major transition metals such as iron (Fe), copper (Cu), and zinc (Zn) are implicated in neurodegenerative conditions

such as Parkinson's disease (PD), Alzheimer's disease (AD), amyotrophic lateral sclerosis (ALS) and Huntington disease (HD) (Bishop et al., 2002; Bossy-Wetzel et al., 2004; Brown, 2009; Bush and Curtain, 2008; Cahill et al., 2009; Gaeta and Hider, 2005; Molina-Holgado et al., 2007; Sayre et al., 1999). Recent discoveries have indicated that the pathogenic proteins involved in PD, AD, ALS, and HD may have the capacity to transmit the associated disease in a prion-like manner (Braak and Del Tredici, 2011; Desplats et al., 2009; Munch et al., 2011; Ren et al., 2009). Manganese (Mn) is an essential trace elemental metal that is required by organisms for normal functioning; however, continued exposure to high concentrations of Mn results in adverse neurological deficits (Aschner, 1999; Dobson et al., 2004; Levy and Nassetta, 2003; Pfeifer et al., 2004). Several lines of evidence suggest that exposure to Mn or Mn-containing compounds induces a variety of cellular changes including mitochondrial dysfunction, increased oxidative stress, glutathione depletion, loss of dopaminergic neurons, impairment of energy metabolism and antioxidant systems, and alterations in various cell signaling pathways (Erikson and Aschner, 2003; Kitazawa et al., 2002; Roth and Garrick, 2003). Prolonged exposure to high levels of Mn results in an irreversible Parkinson-like condition called manganism (Beuter et al., 1994; Gibbs et al., 1999; Myers et al., 2003).

Elevated Mn levels have been observed in both the brain and blood of animals and humans infected with TSE (Hesketh et al., 2007; Hesketh et al., 2008; Thackray et al., 2002; Wong et al., 2001). Additionally, $PrP^{Sc}$ bound to Mn

has been isolated from both humans and animals (Thackray et al., 2002; Wong et al., 2001). Our group recently discovered that $PrP^C$ interacts with Mn to alter the metal toxicity, and that Mn exposure increases $PrP^C$ levels independent of transcription (Choi et al., 2007; Choi et al., 2010; Martin et al., 2011). Despite these findings, the role of Mn in the pathogenesis of TSE is currently unknown. Studies using recombinant prion protein have shown that, despite an apparent lower affinity, Mn can displace Cu and bind to the protein (Brazier et al., 2008; Zhu et al., 2008). Recombinant $PrP^C$ refolded in the presence of Mn was originally thought to bind up to four molecules of Mn at the octapeptide repeat domain, similar to Cu (Brown et al., 2000). However, isothermal titration calorimetry experiments demonstrated that $PrP^C$ binds one molecule of Mn at each of two sites (Brazier et al., 2008). The binding of Mn to $PrP^C$ was irreversible, as was the oxidation of Mn bound to $PrP^C$; however, the biological consequence of Mn replacing Cu in $PrP^C$ or $PrP^{Sc}$ is still unknown. Studies using circular dichroism and Raman optical activity indicate that upon $PrP^C$ binding to Mn, the secondary structure becomes more organized, gaining greater α-helix and β-sheet content than Cu-bound $PrP^C$ (Brazier et al., 2008; Zhu et al., 2008). Limited proteolytic digestion experiments using proteinase K have shown Mn-bound $PrP^C$ gains partial protease resistance, similar to but less profound than the diagnostic proteolytic resistance characteristic of $PrP^{Sc}$ (Brown et al., 2000; Kim et al., 2005). Once bound to Mn, $PrP^C$ can also seed polymerization of soluble oligomers of metal free $PrP^C$ (Abdelraheim et al., 2006; Giese et al.,

2004). Despite the fact that Mn homeostasis is disrupted during TSE and binding of Mn to $PrP^{C}$ induces $PrP^{Sc}$-like biochemical changes within the protein, the role of metals in the disease has yet to be established.

**Materials and methods**

Absolutely RNA Miniprep Kit (Stratagene, La Jolla, CA), RT2 First Strand kit (SABiosciences, Frederick, MD), Absolutely RNA Miniprep Kit (Stratagene, La Jolla, CA), qPCR primer assay specific for murine Prkcd (SABiosciences, Frederick, MD), using a qPCR primer assay specific for murine Mgrn1 (SABiosciences, Frederick, MD),

Cell culture model of prion disease

The CAD-2A2D5 subclone of uninfected and RML scrapie-infected Cath.a-differentiated cells (CAD5) were a generous gift from Dr. Charles Weissmann of the Scripps Institute (Jupiter, FL). The isolation and characterization of CAD5 prion-infected cell culture model has been previously described (Mahal et al., 2007). Uninfected and RML scrapie-infected CAD5 cells were grown under identical conditions in Opti-MEM media supplemented with 50 units penicillin, 50 µg/ml streptomycin, and 10% qualified fetal bovine serum. The propagation of RML scrapie infection was confirmed over five subsequent

passages. Cells were maintained at 37ºC in a humidified atmosphere of 5% $CO_2$.

SDS-PAGE and Western blot

Western blot analysis was carried out as previously described (Anantharam et al., 2002; Kitazawa et al., 2005; Latchoumycandane et al., 2005). Briefly, cells were collected by scraping with a rubber policeman after treatment. Protein concentrations were determined by Bradford assay and equal protein amounts were then separated by SDS-PAGE using a 15% polyacrylamide gel. Samples were then transferred overnight onto nitrocellulose membrane. Membranes were blocked for 1 h in blocking buffer, and then treated with SAF32 anti-PrP monoclonal antibody overnight at 4ºC. Co-treatment with rabbit anti-ß-actin antibody in blocking buffer was done to ensure equal protein loading. After washing, membranes were then treated with anti-mouse and anti-rabbit fluorescent secondary antibodies in blocking buffer for 1 h at room temperature. Visualization was done using an Odyssey scanner (Licor, Lincoln, NE). Band quantification was done using ImageJ software (U.S. National Institutes of Health, Bethesda, MD).

Cytosolic and membrane rich fractionation

Cytosolic and membrane fractions were separated by first allowing the

cells to swell by incubation on ice in hypotonic homogenization buffer (20mM Tris-HCl, 10mM EGTA, 2mM EDTA, 2mM DTT, with protease and phosphatase inhibitor cocktail). Cells were then lysed by shearing the cell membranes by passage through progressively smaller gauge needles. Sheared lysates were then subjected to ultracentrifugation at 100,000 x g for 30 mins to pellet the membrane fraction while the cytosolic fraction remained in the supernatant. The membrane pellet was rehomogenized by addition of 0.5% Triton X-100 and 0.5% sodium deoxycholate and sonication in a cup horn sonicator.

Immunohistochemistry

Mice were treated with 10 mg/kg of Mn in ddH2O by oral gavage for 10 days. At the conclusion of the treatment, mice were perfused with 4% PFA and frozen sections were cut using a cryostat. Coronal sections corresponding to the location of the motor cortex and caudate putamen were then treated with SAF32 anti-PrP antibody (red), anti-Mgrn1 antibody (green) and Hoescht to stain nuclei (blue). Pictures were taken with a Nikon inverted fluorescence microscope (model TE-2000U; Nikon, Tokyo, Japan); images were captured with a SPOT digital camera (Diagnostic Instruments, Sterling Heights, MI).

Quantative real time polymerase chain reaction (qRT-PCR)

Total RNA was isolated from uninfected and scrapie-infected CAD5 cells treated with 300 μM $MnCl_2$ for 20 h using an Absolutely RNA Miniprep Kit. Reverse transcription into first strand complimentary DNA was done using a RT2 First Strand kit. Total RNA was isolated from Mn-treated mice using an Absolutely RNA Miniprep Kit. Reverse transcription into first strand complimentary DNA was done using a RT2 First Strand kit. Quantitative PCR was done with a MX3000P RT-PCR thermocycler (Stratagene, La Jolla, CA) using a qPCR primer assay specific for murine Prkcd. Amplification was performed over 40 cycles and quantified as fold increase calculated by 2^ΔΔCt (ΔΔCt = ΔCt (Mn) - ΔCt (Con) ) as recommended by the manufacturer. 18S RNA was used as a loading control to ensure equal RNA levels per well. Quantitative PCR was done with a MX3000P RT-PCR thermocycler (Stratagene, La Jolla, CA) using a qPCR primer assay specific for murine Mgrn1. Amplification was performed over 40 cycles and quantified as fold increase calculated by 2^-ΔΔCt (ΔΔCt = ΔCt (Mn) - ΔCt (Con) ) as recommended by the manufacturer. 18S RNA was used as a loading control to ensure equal RNA levels per well.

Data Analysis

Statistical analysis was performed with Prism 4.0 software (GraphPad Software, San Diego, CA). Statistical significance among treatments was determined by one-way ANOVA analysis with Tukey's multiple comparison

testing and is indicated by asterisks with @p<0.1, *p<0.05, **p<0.01, and ***p<0.001. Analyses between two data sets were done using Student's t-test. Data typically represent three separate experiments and are expressed as mean ± S.E.M.

**Results**

Mn treatment induces increased cytosolic PrP in a cell culture model of prion disease

Our group has reported that Mn treatment induces increased cytosolic levels of $PrP^C$ in in vitro neuronal cell culture (Choi et al., 2010). In the same study we showed that Mn treatment increased $PrP^C$ levels in CAD5 cells infected with mouse adapted scrapie. In order to determine the consequence of Mn treatment on the localization of $PrP^C$ in the CAD5 cell culture model of TSE, we did subcellular separation of the cytosolic and membrane fractions of Mn-treated uninfected and scrapie-infected CAD5 cells. Cells were treated with 300 μM $MnCl_2$ in Opti-MEM for 16, 20, and 24 h. After treatment, cytosolic and membrane fractions were separated and both fractions were analyzed by immunobot analysis using SAF32 anti-PrP antibodies to determine if $PrP^C$ was present in the cytosol. The protein level loaded for the cytosolic fraction was twice that of the membrane fraction. As seen in Figure 1, the level of $PrP^C$ is

increased in the membrane and cytosolic fractions of both uninfected and RML scrapie-infected cells up to 24 h. The levels of $PrP^{Sc}$ may be likewise increased in RML scrapie-infected cells, but the anti-PrP antibody used does not discriminate between isoforms.

Densitometric analysis of the cytosolic $PrP^{C}$ band in Fig. 1A revealed that Mn-exposure induced a statistically significant increase in $PrP^{C}$ levels in both uninfected and RML-infected CAD5 cells. The $PrP^{C}$ levels increased in a time-dependent manner up to 20 h and then decreased marginally at 24 h; therefore, the 20 h time point was used for subsequent experiments. Further, the extent of the increase in $PrP^{C}$ levels in Mn-treated uninfected cells was significantly higher compared to Mn-treated RML-infected cells.

Subcellular localization of prion protein in Mn-treated CAD5 cells

In order to visualize the localization of $PrP^{C}$ in the cytosol, immunocytochemical analysis was done on Mn treated uninfected and scrapie-infected CAD5 cells. Cells were treated with 300 μM $MnCl_2$ for 20 h in Opti-MEM and then fixed with 4% paraformaldehyde. Cells were then treated with SAF32 anti-PrP, and anti-Mgrn1 primary antibodies. Imaging was done on an Olympus FV1000 confocal microscope (Olympus America Inc., Center Valley, PA). As seen in Figure 2, $PrP^{C}$ aggregates within the cytosol of cells that express Mgrn1 after Mn treatment in both uninfected (Fig. 2A) and RML scrapie-infected (Fig.

2B) CAD5 cells. In infected cells, $PrP^{C}$ or $PrP^{Sc}$ within the cytosol appears to colocalize with Mgrn1 (white arrowheads). The low level of cytosolic $PrP^{C}$ that can be seen adjacent to the nucleus in control untreated CAD5 cells most likely represents newly synthesized $PrP^{C}$ undergoing processing within the endoplasmic reticulum and Golgi apparatus en route to the plasma membrane.

Mn treatment induces increased cytosolic $PrP^{C}$ and colocalization with Mgrn1 in an animal model of Mn toxicity

$PrP^{C}$ is normally attached to the exterior of the plasma membrane by a GPI anchor and is associated with lipid rafts (Baron et al., 2002; Stahl et al., 1987). Interestingly, a small number of neuronal cells were found in the hippocampus, neocortex, and thalamus that have strong staining for $PrP^{C}$ in the cytosol (Mironov et al., 2003). In that study, the cells did not show markers of necrosis or apoptosis, and the GPI anchor machinery functioned normally. To examine the consequence of Mn treatment on $PrP^{C}$ levels in an in vivo mouse model system,

we found a large amount of cells staining positively for $PrP^{C}$ within the cell body in the motor cortex (Figure 3) and to a lesser extent in the lateral septal nucleus (not shown) when compared to control. Both of these brain regions undergo marked neuronal loss and spongiform vacuolation during the course of

experimental scrapie in mice, indicating that increased cytosolic $PrP^{C}$ or $PrP^{Sc}$ levels may play a role in neuronal loss associated with TSE (Fraser and Dickinson, 1968; Fraser and Dickinson, 1973; Jesionek-Kupnicka et al., 1999; Jesionek-Kupnicka et al., 2001).

mice were treated with 10 mg/kg of Mn in ddH2O by oral gavage once daily for 10 days. At the conclusion of the treatment, mice were perfused with 4% PFA and frozen sections were cut using a CM1800 cryostat (Leica Biosystems, Nussloch, Germany). Coronal sections corresponding to the location of the motor cortex were labeled with SAF32 anti-PrP antibody (red), anti-Mgrn1 antibody (green) and/or Hoescht nuclear stain (blue). Figure 3 shows $PrP^{C}$ localization (red) in the motor cortex of vehicle control and Mn-treated mice at 15X magnification. Inset composite images at 90X magnification illustrate cellular redistribution of $PrP^{C}$ within the cell body as a result of Mn treatment (inset, white arrowheads). In terms of brain regions, we found a large amount of cells staining positively for $PrP^{C}$ within the motor cortex (Figure 3) and to a lesser extent in the lateral septal nucleus (not shown) when compared to vehicle control. Figure 4 includes co-labeling of $PrP^{C}$ and Mgrn1 within the motor cortex. Colocalization of Mgrn1 (green) and $PrP^{C}$ (red) can be seen in the cytosolic region of multiple cells in Mn-treated animals, but not in those treated with just vehicle (white arrowheads). Similar to untreated CAD5 cells, vehicle control animals have low levels of $PrP^{C}$ staining within the cell body that may correspond to newly

expressed $PrP^C$ undergoing processing in the endoplasmic reticulum and Golgi apparatus for eventual localization in the cell membrane.

Infectious prion protein alters Mgrn1 response to Mn treatment

Although the inhibition of Mgrn1 function by cytosolic $PrP^C$ has been established (Chakrabarti and Hegde, 2009), the contribution of Mgrn1 to TSE-related spongiform degeneration has not. In order to evaluate the effect Mn treatment has on the expression of Mgrn1 in a cell culture model of prion disease, we did immunoblot analysis on uninfected and RML scrapie infected CAD5 cells treated with 300 μM $MnCl_2$ in Opti-MEM for 16, 20, and 24 h (Figure 5A). Densitometric analysis of the Mgrn1 band in Fig 5A revealed that in uninfected cells, Mn treatment induced a time dependent increase in the expression of Mgrn1, whereas Mgrn1 levels in scrapie-infected cells did not increase with Mn treatment at any time point (Figure 5B).

Transcriptional regulation of Mgrn1 is altered in Mn treated CAD5 cells

We have previously shown that although $PrP^C$ is increased in Mn-treated cells, the increase is not due to transcriptional upregulation (Choi et al., 2010). In order to confirm these results in a cell culture model of prion disease, we evaluated the level of $PrP^C$ mRNA in CAD5 cells treated with 300 μM $MnCl_2$ for

20 h by quantitative real time polymerase chain reaction (qRT-PCR). Although an increase in Mgrn1 protein level is apparent in uninfected cells, there is no corresponding increase in mRNA (Figure 6). Conversely, while there is no increase in Mgrn1 protein level in infected cells, there is a twofold increase in Mgrn1 mRNA. These results indicate that the increase in Mgrn1 levels in in uninfected cells in response to Mn treatment are not due to transcriptional changes, and Mgrn1 levels do not increase in RML scrapie infected cells despite an upregulation of Mgrn1 mRNA.

**Discussion**

Inhibition of protein quality control systems, protein aggregation, and metal dyshomeostasis have all been observed in various models of a variety of neurodegenerative diseases, yet how these processes interact during disease pathogenesis is not well understood (Lee et al., 2011; Tyedmers et al., 2010). Increases in the level of Mn in the brain and blood of both humans and animals infected with TSE have led to the speculation that Mn may play a role in TSE pathogenesis (Hesketh et al., 2007; Hesketh et al., 2008; Thackray et al., 2002; Wong et al., 2001). In the present study we have found Mn exposure induces an increase in cytosolic PrP in a cell culture model of TSE and an animal model of Mn toxicity. An increase in cytosolic $PrP^C$ would act to attenuate Mgrn1 function since the N-terminus of $PrP^C$ has been shown to bind to Mgrn1 and allosterically

inhibit E3 ubiquitin ligase activity, and may contribute to spongiform neurodegeneration (Chakrabarti and Hegde, 2009; He et al., 2003). However, a recent study found that neither overexpression nor knockout of Mgrn1 altered the progression of mouse adapted scrapie indicating that Mgrn1 (Silvius et al., 2013). Truncation studies identified the octapeptide repeat domain as the interaction site of $PrP^C$ and Mgrn1 (Chakrabarti and Hegde, 2009). The N-terminal octapeptide repeat sequences of $PrP^C$ (PHGGG/SWGQ) bind divalent metals such as copper, manganese, and zinc, with the highest affinity being for copper (Hornshaw et al., 1995; Viles et al., 1999). Point mutations, deletions, or duplications of the octapeptide repeats in the prion protein gene have been linked to inherited TSE in humans and animals (Krasemann et al., 1995; Mead et al., 2007; Palmer and Collinge, 1993; Yin et al., 2007). Cu bound by octapeptide repeat domain of $PrP^C$ is able to undergo reversible redox chemistry allowing for antioxidant-like activity (Brown et al., 1999; Brown et al., 2001; Gaggelli et al., 2008; Nadal et al., 2007; Treiber et al., 2007). An additional higher affinity metal binding site has been identified at His 95 and 110 (mouse numbering) (Jackson et al., 2001; Jones et al., 2004). This region was named the “5th site” since the octapeptide repeat domain accounts for only four of the five Cu molecules bound by $PrP^C$ (Brazier et al., 2008; Treiber et al., 2007). Interestingly, mutation of the histidine residues in this region to isoleucine induces a pathogenic transmembrane form of prion protein that has been shown to interact with Mgrn1 (Chakrabarti and Hegde, 2009). Further studies are required to elucidate the role

each metal binding site has in the pathogenesis of TSE.

The affinity of $PrP^C$ for metals is highly dependent upon pH, suggesting a mechanism by which $PrP^C$ can alter the homeostasis of divalent metals in the cell by endocytosis from the cell surface to early endocytotic vesicles with low pH where the metal is released, then cycling back to the cell surface (Brown and Harris, 2003; Burns et al., 2002). Studies have shown both Cu and Zn exposure can induce internalization of $PrP^C$ by endocytosis and that this metal induced endocytosis is dependent upon the presence of the octapeptide repeats (Pauly and Harris, 1998; Perera and Hooper, 2001). Internalized $PrP^C$ is either cycled back to the plasma membrane or rapidly degraded by the ubiquitin proteasomal (UPS) or lysosomal systems (Ciechanover and Brundin, 2003; Kang et al., 2004; Laszlo et al., 1992). These prior studies indicated that Mn did not have the same internalizing effect as Cu and Zn. However, our group recently reported that Mn treatment increases $PrP^C$ levels in neuronal cells independent of transcription (Choi et al., 2010). Furthermore, we found Mn treatment significantly altered the stability of $PrP^C$, suggesting that Mn directly interacts with $PrP^C$.

Although we have established that scrapie infection alone does not change the expression level of Mgrn1 in a cell culture model of TSE, we have discovered that uninfected cells have a time dependent increase in Mgrn1 in response to Mn treatment while cells infected with scrapie do not. The lack of transcriptional upregulation coincident with the increase in Mgrn1 protein levels indicates that Mn increases the protein stability or impairs degradation of the

protein; however, mRNA levels may be altered at earlier time points and a broader mechanistic study is warranted. The fact that the presence of $PrP^{Sc}$ abrogates the increase in Mrgn1 protein levels, despite an apparent upregulation in the message, may indicate a multilevel inhibition of Mgrn1 function through modulation of its expression as well as direct allosteric inhibition in response to Mn toxicity. Since Mn is increased during the course of TSE, our results indicate that metal dyshomeostasis and impairment of protein degradation are interconnected mechanisms in spongiform disease.

**References**

Abdelraheim, S.R., Kralovicova, S., Brown, D.R., 2006. Hydrogen peroxide cleavage of the prion protein generates a fragment able to initiate polymerisation of full length prion protein. Int J Biochem Cell Biol. 38, 1429-40.

Anantharam, V., et al., 2002. Caspase-3-dependent proteolytic cleavage of protein kinase Cdelta is essential for oxidative stress-mediated dopaminergic cell death after exposure to methylcyclopentadienyl manganese tricarbonyl. J Neurosci. 22, 1738-51.

Ardley, H.C., Robinson, P.A., 2004. The role of ubiquitin-protein ligases in neurodegenerative disease. Neurodegener Dis. 1, 71-87.

Aschner, M., 1999. Manganese homeostasis in the CNS. Environ Res. 80, 105-9.

Baron, G.S., et al., 2002. Conversion of raft associated prion protein to the protease-resistant state requires insertion of PrP-res (PrP(Sc)) into contiguous membranes. Embo J. 21, 1031-40.

Belay, E.D., Schonberger, L.B., 2005. The public health impact of prion diseases. Annu Rev Public Health. 26, 191-212.

Bence, N.F., Sampat, R.M., Kopito, R.R., 2001. Impairment of the ubiquitin-proteasome system by protein aggregation. Science. 292, 1552-5.

Bennett, E.J., et al., 2005. Global impairment of the ubiquitin-proteasome system by nuclear or cytoplasmic protein aggregates precedes inclusion body formation. Mol Cell. 17, 351-65.

Beuter, A., et al., 1994. Diadochokinesimetry: a study of patients with Parkinson's disease and manganese exposed workers. Neurotoxicology. 15, 655-64.

Bishop, G.M., et al., 2002. Iron: a pathological mediator of Alzheimer disease? Dev Neurosci. 24, 184-7.

Bockman, J.M., et al., 1985. Creutzfeldt-Jakob disease prion proteins in human brains. N Engl J Med. 312, 73-8.

Bossy-Wetzel, E., Schwarzenbacher, R., Lipton, S.A., 2004. Molecular pathways to neurodegeneration. Nat Med. 10 Suppl, S2-9.

Braak, H., Del Tredici, K., 2011. Alzheimer's pathogenesis: is there neuron-to-neuron propagation? Acta Neuropathol. 121, 589-95.

Brazier, M.W., et al., 2008. Manganese binding to the prion protein. J Biol Chem. 283, 12831-9.

Brown, D.R., et al., 1999. Normal prion protein has an activity like that of superoxide dismutase. Biochem J. 344 Pt 1, 1-5.

Brown, D.R., et al., 2000. Consequences of manganese replacement of copper for prion protein function and proteinase resistance. Embo J. 19, 1180-6.

Brown, D.R., Clive, C., Haswell, S.J., 2001. Antioxidant activity related to copper binding of native prion protein. J Neurochem. 76, 69-76.

Brown, D.R., Sassoon, J., 2002. Copper-dependent functions for the prion protein. Mol Biotechnol. 22, 165-78.

Brown, D.R., 2004. Metallic prions. Biochem Soc Symp. 193-202.

Brown, D.R., 2009. Brain proteins that mind metals: a neurodegenerative perspective. Dalton Trans. 4069-76.

Brown, L.R., Harris, D.A., 2003. Copper and zinc cause delivery of the prion protein from the plasma membrane to a subset of early endosomes and the Golgi. J Neurochem. 87, 353-63.

Brown, P., Gajdusek, D.C., 1991. The human spongiform encephalopathies: kuru, Creutzfeldt-Jakob disease, and the Gerstmann-Straussler-Scheinker syndrome. Curr Top Microbiol Immunol. 172, 1-20.

Burns, C.S., et al., 2002. Molecular features of the copper binding sites in the octarepeat domain of the prion protein. Biochemistry. 41, 3991-4001.

Bush, A.I., Curtain, C.C., 2008. Twenty years of metallo-neurobiology: where to now? Eur Biophys J. 37, 241-5.

Cahill, C.M., et al., 2009. Amyloid precursor protein and alpha synuclein translation, implications for iron and inflammation in neurodegenerative diseases. Biochim Biophys Acta. 1790, 615-28.

Chakrabarti, O., Hegde, R.S., 2009. Functional depletion of mahogunin by cytosolically exposed prion protein contributes to neurodegeneration. Cell. 137, 1136-47.

Chen, S., et al., 2003. Prion protein as trans-interacting partner for neurons is involved in neurite outgrowth and neuronal survival. Mol Cell Neurosci. 22, 227-33.

Chiarini, L.B., et al., 2002. Cellular prion protein transduces neuroprotective signals. Embo J. 21, 3317-26.

Choi, C.J., et al., 2007. Normal Cellular Prion Protein Protects against Manganese-Induced Oxidative Stress and Apoptotic Cell Death. Toxicol Sci. 98, 495-509.

Choi, C.J., et al., 2010. Manganese upregulates cellular prion protein and contributes to altered stabilization and proteolysis: relevance to role of metals in pathogenesis of prion disease. Toxicol Sci. 115, 535-46.

Ciechanover, A., Brundin, P., 2003. The ubiquitin proteasome system in neurodegenerative diseases: sometimes the chicken, sometimes the egg. Neuron. 40, 427-46.

Desplats, P., et al., 2009. Inclusion formation and neuronal cell death through neuron-to-neuron transmission of alpha-synuclein. Proc Natl Acad Sci U S A. 106, 13010-5.

Dobson, A.W., Erikson, K.M., Aschner, M., 2004. Manganese neurotoxicity. Ann N Y Acad Sci. 1012, 115-28.

Erikson, K.M., Aschner, M., 2003. Manganese neurotoxicity and glutamate-GABA interaction. Neurochem Int. 43, 475-80.

Fraser, H., Dickinson, A.G., 1968. The sequential development of the brain lesion of scrapie in three strains of mice. J Comp Pathol. 78, 301-11.

Fraser, H., Dickinson, A.G., 1973. Scrapie in mice. Agent-strain differences in the distribution and intensity of grey matter vacuolation. J Comp Pathol. 83, 29-40.

Gaeta, A., Hider, R.C., 2005. The crucial role of metal ions in neurodegeneration: the basis for a promising therapeutic strategy. Br J Pharmacol. 146, 1041-59.

Gaggelli, E., et al., 2008. Structural characterization of the intra- and inter-repeat copper binding modes within the N-terminal region of "prion related protein" (PrP-rel-2) of zebrafish. J Phys Chem B. 112, 15140-50.

Gibbs, J.P., et al., 1999. Focused medical surveillance: a search for subclinical movement disorders in a cohort of U.S. workers exposed to low levels of manganese dust. Neurotoxicology. 20, 299-313.

Giese, A., et al., 2004. Effect of metal ions on de novo aggregation of full-length prion protein. Biochem Biophys Res Commun. 320, 1240-6.

He, L., et al., 2003. Spongiform degeneration in mahoganoid mutant mice. Science. 299, 710-2.

Hesketh, S., et al., 2007. Elevated manganese levels in blood and central nervous system occur before onset of clinical signs in scrapie and bovine spongiform encephalopathy. J Anim Sci. 85, 1596-609.

Hesketh, S., et al., 2008. Elevated manganese levels in blood and CNS in human prion disease. Mol Cell Neurosci. 37, 590-8.

Holmberg, C.I., et al., 2004. Inefficient degradation of truncated polyglutamine proteins by the proteasome. EMBO J. 23, 4307-18.

Hornshaw, M.P., McDermott, J.R., Candy, J.M., 1995. Copper binding to the N-terminal tandem repeat regions of mammalian and avian prion protein. Biochem Biophys Res Commun. 207, 621-9.

Jackson, G.S., et al., 2001. Location and properties of metal-binding sites on the human prion protein. Proc Natl Acad Sci U S A. 98, 8531-5.

Jesionek-Kupnicka, D., et al., 1999. The ultrastructural study of primary intracranial germ tumors. Folia Neuropathol. 37, 171-4.

Jesionek-Kupnicka, D., et al., 2001. Apoptosis in relation to neuronal loss in experimental Creutzfeldt-Jakob disease in mice. Acta Neurobiol Exp (Wars). 61, 13-9.

Jones, C.E., et al., 2004. Preferential Cu2+ coordination by His96 and His111 induces beta-sheet formation in the unstructured amyloidogenic region of the prion protein. J Biol Chem. 279, 32018-27.

Kang, S.C., et al., 2004. Prion protein is ubiquitinated after developing protease resistance in the brains of scrapie-infected mice. J Pathol. 203, 603-8.

Kim, N.H., et al., 2005. Effect of transition metals (Mn, Cu, Fe) and deoxycholic acid (DA) on the conversion of PrPC to PrPres. Faseb J. 19, 783-5.

Kitazawa, M., et al., 2002. Oxidative stress and mitochondrial-mediated apoptosis in dopaminergic cells exposed to methylcyclopentadienyl manganese tricarbonyl. J Pharmacol Exp Ther. 302, 26-35.

Kitazawa, M., et al., 2005. Activation of protein kinase C delta by proteolytic cleavage contributes to manganese-induced apoptosis in dopaminergic cells: protective role of Bcl-2. Biochem Pharmacol. 69, 133-46.

Krasemann, S., et al., 1995. Prion disease associated with a novel nine octapeptide repeat insertion in the PRNP gene. Brain Res Mol Brain Res. 34, 173-6.

Laszlo, L., et al., 1992. Lysosomes as key organelles in the pathogenesis of prion encephalopathies. J Pathol. 166, 333-41.

Latchoumycandane, C., et al., 2005. Protein kinase Cdelta is a key downstream mediator of manganese-induced apoptosis in dopaminergic neuronal cells. J Pharmacol Exp Ther. 313, 46-55.

Lee, S.J., et al., 2011. Protein aggregate spreading in neurodegenerative diseases: problems and perspectives. Neurosci Res. 70, 339-48.

Levy, B.S., Nassetta, W.J., 2003. Neurologic effects of manganese in humans: a review. Int J Occup Environ Health. 9, 153-63.

Mahal, S.P., et al., 2007. Prion strain discrimination in cell culture: the cell panel assay. Proc Natl Acad Sci U S A. 104, 20908-13.

Mange, A., et al., 2002. PrP-dependent cell adhesion in N2a neuroblastoma cells. FEBS Lett. 514, 159-62.

Martin, D.P., et al., 2011. Infectious prion protein alters manganese transport and neurotoxicity in a cell culture model of prion disease. Neurotoxicology. 32, 554-62.

Mead, S., et al., 2007. Inherited prion disease with 5-OPRI: phenotype modification by repeat length and codon 129. Neurology. 69, 730-8.

Mironov, A., Jr., et al., 2003. Cytosolic prion protein in neurons. J Neurosci. 23, 7183-93.

Molina-Holgado, F., et al., 2007. Metals ions and neurodegeneration. Biometals. 20, 639-54.

Munch, C., O'Brien, J., Bertolotti, A., 2011. Prion-like propagation of mutant superoxide dismutase-1 misfolding in neuronal cells. Proc Natl Acad Sci U S A. 108, 3548-53.

Myers, J.E., et al., 2003. The nervous system effects of occupational exposure on workers in a South African manganese smelter. Neurotoxicology. 24, 885-94.

Nadal, R.C., et al., 2007. Prion protein does not redox-silence Cu2+, but is a sacrificial quencher of hydroxyl radicals. Free Radic Biol Med. 42, 79-89.

Palmer, M.S., Collinge, J., 1993. Mutations and polymorphisms in the prion protein gene. Hum Mutat. 2, 168-73.

Pauly, P.C., Harris, D.A., 1998. Copper stimulates endocytosis of the prion protein. J Biol Chem. 273, 33107-10.

Perera, W.S., Hooper, N.M., 2001. Ablation of the metal ion-induced endocytosis of the prion protein by disease-associated mutation of the octarepeat region. Curr Biol. 11, 519-23.

Pfeifer, G.D., et al., 2004. Health and environmental testing of manganese exhaust products from use of methylcyclopentadienyl manganese tricarbonyl in gasoline. Sci Total Environ. 334-335, 397-408.

Prusiner, S.B., 1982. Novel proteinaceous infectious particles cause scrapie. Science. 216, 136-44.

Prusiner, S.B., et al., 1983. Scrapie prions aggregate to form amyloid-like birefringent rods. Cell. 35, 349-58.

Prusiner, S.B., 1985. Scrapie prions, brain amyloid, and senile dementia. Curr Top Cell Regul. 26, 79-95.

Ren, P.H., et al., 2009. Cytoplasmic penetration and persistent infection of mammalian cells by polyglutamine aggregates. Nat Cell Biol. 11, 219-25.

Roth, J.A., Garrick, M.D., 2003. Iron interactions and other biological reactions mediating the physiological and toxic actions of manganese. Biochem Pharmacol. 66, 1-13.

Sakudo, A., et al., 2004. Prion protein suppresses perturbation of cellular copper homeostasis under oxidative conditions. Biochem Biophys Res Commun. 313, 850-5.

Sarge, K.D., Park-Sarge, O.K., 2011. SUMO and its role in human diseases. Int Rev Cell Mol Biol. 288, 167-83.

Sayre, L.M., Perry, G., Smith, M.A., 1999. Redox metals and neurodegenerative disease. Curr Opin Chem Biol. 3, 220-5.

Silvius, D., et al., 2013. Levels of the Mahogunin Ring Finger 1 E3 ubiquitin ligase do not influence prion disease. PLoS One. 8, e55575.

Stahl, N., et al., 1987. Scrapie prion protein contains a phosphatidylinositol glycolipid. Cell. 51, 229-40.

Tai, H.C., Schuman, E.M., 2008. Ubiquitin, the proteasome and protein degradation in neuronal function and dysfunction. Nat Rev Neurosci. 9, 826-38.

Taylor, J.P., Hardy, J., Fischbeck, K.H., 2002. Toxic proteins in neurodegenerative disease. Science. 296, 1991-5.

Thackray, A.M., et al., 2002. Metal imbalance and compromised antioxidant function are early changes in prion disease. Biochem J. 362, 253-8.

Treiber, C., et al., 2007. Copper is required for prion protein-associated superoxide dismutase-I activity in Pichia pastoris. Febs J. 274, 1304-11.

Tyedmers, J., Mogk, A., Bukau, B., 2010. Cellular strategies for controlling protein aggregation. Nat Rev Mol Cell Biol. 11, 777-88.

Viles, J.H., et al., 1999. Copper binding to the prion protein: structural implications of four identical cooperative binding sites. Proc Natl Acad Sci U S A. 96, 2042-7.

Wong, B.S., et al., 2001. Oxidative impairment in scrapie-infected mice is associated with brain metals perturbations and altered antioxidant activities. J Neurochem. 79, 689-98.

Yin, S., et al., 2007. Human prion proteins with pathogenic mutations share common conformational changes resulting in enhanced binding to glycosaminoglycans. Proc Natl Acad Sci U S A. 104, 7546-51.

Zhu, F., et al., 2008. Raman optical activity and circular dichroism reveal dramatic differences in the influence of divalent copper and manganese ions on prion protein folding. Biochemistry. 47, 2510-7.

## Figures

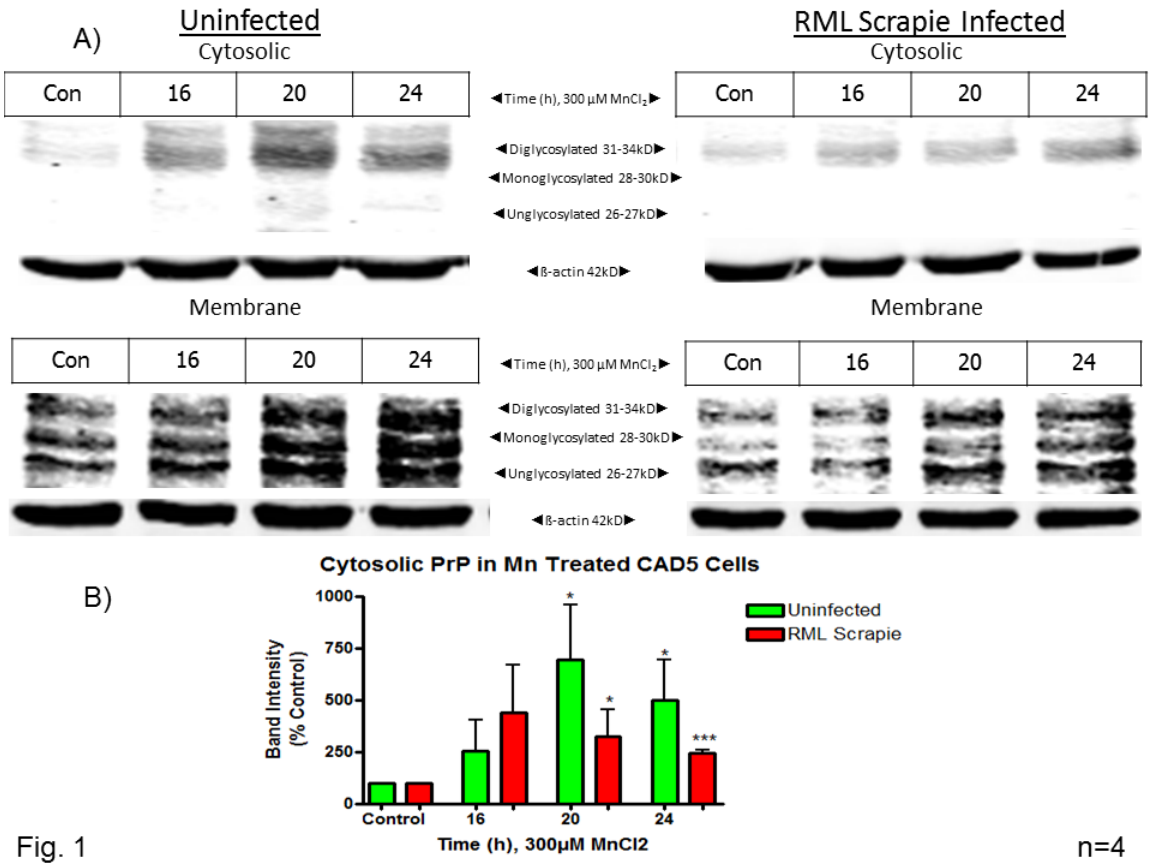


**Figure 1. Manganese induces an increase in cytosolic PrP.** Uninfected and RML scrapie-infected CAD5 cells were treated with 300 µM $MnCl_2$ for 16, 20, and 24 h and subcellular fractionation was done to isolate cytocolic and membrane rich fractions. The level of $PrP^C$ in each fraction was assayed by immunoblot using SAF32 anti-PrP antibody. A) Mn treatment induces an increase in cytosolic and membrane rich fractions in both uninfected and infected CAD5 cells. B) Quantification of cytosolic bands. Levels indicate total PrP since SAF32 does not discriminate between PrP isoforms. Membranes were cotreated with anti-ß-actin antibody to ensure equal protein loading. Asterisks represent * $p<0.05$, ** $p<0.01$,

and *** p<0.001 compared to control untreated cells. Data represent mean percent control untreated cells ± SEM from four individual experiments.

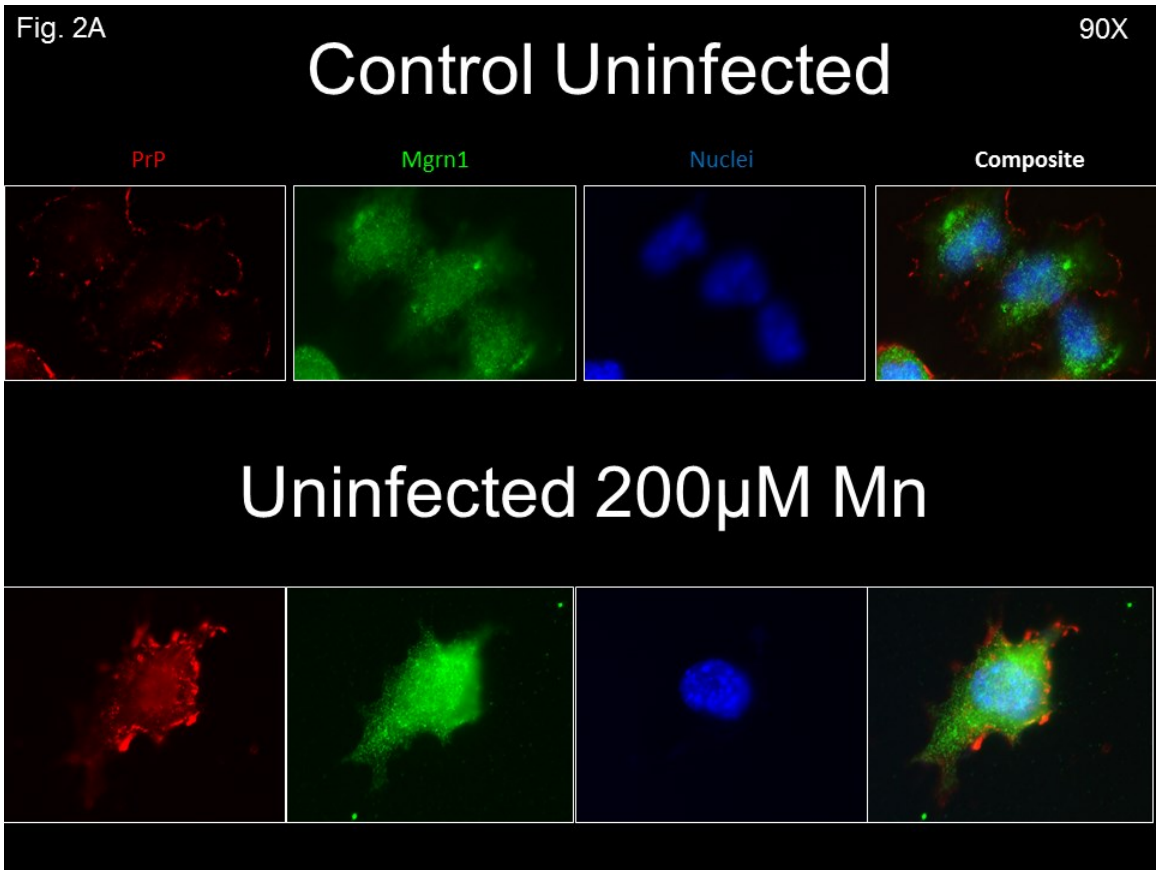

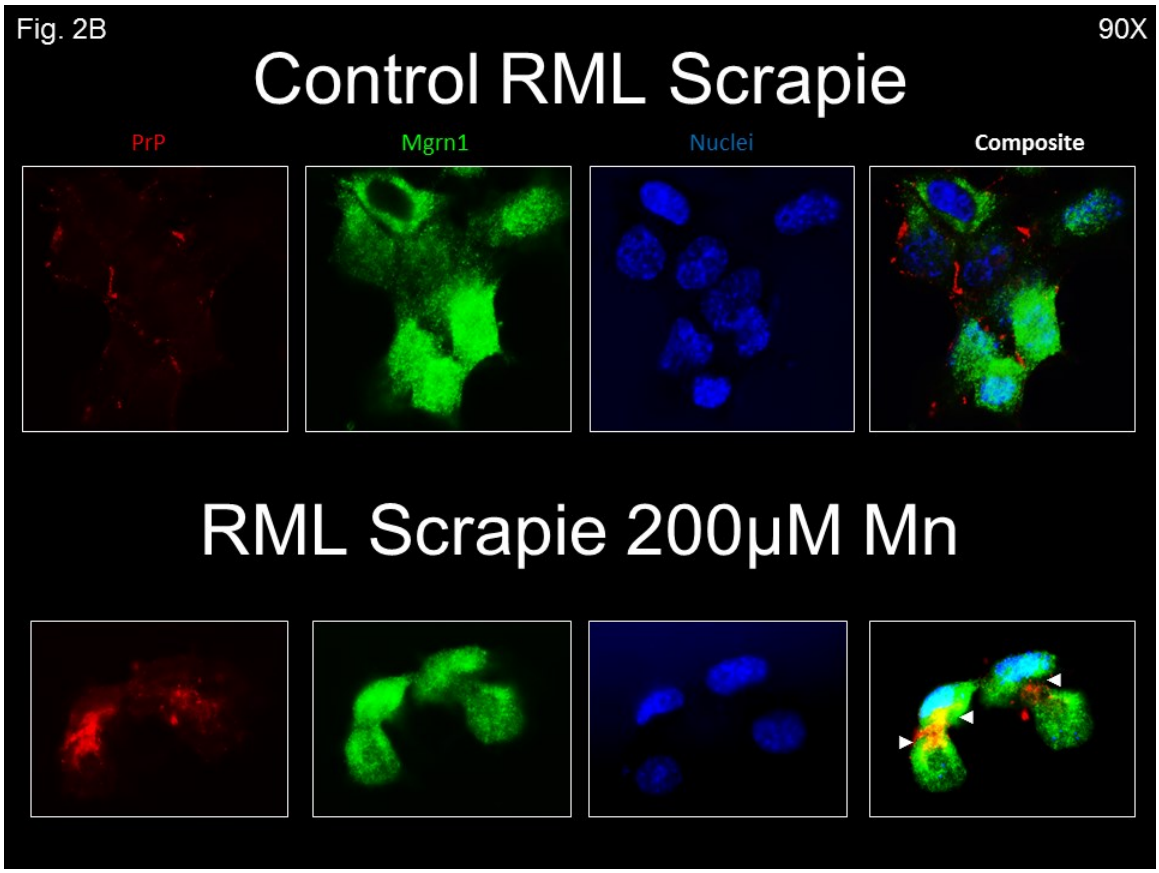


**Figure 2. Cytosolic PrP colocalizes with Mgrn1 in Mn treated CAD5 cells.** Uninfected and RML scrapie-infected CAD5 cells were treated with 200 μM $MnCl_2$ for 24 h and fixed with 4% paraformaldehyde. Cells were immunohistochemically labeled with SAF32 anti-PrP and anti-Mgrn1 antibodies and examined by fluorescent microscopy. A) In untreated uninfected CAD5 cells, $PrP^C$ (red) localizes to the plasma membrane, while Mgrn1 (green) is cytosolically localized. Treatment with Mn induces internal punctate localization of $PrP^C$. B) In untreated RML scrapie-infected CAD5 cells, PrP distribution appears more condensed, but remains at the cell periphery. Mn treatment induces increased internal $PrP^C$ and/or $PrP^{Sc}$ levels that colocalize with Mrgn1

(white arrowheads). Cells were costained with Hoechst nuclear stain to visualize nuclei (blue).

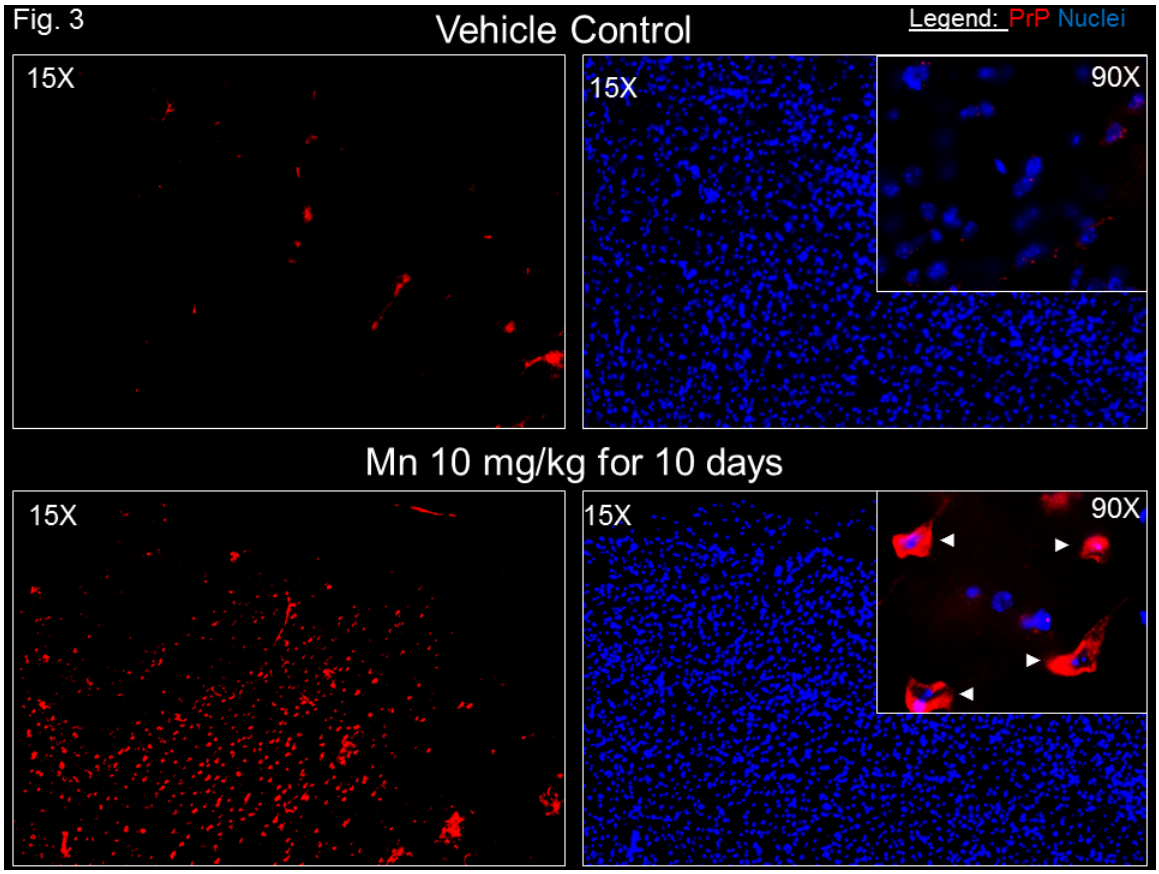


**Figure 3. Mn treatment induces cytosolically localized PrP in C57 mouse motor cortex.** Mice were treated for 10 days with 10 mg/kg of Mn by oral gavage. Control animals were treated with $ddH_2O$ vehicle. Animals were perfused with 4% paraformaldehyde, brains were removed and cut in 30 µm frozen sections with a cryostat, and immunohistochemically labeled with SAF32 anti-PrP antibody. In the motor cortex of Mn treated animals, cells with neuronal morphology appear to have a large redistribution of $PrP^C$ (red) internally within the cytosol (white arrowheads, inset). Cells were costained with Hoechst nuclear

stain to visualize nuclei (blue). This pattern of redistribution appeared in the lateral septal nucleus as well (data not shown).

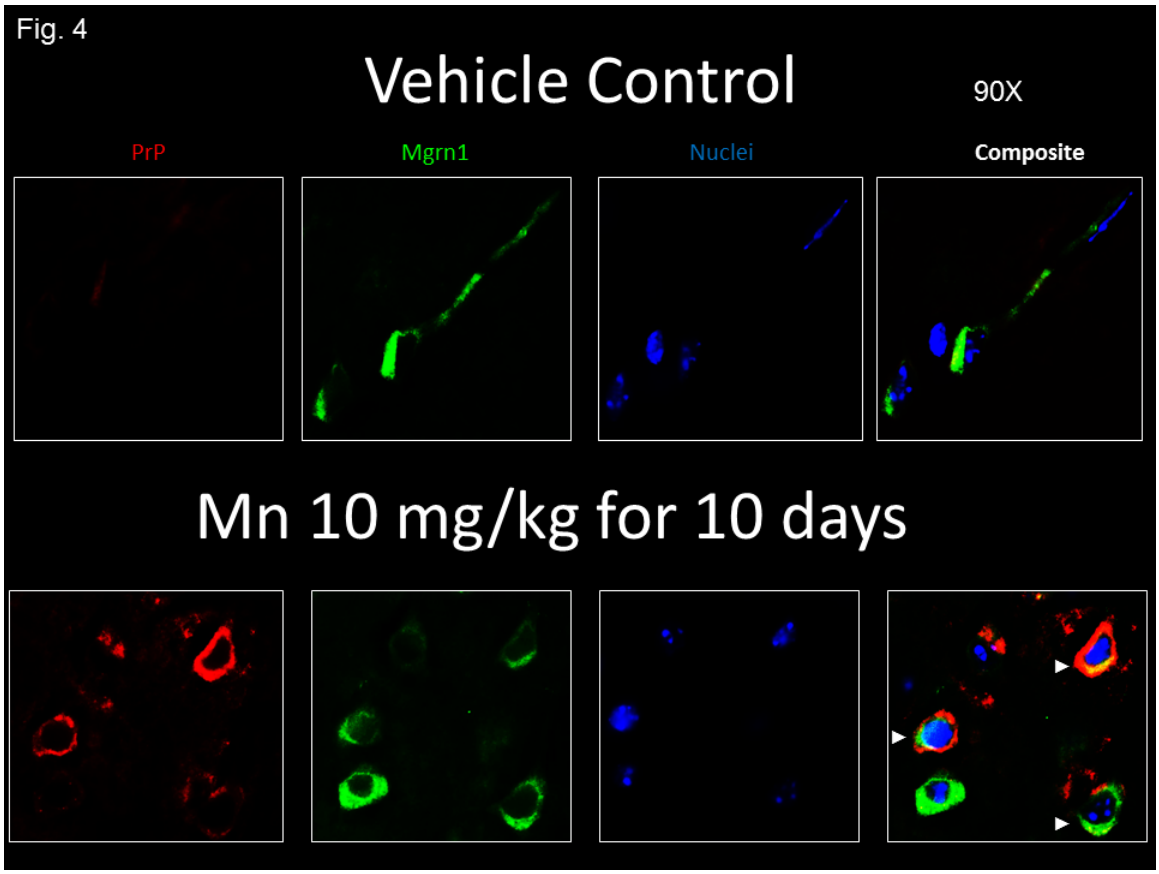


**Figure 4. Cytosolic PrP and Mgrn1 colocalize in the motor cortex of Mn treated mice.** Mice were treated for 10 days with 10 mg/kg of Mn by oral gavage. Control animals were treated with dd$H_2O$ vehicle. Animals were perfused with 4% paraformaldehyde and brains were cryosectioned. Immunohistochemical labeling with SAF32 anti-PrP antibody and Mgrn1 show colocalization of cytosolic $PrP^C$ (red) and Mgrn1 (green) in mouse motor cortex of Mn treated animals. Cells were costained with Hoechst nuclear stain to visualize nuclei (blue).

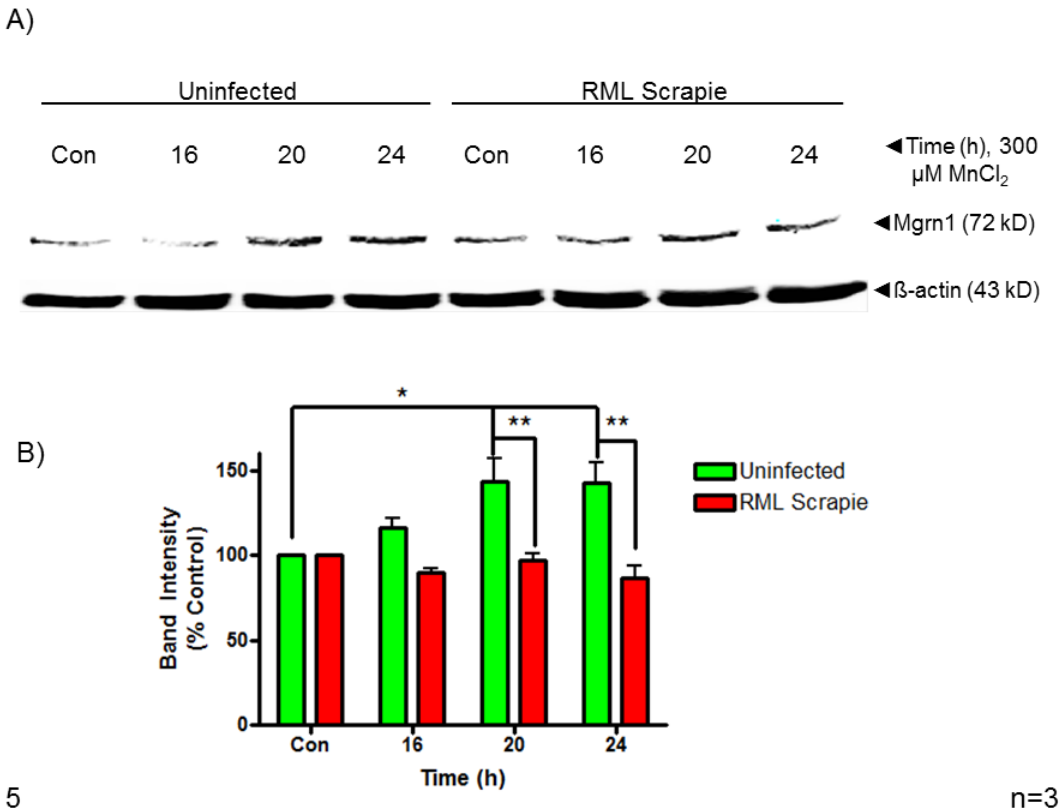


Fig. 5 n=3

**Figure 5. RML scrapie-infected CAD5 cells have altered Mgrn1 levels in response to Mn treatment.** Uninfected and RML scrapie-infected cells were treated with 300 μM $MnCl_2$ for 16, 20, and 24 hours. Cell lysate was analyzed by SDS-PAGE and immunoblotting with anti-Mgrn1 antibody. A) Uninfected cells displayed a significant increase in Mgrn1 protein levels with Mn treatment at 20 and 24 hours while Mgrn1 levels in RML scrapie-infected cells remained unchanged. B) Densitometric analysis of Mgrn1 protein levels in uninfected and RML scrapie infected cells. Membranes were colabeled with anti-ß-actin antibody and Mgrn1 values were normalized to ß-actin levels to ensure equal protein concentrations. Asterisks represent * $p<0.05$ and ** $p<0.01$. Data represent mean

± SEM from three individual experiments.

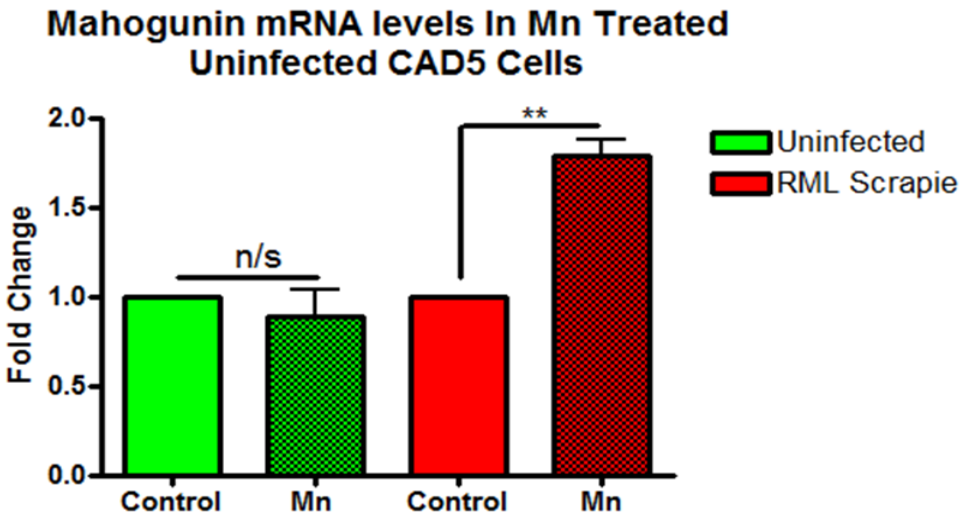


Fig. 6 n=3

**Figure 6. Transcriptional regulation of Mgrn1 is altered in RML scrapie-infected CAD5 cells.** Uninfected and RML scrapie-infected cells were treated with 300 μM $MnCl_2$ for 20 hours and total RNA was isolated. RNA was quantified by NanoDrop and RNA levels were equalized. Reverse transcription was done to produce cDNA and the level of Mgrn1 was assayed by SYBR-green real time quantitative PCR analysis. Despite an increase in Mgrn1 protein levels, Mgrn1 mRNA is unchanged in uninfected CAD5 cells. However, in RML scrapie-infected cells, Mgrn1 gene transcription is slightly but significantly upregulated. Asterisks represent ** $p<0.01$. Data represent mean ± SEM from three individual experiments each with two replicates.

# CHAPTER 4: PROTEOLYTIC ACTIVATION OF PROTEIN KINASE C DELTA CONTRIBUTES TO TRANSMISSIBLE SPONGIFORM ENCEPHALOPATHY-RELATED NEURODEGENERATION

A manuscript to be communicated to the journal Prion

Dustin Martin[1], Juergen Richt[2], Vellareddy Anantharam[1], Arthi Kanthasamy[1] and Anumantha G. Kanthasamy*[1]

1Department of Biomedical Sciences, Iowa Center for Advanced Neurotoxicity, Iowa State University, Ames, IA 50011

2 Department of Diagnostic Medicine/Pathobiology, Kansas State University, Manhattan, KS 66506

*Corresponding Author

## Abstract

An abnormal isoform of the endogenous prion protein is the putative pathogenic agent of transmissible spongiform encephalopathy (TSE). TSE is characterized by extensive gliosis, neuronal loss, and spongiform vacuolization in the central nervous system of infected humans and animals. Despite considerable

effort, the process of conversion from the normal cellular isoform ($PrP^{C}$) to the pathogenic conformation ($PrP^{Sc}$), as well as the endogenous function of $PrP^{C}$ have yet to be deciphered. Biochemical signs in the CNS of TSE-infected organisms include accumulation of protease resistant $PrP^{Sc}$, neuronal loss, oxidative stress, DNA fragmentation, and caspase-3 activation implicating apoptotic cell death as the probable cause of neuronal loss observed in TSEs. In order to design effective treatments for TSE, the molecules involved in TSE-related neuronal apoptosis must be more clearly understood. Our lab has extensively characterized the proteolytic activation of a novel protein kinase C, PKCδ, in the pathogenic apoptotic cell death of dopaminergic neuronal cells in Parkinson's disease. Therefore, in this study, we characterized the role of PKCδ in neuronal apoptosis associated with TSE. Our results have identified constitutive activation of PKCδ by cleavage in multiple brain regions in a mouse-adapted scrapie model. We also report changes in the phosphorylation of PKCδ at two regulatory sites: T505 within the activation loop of PKCδ to evaluate activation of native kinase activity and Y311 which flanks the caspase-3 cleavage site of PKCδ and precedes proteolytic activation. Additionally, we have discovered that PKCδ knockout animals display a significant delay in the onset of motor symptoms associated with TSE and have an altered pattern of oxidative damage and neuronal degeneration. These data indicate that PKCδ signaling may contribute to neurodegeneration observed during the course of TSE.

## Introduction

The prion protein undergoes a conversion from endogenous membrane bound protein ($PrP^{C}$) to transmissible neurodegenerative pathogen ($PrP^{Sc}$) through changes in its secondary and tertiary structure by an as yet unidentified process (Chatigny and Prusiner, 1980; Prusiner, 1982). Misfolded prion protein has been identified as the sole causative agent in transmissible spongiform encephalopathy (TSE), yet these diseases do not share a common etiology or pathology. A variety of potential apoptotic stimuli have been implicated in TSE related apoptosis, including oxidative and endoplasmic reticulum stress (Fairbairn et al., 1994; Ferreiro et al., 2006; Ferreiro et al., 2008; Hetz et al., 2003; Kim and Smith, 2001; Milhavet and Lehmann, 2002; Soto, 2008). Several hallmarks of apoptotic cell death have been observed in relation to TSE-related neurodegeneration in both *in vitro* and *in vivo* models, including caspase activation and DNA fragmentation (Bourteele et al., 2007; Fairbairn et al., 1994; Hetz et al., 2003; Offen et al., 2000). Additionally, our group has discovered that expression of $PrP^{C}$ exacerbates apoptosis induced by the ER stress-inducing agent tunicamysin (Anantharam et al., 2008). Despite these discoveries, the signaling cascades leading to prion-induced apoptosis are still unclear.

The delta isoform of protein kinase C (PKCδ) has emerged as a molecule of diverse function and marked importance. The normal cellular functions of this ubiquitously expressed, diacylglycerol (DAG) dependent, calcium independent

serine/threonine kinase include cellular differentiation, proliferation, secretion, and apoptosis (Benes and Soltoff, 2001; Kanthasamy et al., 2003; Kikkawa et al., 2002; Miyamoto et al., 2002; Orosco et al., 2006; Reyland, 2007). Under a variety of apoptotic stimuli, most notably agents of oxidative or endoplasmic reticulum stress, PKCδ is proteolytically cleaved by the effector caspase, caspase-3, into two subunits: regulatory and catalytic (Kanthasamy et al., 2003; Kikkawa et al., 2002; Kitazawa et al., 2005; Reyland, 2007; Yang et al., 2004). Separation of the regulatory domain from the catalytic domain produces a persistently active kinase that translocates to several different cellular organelles, including the cell membrane, nucleus, and mitochondria, and induces apoptosis (Kanthasamy et al., 2003; Kikkawa et al., 2002; Reyland, 2007; Yoshida, 2007). Indeed, expression of the catalytic domain alone is sufficient to induce apoptosis in cells (Denning et al., 2002). Inhibition of caspase-3 or PKCδ activity protects cells from both oxidative and endoplasmic reticulum stress-related apoptosis (Anantharam et al., 2004; Choi et al., 2007; Hetz et al., 2003; Kaul et al., 2003; Kitazawa et al., 2003; Kitazawa et al., 2004; Latchoumycandane et al., 2005; Yang et al., 2004). PKCδ activity is regulated by multiple internal phosphorylation sites. Phosphorylation of the tyrosine at site 311 which flanks the caspase-3 cleavage site has been implicated in the proteolytic activation of PKCδ (Kaul et al., 2005; Konishi et al., 1997; Rybin et al., 2004; Saminathan et al., 2011). Conversely, an increase in native full length activity or low levels of proteolytic activation of PKCδ have been shown to exert an antiapoptotic effect (Asaithambi et al., 2011; Brodie and Blumberg, 2003; McCracken et al., 2003).

Phosphorylation of T505 in the activation loop of PKCδ has been associated with an increase in native kinase activity and pro-survival signaling (Orosco et al., 2006).

**Materials and methods**

Chemicals and antibodies

PKCδ polyclonal antibody (Santa Cruz cat# sc-213), anti-p-T507 PKCδ antibody (Santa Cruz cat# sc-11770), anti-p-Y311 PKCδ antibody (Santa Cruz cat# sc-18364-R), anti-caspase-3 antibody (Santa Cruz cat# sc-22140), anti-4-hydroxynonenal (R&D Systems, Minneapolis, MN), 6H4 anti-PrP antibody (Prionics, Schlieren, Switzerland), Fluorojade C (Millipore, Bilerica, MA), Absolutely RNA Miniprep Kit (Stratagene, La Jolla, CA), RT2 First Strand kit (SABiosciences, Frederick, MD), Absolutely RNA Miniprep Kit (Stratagene, La Jolla, CA), qPCR primer assay specific for murine PKCδ (SABiosciences, Frederick, MD), electrochemiluminescence (ECL) detection kit (GE Healthcare, Piscataway, NJ).

Mouse models of murine scrapie

The animals and protocol procedures were approved and supervised by the Committee on Animal Care (COAC) at Iowa State University. C57Bl/6 and PKCδ(-/-) mice at postnatal week 6-8 were arranged by weight and randomized into 8 groups

(four mock and four scrapie inoculations ending at 60, 90, 120, and 150 DPI). PKCδ knockout animals were kindly provided by Dr. Keiichi Nakayama's Laboratory, Medical Institute of Bioregulation, Kyushu University, Fukuoka, Japan (Miyamoto et al., 2002). The rationale for time points selected in the study were to determine the effect of PKCδ on TSE progression ranging from early stages of the disease prior to the onset of motor symptoms to the terminal stage. Infection with the RML strain of mouse adapted scrapie protein results in severe clinical presentation within 150-160 days. Brain homogenate from RML infected mice was generously provided by Dr. Juergen Richt, Kansas State University, Manhattan, KS. RML infection was performed by intracerebrally injecting 30 µl of 1% (w/v) RML infected brain homogenate in PBS. Mock control inoculations were done with 30 µl of 1% uninfected brain homogenate. At 60, 90, 120 and 150 DPI WT and PKCδ(-/-) mice used in the behavioral experiments were humanely sacrificed and the following brain regions were harvested: motor cortex, striatum, thalamus, pons, medulla oblongata, and cerebellum. The tissues were dissected out and frozen immediately at -80ºC for biochemical evaluation.

SDS-PAGE and Western blot

Western blot analysis was performed as described previously (Anantharam et al., 2002; Kitazawa et al., 2005; Latchoumycandane et al., 2005). Following Mn treatment, cells were collected by scraping with a rubber scraper, washed once with

ice cold PBS, and then lysed in RIPA (Radio-Immunoprecipitation Assay) buffer with phosphatase and protease inhibitor cocktail. Protein concentrations of samples were determined using Bradford assay and samples were then separated by SDS-PAGE using a 10-15% polyacrylamide gel and transferred onto nitrocellulose membrane. After 1 h in blocking buffer, the membranes were treated with either anti-PKCδ, anti-caspase-3, or anti-4-hydroxynonenal at 4ºC overnight. Membranes were co-treated with anti-ß-actin antibody in blocking buffer to ensure equal protein loading. Membranes were then treated with anti-mouse, anti-goat, or anti-rabbit fluorescent secondary antibodies for 1 h at room temperature. Visualization was done using an Odyssey scanner (Licor, Lincoln, NE). Image analysis and band quantification was doing with ImageJ (NIH, Bethesda, MD).

Limited proteolysis

Dissected rain regions from mock infected and RML scrapie-infected mice were homogenized with a pellet pestle in lysis buffer (150 mM NaCl, 50 mM Tris-HCl pH 7.4, 5 mM EDTA, 2% Triton X, and 2% sodium deoxycholate). Lysate was sonicated for 5 mins in a cup horn sonicator and incubated at 4ºC for 20 mins. Protein concentrations were determined by Bradford assay, and 2 mg of protein from each sample were brought to equal volume with addition of excess lysis buffer. Limited proteolysis was begun by addition of 20 µg/ml PK to each sample and incubated at 37°C for 1 h. Reaction was quenched by the addition of 2 mM PMSF

(final concentration). After PK digestion, samples were ultracentrifuged at 120,000 X g for 2 h using an Optima Max Ultracentrifuge (Beckman-Coulter, Brea, CA) to pellet the PK-resistant fraction. The supernatant was discarded and 30 µl of PAGE loading buffer with DTT was added directly to the pellet. The samples were then sonicated for 5 mins in a cup horn sonicator, boiled for 10 mins, and separated by SDS-PAGE on a 15% polyacrylamide gel and transferred to nitrocellulose membrane. The membranes were treated with 6H4 anti-PrP monoclonal antibody overnight at 4ºC. 6H4 antibody has been used extensively to detect the PK resistant core of the pathogenic $PrP^{Sc}$ (Enari et al., 2001; Flechsig et al., 2000; Montrasio et al., 2000; Moynagh and Schimmel, 1999; Zou et al., 2004). Membranes were then incubated with HRP-conjugated secondary anti-mouse IgG antibody for 1 h at room temperature. Detection was done with an ECL detection kit and visualized using x-ray film (Kodak, Rochester, NY).

Quantative real time polymerase chain reaction (qRT-PCR)

Total RNA was isolated from uninfected and RML scrapie-infected C57Bl/6 mice using an Absolutely RNA Miniprep Kit. Reverse transcription into first strand complimentary DNA was done using a RT2 First Strand kit. Quantitative PCR was done with a MX3000P RT-PCR thermocycler (Stratagene, La Jolla, CA) using a qPCR primer assay specific for murine Prkcd. Amplification was performed over 40 cycles and quantified as fold increase calculated by 2^(-ΔΔCt) (ΔΔCt = ΔCt (Mn) -

ΔCt (Con) as recommended by the manufacturer. 18S RNA was used as a loading control to ensure equal RNA levels per well.

Behavioral evaluations

Extensive neuronal loss during the course of transmissible spongiform encephalopathy (TSE) produces progressive motor deficits in humans and animals including ataxia, tremor, and postural instability. Grip stamina and motor control were evaluated using the horizontal bar test (Guenther et al., 2001; Mallucci et al., 2007). Each mouse was held by the tail and allowed to grip a 0.2 cm diameter brass rod 50 cm above a padded cage with its forelimbs. The padded Innovive (San Francisco, CA, USA) mouse cage was placed below the bar to protect the mice from injury by falling. The mouse was quickly released and the time it took for the mouse to fall was recorded. Scores were given based on the following paradigm: 0-5s = 1; 6-10s = 2; 11-20s = 3; 21-29s = 4; and 30s or reaching the side support = 5.

The Columbus Instrument (Columbus, OH, USA) grip strength meter was used to determine the maximal amount of force each animal was apply to a specially designed bar with their forelimbs (LaMonte et al., 2002; Lepore et al., 2008). For all measurements, gauge was measured in PEAK mode and units were set to kgF. Animals were gripped firmly but gently at the base of the tail and the animal's forelimbs were placed on grip bar. Once the animal gripped the bar with both forelimbs, it was steadily pulled directly away from the digital strength meter. This

process was repeated 2-3 times to get peak strength reading.

Behavioral evaluations were done by trained personnel in cooperation with Iowa State University Laboratory Animal Resources. We evaluated uninfected and RML scrapie-infected C57Bl/6 and PKCδ(-/-) mice once weekly for differences in motor signs that reflected difficulty initiating ambulatory activities and changes in ambulatory activity patterns. Motor performance was scored on a scale from 0 to 4 with 0 = normal movement, 1 = slight alteration in ambulation, 2 = obvious intermittent motor signs, 3 = continuous pronounced motor signs, and 4 = almost complete lethargy. Test animals were monitored for changes in behavioral motor deficits over a period of several minutes. Mice were also evaluated for clasping of limbs when held aloft by the tail.

Data Analysis

Statistical analysis was performed with Prism 4.0 software (GraphPad Software, San Diego, CA). Statistical analysis between uninfected and infected data sets were done using Student's t-test and is indicated as follows: @$p<0.1$, *$p<0.05$, **$p<0.01$, and ***$p<0.001$. Data typically represent three to four separate experiments and are expressed as mean ± S.E.M.

## Results

### PKCδ is proteolytically activated in RML scrapie-infected mice

Apoptosis has been identified as the probable cause of neuronal loss associated with spongiform neurodegeneration (Bourteele et al., 2007; Carimalo et al., 2005; Fairbairn et al., 1994; Hetz et al., 2003; Offen et al., 2000). During apoptosis in neuronal cells induced by a variety of stimuli, PKCδ is cleaved by capsase-3 to produce a constitutively active catalytic fragment (Kanthasamy et al., 2003; Reyland, 2007). In order to evaluate the proteolytic activation of PKCδ during TSE disease progression, we examined murine-adapted RML scrapie-inoculated mice at 60, 90, 120, and 150 dpi for the presence of the cleaved fragment of PKCδ by immunoblot analysis. An increase in cleaved PKCδ in RML scrapie-infected animals when compared to mock infected mice was observed in the early preclinical stages of TSE (60 and 90 DPI) in the motor cortex (Figure 1A), although the difference was not statistically significant ($p>0.05$). However, a significant increase in cleaved PKCδ was detected in the striatum of infected animals at 120 DPI (Figure 1B). Although a peak in cleaved PKCδ was observed at 90 DPI in the thalamus, it was not statistically significant ($p>0.05$) (Figure 1C). Interestingly, the pons showed a significant decrease at 150 DPI compared to WT (Figure 1D). No cleavage was detected in the medulla oblongata at any time point (Figure 1 E). However, in the cerebellum cleaved PKCδ was evident at both 90 and 120 DPI of infected mice,

although only the 120 DPI time point was significant (Figure 1F).

Previous studies have found a reduction in native PKCδ protein levels during the terminal stage of TSE in mice and humans (Rodriguez et al., 2005; Rodriguez et al., 2006). A significant decrease in native PKCδ was detected at 150 DPI in the motor cortex, striatum, and pons, but not in the thalamus, medulla oblongata, and cerebellum of RML scrapie-infected animals compared to mock (Figure 1A-F). A surprising increase in native PKCδ was found in the striatum at 120 DPI (Figure 1B) and the medulla oblongata at 90 DPI (Figure 1E).

PKCδ phosphorylations at T505 and Y311 are altered during murine scrapie

We systematically examined the phosphorylation of PKCδ at two regulatory sites: T505 within the activation loop and Y311 flanking the caspase-3 cleavage site of PKCδ. Phosphorylation of T505 is associated with an increase in native kinase activity and may induce an antiapoptotic effect (Brodie and Blumberg, 2003; Orosco et al., 2006). Y311 phosphorylation has been associated with the proteolytic activation of PKCδ (Konishi et al., 1997). Mutation of this tyrosine residue prevents proteolytic activation of PKCδ by caspase-3 and protects neurons from apoptosis induced by oxidative stress (Kaul et al., 2005). A significant increase in T505 phosphorylation was detected in the motor cortex of RML scrapie-infected mice at 120 DPI (Figure 2A). Despite a slight increase in cleaved PKCδ at 60 and 90 DPI, no increase in Y311 phosphorylation was detected in the motor cortex of infected mice

at any timepoint. When normalized to native PKCδ protein levels, a significant decrease was detected at both phospho sites at 60 DPI.

In the striatum of infected mice, an increase in p-Y311 was detected that corresponds to the cleavage of PKCδ at 120 DPI (Figure 2B). An increase in p-T505 was detected at this time point as well. However, at 60 and 150 DPI p-T505 was significantly decreased in comparison to uninfected animals. When normalized to native PKCδ protein levels, p-Y311 became significantly reduced in comparison to the striatum of uninfected animals indicating that the phosphorylation of Y311 within the striatum may be context and/or cell type specific.

In the thalamus of infected animals, p-T505 was decreased compared to mock uninfected at 120 and 150 DPI which may indicate a loss of antiapoptotic signaling at these time points (Figure 2C). Phosphorylation of Y311 was decreased at 60 DPI as well. However, in the pons of RML scrapie infected mice, p-Y311 was increased at 120 DPI, (Figure 2D) although there was not a significant increase in cleaved PKCδ. T505 phosphorylation was likewise increased as 150 DPI, but the increase was not significant until normalized to native PKCδ. There was no significant difference in phosphorylation at T505 in the medulla oblongata of mock and scrapie-infected animals (Figure 2E). However, there was a significant decrease in p-Y311 when normalized to native protein levels. In the cerebellum of infected mice we found increased p-T505 at 60 DPI compared to control but no significant change at any time point after that. We additionally found an increase in p-Y311 at 90 and 120 DPI (Figure 2F). The phosphorylation of Y311 in the cerebellum

corresponds to the increases in PKCδ cleavage at 90 and 120 DPI.

PKCδ kinase activity is persistently activated in RML scrapie-infected mice

To confirm increased DAG-independent kinase activity of PKCδ cleaved fragments in RML infected mouse brain, PKCδ was immunoprecipitated from the homogenate of the motor cortex at 60 DPI and thalamus at 90 DPI using a PKCδ polyclonal antibody. In order to visualize the level of kinase activity in the immunoprecipitated protein, the known substrate of PKCδ, histone 2B, was added along with $^{32}$P-ATP, with or without DAG. The samples were then run on a 12% polyacrylamide gel and imaged using a Fujifilm FLA-5100 phosphoimager (Fujifilm Life Science, Woodbridge, CT). Figure 3B shows a significant increase in DAG-independent phosphorylation activity in the RML infected thalamus at 90 dpi ($p<0.01$). An increase in the kinase activity in the motor cortex was evident at 60 dpi however the p value was slightly above 0.05 (Figure 3A). The presence of kinase activity in the absence of DAG is indicative of persistent kinase activity in the motor cortex and thalamus of mice infected with RML scrapie and corresponds to proteolytic activation of PKCδ.

The decrease in PKCδ native protein levels at 150 DPI is not transcriptionally regulated

During the terminal stages of both BSE in transgenic mice and in human CJD, Rodríguez and colleagues observed a reduction in native PKCδ protein expression (Rodriguez et al., 2005; Rodriguez et al., 2006). However, in another study PKCδ mRNA was found to be upregulated in murine scrapie in a microarray experiment (Sorensen et al., 2008). In an effort to elucidate this discrepancy between protein and mRNA expression between different species during the course of TSE we assayed the PKCδ mRNA levels in brain regions that displayed significant decrease in native PKCδ protein levels at 150 DPI. Surprisingly, at this time point PKCδ mRNA was actually increased in striatum, but no change was detected in the motor cortex or pons indicating that the decrease in PKCδ protein levels is not due to transcriptional regulation (Figure 3C).

PKCδ knockout mice display altered pattern of protease resistant $PrP^{Sc}$

Upon conversion from $PrP^{C}$ to $PrP^{Sc}$, prion protein becomes highly resistant to denaturation and digestion by proteases. Therefore, limited proteolytic digestion of infected tissue using proteinase K (PK) and detection of $PrP^{Sc}$ by Western blot or ELISA has become a standard assay for the diagnosis of TSE. In order to further explicate the biological significance of PKCδ signaling in TSE-related apoptosis, we evaluated the progression of murine-adapted RML scrapie in a PKCδ knockout (PKCδ(-/-)) mouse line that has been used previously by our lab (Zhang et al., 2007). Presence of $PrP^{Sc}$ was determined by limited proteolysis of lysate from the

remaining cortical brain tissue using 20 µg/ml PK for one hour at 37ºC and subsequent Western blot. Figure 4 shows that both C57 and PKCδ(-/-) animals are susceptible to infection with RML scrapie. Interestingly, PKCδ(-/-) animals display an altered pattern of $PrP^{Sc}$ in early stages of RML scrapie when compared to WT C57. Only the band corresponding to the diglycosylated glycoform of $PrP^{Sc}$ appeared in all PKCδ(-/-) animals assayed at 90 DPI while all three glycoforms of $PrP^{Sc}$ appeared in WT animals. Bands corresponding to all three glycoforms are apparent at 150 DPI in both WT and PKCδ(-/-) animals. No protease resistant $PrP^{Sc}$ was found in mock infected animals.

TSE-related behavioral abnormalities are delayed in PKCδ(-/-) mice

The neurological symptoms of mice infected with mouse adapted scrapie include kyphosis, tremor, cachexia, and ataxia (Aguzzi and Heikenwalder, 2006; Brandner, 2003; Geissen et al., 2007; Johnson, 2005; Liberski and Brown, 2004; Strandberg Pedersen, 2003; Tatzelt and Schatzl, 2007; Unterberger et al., 2005; Wolferstan, 2003). Additionally, infected mice display clasping of limbs when held aloft by the tail (Wang et al., 2011). If PKCδ signaling contributes significantly to the neurodegeneration associated with TSE, inhibition of PKCδ function may delay onset of the disease. In order to further explicate the biological significance of PKCδ signaling in TSE-related apoptosis, we evaluated the motor function of mice following inoculation with murine-adapted RML scrapie in a PKCδ knockout (PKCδ(-

/-)) mouse line that has been used previously by our lab (Zhang et al., 2007). Mice were evaluated weekly using the horizontal bar test and grip strength meter to evaluate grip strength, stamina, and coordination. Beginning at week 14, WT infected animals displayed a significant reduction in forelimb strength (Figure 5A). Conversely, PKCδ(-/-) animals retained forelimb strength comparable to uninfected mice until sacrificed at 150 DPI. For the horizontal bar test (Figure 5B), mice were scored based on the time they were able to hang from a suspended metal bar. The scores were as follows: 0-5s = 1; 6-10s = 2; 11-20s = 3; 21-29s = 4; and 30s or reaching the side support = 5. Infected WT animals began showing difficulty staying on the bar at week 18 but the score significantly decreased at week 21 (Figure 5B). PKCδ(-/-) mice showed no significant reduction during the course of infection.

Clinical evaluation of all mice was done weekly in order to identify behavioral signs of RML scrapie-induced motor deficits. We evaluated both C57Bl/6 and PKCδ(-/-) mice for differences in motor signs that reflect difficulty initiating ambulatory activities and changes in ambulatory activity patterns and scored their pathology on a scale from 0 to 4 with 0 indicating normal movement and 4 indicating almost complete lethargy (Figure 5C). Test animals were monitored over a period of several minutes for changes in behavioral motor deficits reflecting postural instability and difficulty in open field ambulation. Symptoms began appearing in WT mice at week 17 and became progressively more pronounced over the course of monitoring (Figure 5C). Conversely, PKCδ(-/-) mice showed a delayed onset of TSE-related ataxia and a reduction in the severity of observable motor signs. Additionally, mice

were tested for the clasping of limbs when held aloft by the tail. PKCδ(-/-) mice likewise showed a delay in the onset of clasping, as well as a reduction in the severity (Figure 5D). Taken together, these results indicated that lack of PKCδ catalytic activity delayed the onset of neurological signs associated with mouse adapted scrapie.

RML scrapie-infected PKCδ knockout mice have altered caspase-3 cleavage and markers of oxidative stress

Markers of oxidative stress have been observed in various prion diseases including products of lipid peroxidation and oxidized amino acid side chains such as 4-hydroxynonenal and 3-nitrotyrosine (Andreoletti et al., 2002; Freixes et al., 2006; Yun et al., 2006). The molecular pathway of apoptotic neuronal loss in TSE includes activation of the effector caspase-3 (Engelstein et al., 2005; Jamieson et al., 2001). The level of oxidative damage and subsequent caspase-3 activation were assayed in mock infected and RML scrapie-infected C57 and PKCδ(-/-) mouse brain regions at 90 and 150 DPI by Western blot analysis using anti-4-HNE and anti-caspase-3 antibodies, respectively. At 90 DPI, oxidative damage was increased in RML scrapie-infected PKCδ(-/-) animals compared to WT as indicated by an increase in 4-HNE within the motor cortex, striatum, and thalamus (Figure 6A) but not in the medulla oblongata and pons (Figure 6B). A slight increase in 4-HNE was also observed in the cerebellum, although $p>0.05$ for this value (Figure 6B). At 150 DPI,

we observed marginal increases in 4-HNE accumulation in the pons and medulla oblongata but not in the motor cortex, striatum, thalamus or cerebellum of RML scrapie-infected PKCδ(-/-) animals when compared to WT (Figures 6D and E).

Next we measured the protein levels cleaved caspase-3, another marker of apoptosis by Western blot. At 90 DPI cleaved caspase-3 was surprisingly increased in the striatum and thalamus (Figure 7A) but not the pons or cerebellum (Figure 7B) of RML scrapie-infected PKCδ(-/-) mice compared to WT (Figure 7A). However, cleaved caspase-3 levels were decreased in the medulla oblongata and motor cortex at the same time point (Figure 7A-B). However, at 150 DPI cleaved caspase-3 was increased in motor cortex and thalamus (Figure 7C); but decreased in the pons and medulla oblongata of RML scrapie-infected PKCδ(-/-) mice (Figure 7D). These data indicate an altered pattern of apoptotic cell death and oxidative stress in RML scrapie-infected PKC(-/-) mice when compared to WT.

RML scrapie-infected PKCδ knockout mice have an altered pattern of Fluorojade positive cells

In order to more thoroughly examine the pattern of apoptotic neuronal loss in WT and PKC(-/-) mice, the motor cortex, striatum, thalamus, and cerebellum of terminally ill (150 DPI) were examined using Fluorojade C, a dye used to label degenerating neurons and activated glial cells (Damjanac et al., 2007; Ye et al., 2001). Comparison of these histopathological changes in the various brain regions

of the WT and PKCδ(-/-) mice were used to identify regional differences in importance of PKCδ in TSE-induced apoptosis. At 150 DPI, animals were perfused with 4% paraformaldehyde and processed for sectioning. 30 μm sections were cut with a cryostat and stained as per manufacturer instructions. Mock infected WT and PKCδ(-/-) animals display little to no Fluorojade staining, indicating specificity of the Fluorojade dye for degenerating neurons and activated glial cells related to RML scrapie infection (Figure 8A). In RML scrapie-infected C57 animals, widespread Fluorojade-positive cells were evident throughout the motor cortex, striatum, thalamus, and cerebellum. Conversely, in PKCδ(-/-) animals, a similar distribution of Fluorojade positive cells were evident in motor cortex, striatum, and thalamus; however, in motor cortex and striatum many of these cells displayed altered morphology from WT animals (Figure 8B). Both morphology as well as distribution of Fluorojade-positive cells between infected WT and PKCδ(-/-) animals were unchanged in the thalamus. The cerebellum of infected PKCδ(-/-) animals, on the other hand, showed marked reduction of Fluorojade positive cells (Figure 8B).

**Discussion**

In the present study we report activation of PKCδ by proteolytic cleavage during the course of murine scrapie in multiple brain regions. Upon cleavage by caspase-3, the catalytic domain of PKCδ translocates to different cellular organelles including the nucleus, mitochondria, and plasma membrane and induces apoptosis,

although the exact substrates involved in this cascade are still under investigation. (Kanthasamy et al., 2003; Kikkawa et al., 2002; Kitazawa et al., 2005; Reyland, 2007; Yang et al., 2004). The incidence of PKCδ cleavage prior to the onset of clinical symptoms and accumulation of $PrP^{Sc}$ in mice infected with RML scrapie coincides with studies that have detected signs of oxidative stress in mice infected with TSE prior to the development of clinical pathology (Yun et al., 2006).

We have further characterized the decrease in PKCδ protein levels in terminal TSE first described by Rodriguez and colleagues (Rodriguez et al., 2005; Rodriguez et al., 2006). The changes in the protein level of PKCδ during the course of TSE are seemingly not correlated to transcriptional regulation. This discrepancy between transcriptional regulation and protein expression may be due to pathogenic modulation of the protein degradation systems. Disruption of the ubiquitin proteosomal system (UPS) has long been linked to various amyloidogenic proteinopathies (Tyedmers et al., 2010). Intracellular oligomeric aggregation of proteins directly inhibit the UPS and have been implicated in disease pathogenesis (Bence et al., 2001; Bennett et al., 2005; Holmberg et al., 2004). Widespread changes in the specificity and function of the UPS and sequesteration of signaling molecules may cause ectopic function and promote neurodegeneration. Additionally, expression of PKCδ sensitizes neuronal cells to oxidative stress (Marengo et al., 2011). Neurons expressing higher levels of PKCδ may be more susceptible to TSE-related oxidative stress and undergo apoptoic cell death during earlier stages of the disease. Therefore reduced levels of PKCδ found in the later stages of TSE may be

a result of the loss of cells that normally express higher levels of PKCδ.

A recent study uncovered evidence that caspase activation and PKCδ cleavage mediate microglial activation and therefore promote neuroinflammation (Burguillos et al., 2011). Widespread microglial activation and astrogliosis have been observed in various models of TSE (Diedrich et al., 1991). The delay in the onset of clinical symptoms of TSE in PKCδ(-/-) animals observed in this study as a result of an attenuation in TSE-related inflammatory events cannot be ruled out. The change in distribution of cleaved caspase-3 and the observed difference in the cell morphology of Fluorojade-positive cells in the striatum and motor cortex of RML scrapie-infected PKC(-/-) animals compared to WT may indicate these cells are activated astrocytes since Fluorojade is known to stain not only degenerating neurons, but activated glial cells as well. These results may indicate an altered pattern of TSE-related inflammatory neuroinflammation in PKCδ(-/-) animals. However, a more detailed investigation is needed to elucidate altered glial activation as a result of PKCδ inhibition.

Despite the increase in markers of oxidative damage and activation of caspase-3 we observed in some brain regions of PKCδ(-/-) animals infected with RML scrapie, the lack of PKCδ catalytic activity in mutant mice delayed the onset of motor deficits associated with TSE and may be a potential target for pharmaceutical intervention. A study done by our lab indicated that the PKCδ inhibitor rottlerin protects mice treated with the Parkinsonian toxin MPTP, a known inducer of oxidative stress (Zhang et al., 2007). Animals treated with rottlerin had increased

locomotor function and dopamine levels when compared to animals only treated with toxin. The successful attenuation of scrapie-induced neurodegeration by pharmacological inhibitors of PKCδ could provide a basis for the development of effective therapies prior to the onset of widespread spongiform neurodegeneration and motor deficits in TSE.

In conclusion, we have identified altered regulatory phosphorylation and proteolytic activation of PKCδ in multiple brain regions at various time points during the progression of mouse adapted scrapie. Knockout of PKCδ resulted in a delayed onset of scrapie-induced motor symptoms and an altered pattern of markers of oxidative damage and neurodegeneration. Detailed mechanistic studies will help to elucidate the context specific contribution of PKCδ to the neurodegenerative and neuroinflammatory processes during the course of prion disease.

**References**

Aguzzi, A., Heikenwalder, M., 2006. Pathogenesis of prion diseases: current status and future outlook. Nat Rev Microbiol. 4, 765-75.

Anantharam, V., et al., 2002. Caspase-3-dependent proteolytic cleavage of protein kinase Cdelta is essential for oxidative stress-mediated dopaminergic cell death after exposure to methylcyclopentadienyl manganese tricarbonyl. J Neurosci. 22, 1738-51.

Anantharam, V., et al., 2004. Blockade of PKC{delta} Proteolytic Activation by Loss of Function Mutants Rescues Mesencephalic Dopaminergic Neurons from Methylcyclopentadienyl Manganese Tricarbonyl (MMT)-Induced Apoptotic Cell Death. Ann N Y Acad Sci. 1035, 271-89.

Anantharam, V., et al., 2008. Opposing roles of prion protein in oxidative stress- and ER stress-induced apoptotic signaling. Free Radic Biol Med. 45, 1530-41.

Andreoletti, O., et al., 2002. Astrocytes accumulate 4-hydroxynonenal adducts in murine scrapie and human Creutzfeldt-Jakob disease. Neurobiol Dis. 11, 386-93.

Asaithambi, A., et al., 2011. Protein kinase D1 (PKD1) activation mediates a compensatory protective response during early stages of oxidative stress-induced neuronal degeneration. Mol Neurodegener. 6, 43.

Bence, N.F., Sampat, R.M., Kopito, R.R., 2001. Impairment of the ubiquitin-proteasome system by protein aggregation. Science. 292, 1552-5.

Benes, C., Soltoff, S.P., 2001. Modulation of PKCdelta tyrosine phosphorylation and activity in salivary and PC-12 cells by Src kinases. Am J Physiol Cell Physiol. 280, C1498-510.

Bennett, E.J., et al., 2005. Global impairment of the ubiquitin-proteasome system by nuclear or cytoplasmic protein aggregates precedes inclusion body formation. Mol Cell. 17, 351-65.

Bourteele, S., et al., 2007. Alteration of NF-kappaB activity leads to mitochondrial apoptosis after infection with pathological prion protein. Cell Microbiol. 9, 2202-17.

Brandner, S., 2003. CNS pathogenesis of prion diseases. Br Med Bull. 66, 131-9.

Brodie, C., Blumberg, P.M., 2003. Regulation of cell apoptosis by protein kinase c delta. Apoptosis. 8, 19-27.

Burguillos, M.A., et al., 2011. Caspase signalling controls microglia activation and neurotoxicity. Nature. 472, 319-24.

Carimalo, J., et al., 2005. Activation of the JNK-c-Jun pathway during the early phase of neuronal apoptosis induced by PrP106-126 and prion infection. Eur J Neurosci. 21, 2311-9.

Chatigny, M.A., Prusiner, S.B., 1980. Biohazards of investigations on the transmissible spongiform encephalopathies. Rev Infect Dis. 2, 713-24.

Choi, C.J., et al., 2007. Normal Cellular Prion Protein Protects against Manganese-Induced Oxidative Stress and Apoptotic Cell Death. Toxicol Sci. 98, 495-509.

Damjanac, M., et al., 2007. Fluoro-Jade B staining as useful tool to identify activated microglia and astrocytes in a mouse transgenic model of Alzheimer's disease. Brain Res. 1128, 40-9.

Denning, M.F., et al., 2002. Caspase activation and disruption of mitochondrial membrane potential during UV radiation-induced apoptosis of human keratinocytes requires activation of protein kinase C. Cell Death Differ. 9, 40-52.

Diedrich, J.F., et al., 1991. Scrapie-associated prion protein accumulates in astrocytes during scrapie infection. Proc Natl Acad Sci U S A. 88, 375-9.

Enari, M., Flechsig, E., Weissmann, C., 2001. Scrapie prion protein accumulation by scrapie-infected neuroblastoma cells abrogated by exposure to a prion protein antibody. Proc Natl Acad Sci U S A. 98, 9295-9.

Engelstein, R., et al., 2005. Inhibition of P53-related apoptosis had no effect on PrP(Sc) accumulation and prion disease incubation time. Neurobiol Dis. 18, 282-5.

Fairbairn, D.W., et al., 1994. Detection of apoptosis induced DNA cleavage in scrapie-infected sheep brain. FEMS Microbiol Lett. 115, 341-6.

Ferreiro, E., et al., 2006. An endoplasmic-reticulum-specific apoptotic pathway is involved in prion and amyloid-beta peptides neurotoxicity. Neurobiol Dis. 23, 669-78.

Ferreiro, E., et al., 2008. Involvement of mitochondria in endoplasmic reticulum stress-induced apoptotic cell death pathway triggered by the prion peptide PrP(106-126). J Neurochem. 104, 766-76.

Flechsig, E., et al., 2000. Prion protein devoid of the octapeptide repeat region restores susceptibility to scrapie in PrP knockout mice. Neuron. 27, 399-408.

Freixes, M., et al., 2006. Oxidation, glycoxidation, lipoxidation, nitration, and responses to oxidative stress in the cerebral cortex in Creutzfeldt-Jakob disease. Neurobiol Aging. 27, 1807-15.

Geissen, M., et al., 2007. Understanding the natural variability of prion diseases. Vaccine. 25, 5631-6.

Guenther, K., et al., 2001. Early behavioural changes in scrapie-affected mice and the influence of dapsone. Eur J Neurosci. 14, 401-9.

Hetz, C., et al., 2003. Caspase-12 and endoplasmic reticulum stress mediate neurotoxicity of pathological prion protein. Embo J. 22, 5435-45.

Holmberg, C.I., et al., 2004. Inefficient degradation of truncated polyglutamine proteins by the proteasome. EMBO J. 23, 4307-18.

Jamieson, E., et al., 2001. Activation of Fas and caspase 3 precedes PrP accumulation in 87V scrapie. Neuroreport. 12, 3567-72.

Johnson, R.T., 2005. Prion diseases. Lancet Neurol. 4, 635-42.

Kanthasamy, A.G., et al., 2003. Role of proteolytic activation of protein kinase Cdelta in oxidative stress-induced apoptosis. Antioxid Redox Signal. 5, 609-20.

Kaul, S., et al., 2003. Caspase-3 dependent proteolytic activation of protein kinase C delta mediates and regulates 1-methyl-4-phenylpyridinium (MPP+)-induced apoptotic cell death in dopaminergic cells: relevance to oxidative stress in dopaminergic degeneration. Eur J Neurosci. 18, 1387-401.

Kaul, S., et al., 2005. Tyrosine phosphorylation regulates the proteolytic activation of protein kinase Cdelta in dopaminergic neuronal cells. J Biol Chem. 280, 28721-30.

Kikkawa, U., Matsuzaki, H., Yamamoto, T., 2002. Protein Kinase Cdelta (PKCdelta): Activation Mechanisms and Functions. J Biochem (Tokyo). 132, 831-9.

Kim, J.H., Smith, A., 2001. Distribution of organochlorine pesticides in soils from South Korea. Chemosphere. 43, 137-40.

Kitazawa, M., Anantharam, V., Kanthasamy, A.G., 2003. Dieldrin induces apoptosis by promoting caspase-3-dependent proteolytic cleavage of protein kinase Cdelta in dopaminergic cells: relevance to oxidative stress and dopaminergic degeneration. Neuroscience. 119, 945-64.

Kitazawa, M., et al., 2004. Dieldrin Promotes Proteolytic Cleavage of Poly(ADP-Ribose) Polymerase and Apoptosis in Dopaminergic Cells: Protective Effect of Mitochondrial Anti-Apoptotic Protein Bcl-2. Neurotoxicology. 25, 589-98.

Kitazawa, M., et al., 2005. Activation of protein kinase C delta by proteolytic cleavage contributes to manganese-induced apoptosis in dopaminergic cells: protective role of Bcl-2. Biochem Pharmacol. 69, 133-46.

Konishi, H., et al., 1997. Activation of protein kinase C by tyrosine phosphorylation in response to H2O2. Proc Natl Acad Sci U S A. 94, 11233-7.

LaMonte, B.H., et al., 2002. Disruption of dynein/dynactin inhibits axonal transport in motor neurons causing late-onset progressive degeneration. Neuron. 34, 715-27.

Latchoumycandane, C., et al., 2005. Protein kinase Cdelta is a key downstream mediator of manganese-induced apoptosis in dopaminergic neuronal cells. J Pharmacol Exp Ther. 313, 46-55.

Lepore, A.C., et al., 2008. Selective ablation of proliferating astrocytes does not affect disease outcome in either acute or chronic models of motor neuron degeneration. Exp Neurol. 211, 423-32.

Liberski, P.P., Brown, P., 2004. Kuru: a half-opened window onto the landscape of neurodegenerative diseases. Folia Neuropathol. 42 Suppl A, 3-14.

Mallucci, G.R., et al., 2007. Targeting cellular prion protein reverses early cognitive deficits and neurophysiological dysfunction in prion-infected mice. Neuron. 53, 325-35.

Marengo, B., et al., 2011. PKCdelta sensitizes neuroblastoma cells to L-buthionine-sulfoximine and etoposide inducing reactive oxygen species overproduction and DNA damage. PLoS One. 6, e14661.

McCracken, M.A., et al., 2003. Protein kinase C delta is a prosurvival factor in human breast tumor cell lines. Mol Cancer Ther. 2, 273-81.

Milhavet, O., Lehmann, S., 2002. Oxidative stress and the prion protein in transmissible spongiform encephalopathies. Brain Res Brain Res Rev. 38, 328-39.

Miyamoto, A., et al., 2002. Increased proliferation of B cells and auto-immunity in mice lacking protein kinase Cdelta. Nature. 416, 865-9.

Montrasio, F., et al., 2000. Impaired prion replication in spleens of mice lacking functional follicular dendritic cells. Science. 288, 1257-9.

Moynagh, J., Schimmel, H., 1999. Tests for BSE evaluated. Bovine spongiform encephalopathy. Nature. 400, 105.

Offen, D., Elkon, H., Melamed, E., 2000. Apoptosis as a general cell death pathway in neurodegenerative diseases. J Neural Transm Suppl. 153-66.

Orosco, A., et al., 2006. Dual involvement of protein kinase C delta in apoptosis induced by syndecan-2 in osteoblasts. J Cell Biochem. 98, 838-50.

Prusiner, S.B., 1982. Novel proteinaceous infectious particles cause scrapie. Science. 216, 136-44.

Reyland, M.E., 2007. Protein kinase Cdelta and apoptosis. Biochem Soc Trans. 35, 1001-4.

Rodriguez, A., et al., 2005. Metabotropic glutamate receptor/phospholipase C pathway: a vulnerable target to Creutzfeldt-Jakob disease in the cerebral cortex. Neuroscience. 131, 825-32.

Rodriguez, A., et al., 2006. Group I mGluR signaling in BSE-infected bovine-PrP transgenic mice. Neurosci Lett. 410, 115-20.

Rybin, V.O., et al., 2004. Stimulus-specific differences in protein kinase C delta localization and activation mechanisms in cardiomyocytes. J Biol Chem. 279, 19350-61.

Saminathan, H., et al., 2011. Environmental neurotoxic pesticide dieldrin activates a non receptor tyrosine kinase to promote PKCdelta-mediated dopaminergic apoptosis in a dopaminergic neuronal cell model. Neurotoxicology. 32, 567-77.

Sorensen, G., et al., 2008. Comprehensive transcriptional profiling of prion infection in mouse models reveals networks of responsive genes. BMC Genomics. 9, 114.

Soto, C., 2008. Endoplasmic reticulum stress, PrP trafficking, and neurodegeneration. Dev Cell. 15, 339-41.

Strandberg Pedersen, N., 2003. Prion diseases in man and animals. Acta Vet Scand Suppl. 100, 59-63.

Tatzelt, J., Schatzl, H.M., 2007. Molecular basis of cerebral neurodegeneration in prion diseases. Febs J. 274, 606-11.

Tyedmers, J., Mogk, A., Bukau, B., 2010. Cellular strategies for controlling protein aggregation. Nat Rev Mol Cell Biol. 11, 777-88.

Unterberger, U., Voigtlander, T., Budka, H., 2005. Pathogenesis of prion diseases. Acta Neuropathol. 109, 32-48.

Wang, F., Wang, X., Ma, J., 2011. Conversion of bacterially expressed recombinant prion protein. Methods. 53, 208-13.

Wolferstan, F., 2003. Slow neurodegeneration and transmissible spongiform encephalopathies/prion diseases. Hypothesis: a cycle involving repeated tyrosine kinase A activation could drive the development of TSEs. Med Hypotheses. 60, 52-64.

Yang, Y., et al., 2004. Suppression of caspase-3-dependent proteolytic activation of protein kinase C delta by small interfering RNA prevents MPP+-induced dopaminergic degeneration. Mol Cell Neurosci. 25, 406-21.

Ye, X., et al., 2001. Fluoro-Jade and silver methods: application to the neuropathology of scrapie, a transmissible spongiform encephalopathy. Brain Res Brain Res Protoc. 8, 104-12.

Yoshida, K., 2007. PKCdelta signaling: mechanisms of DNA damage response and apoptosis. Cell Signal. 19, 892-901.

Yun, S.W., et al., 2006. Oxidative stress in the brain at early preclinical stages of mouse scrapie. Exp Neurol. 201, 90-8.

Zhang, D., et al., 2007. Neuroprotective effect of protein kinase C delta inhibitor rottlerin in cell culture and animal models of Parkinson's disease. J Pharmacol Exp Ther. 322, 913-22.

Zou, W.Q., et al., 2004. Antibody to DNA detects scrapie but not normal prion protein. Proc Natl Acad Sci U S A. 101, 1380-5.

## Figures

A)

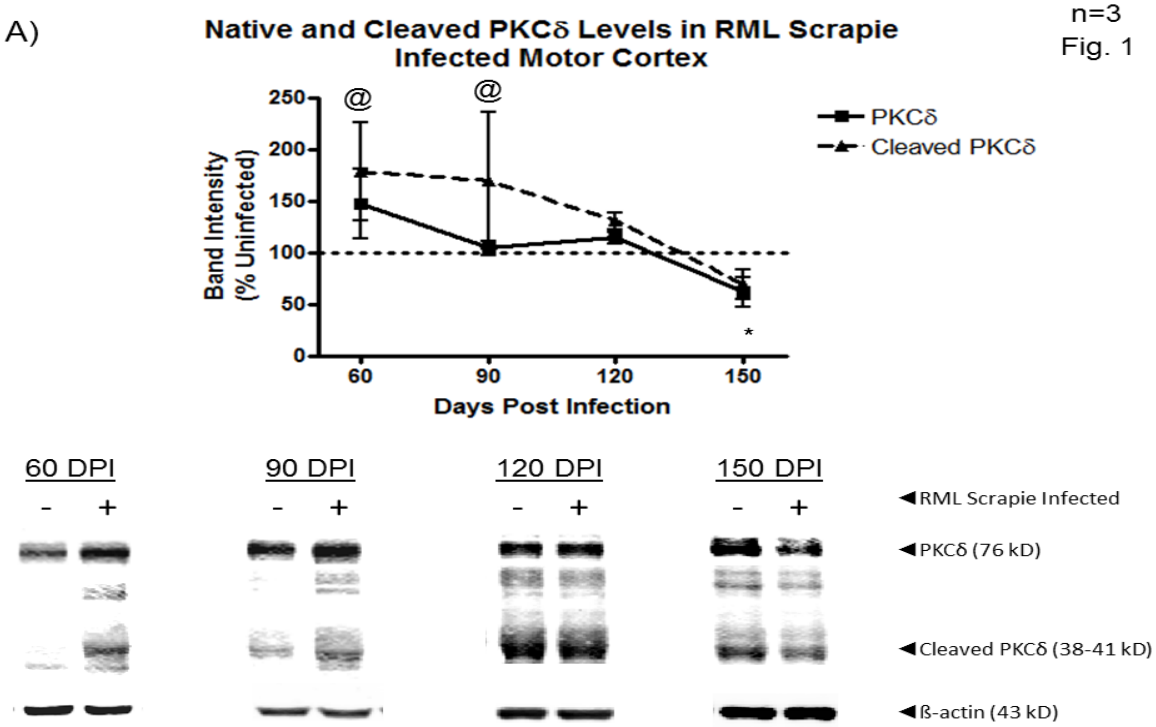


B)

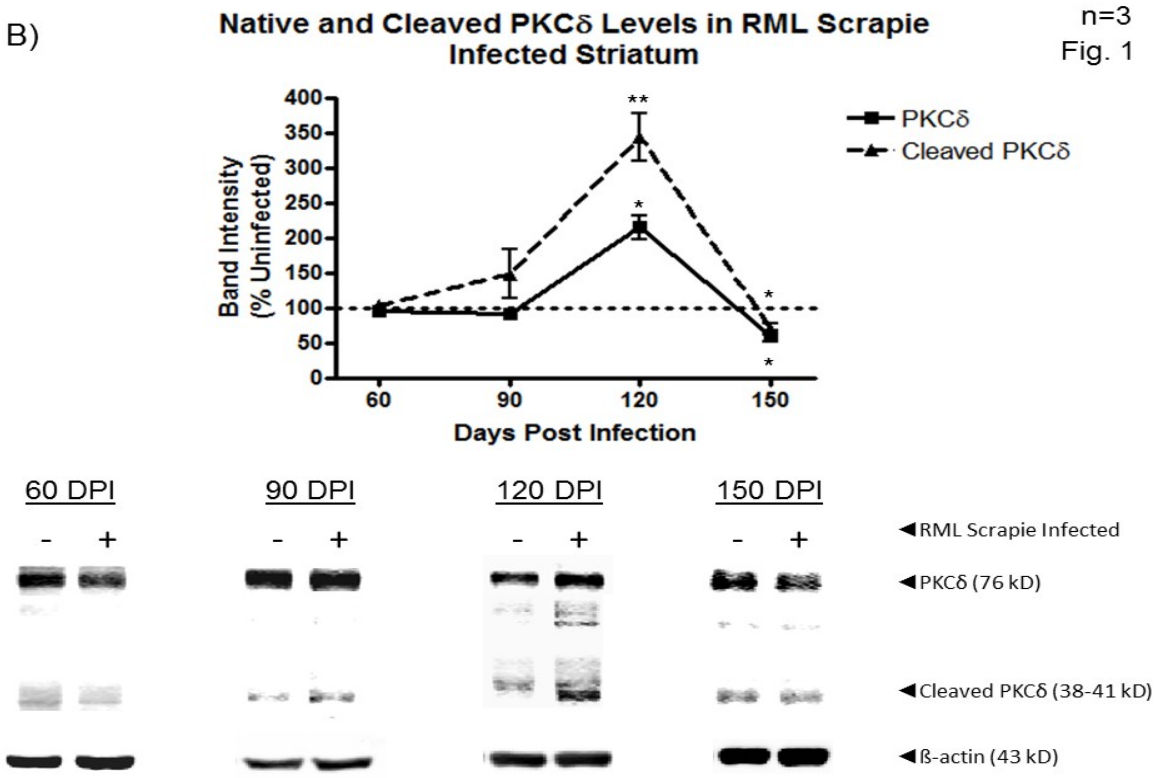

C)

**Native and Cleaved PKCδ Levels in RML Scrapie Infected Thalamus**

n=3
Fig. 1

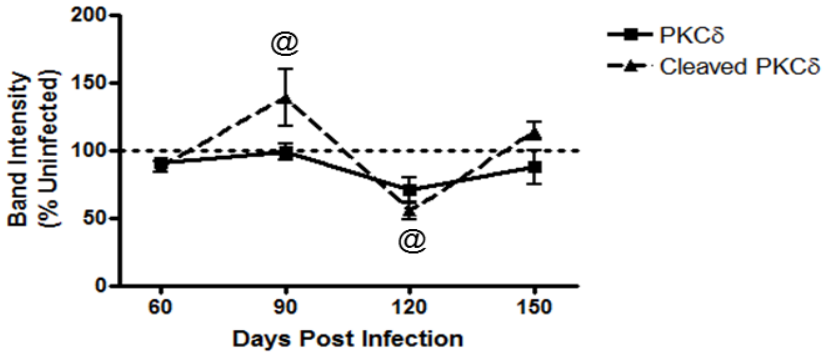


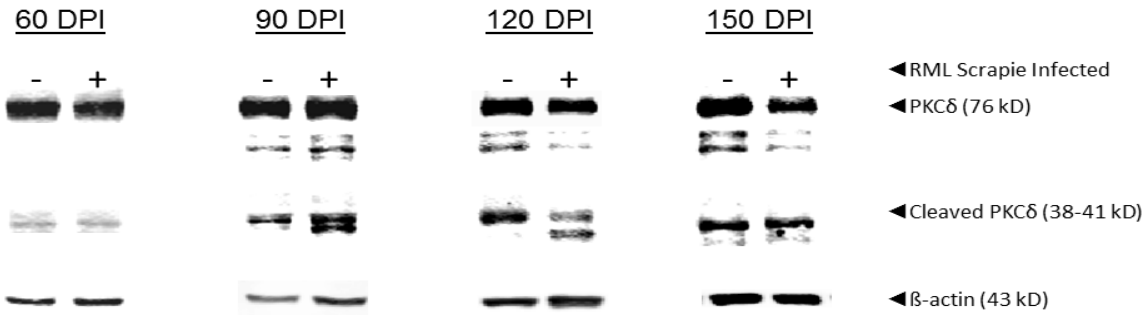


D)

**Native and Cleaved PKCδ Levels in RML Scrapie Infected Pons**

n=3
Fig. 1

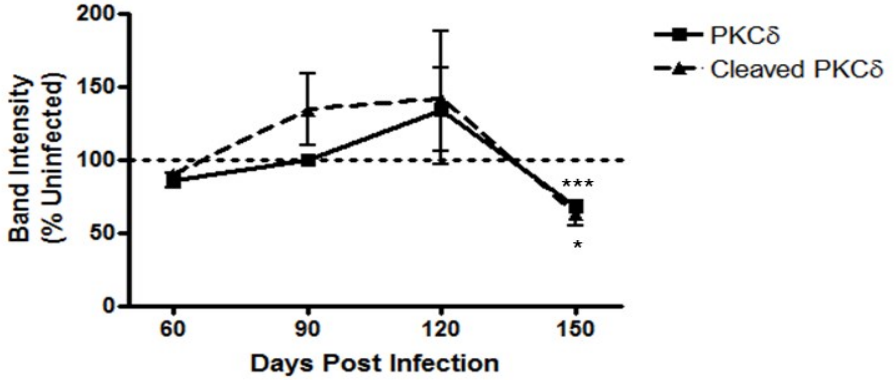


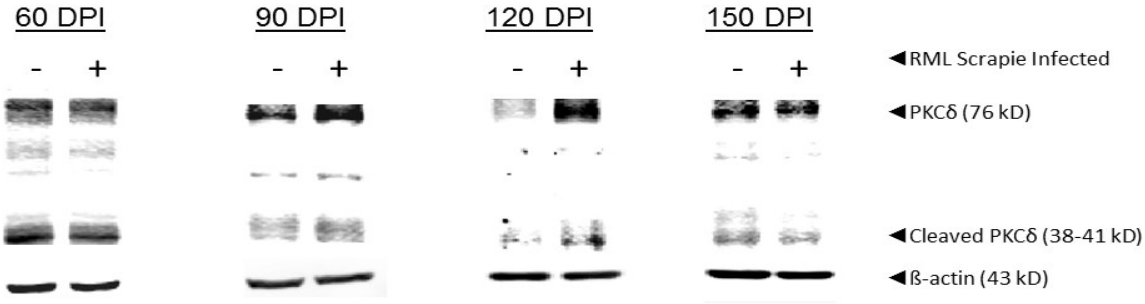

E)

**Native and Cleaved PKCδ Levels in RML Scrapie Infected Medulla Oblongata**

n=3
Fig. 1

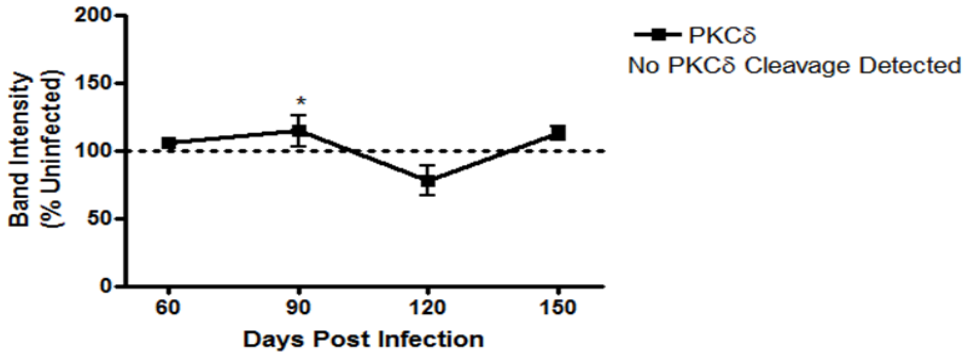


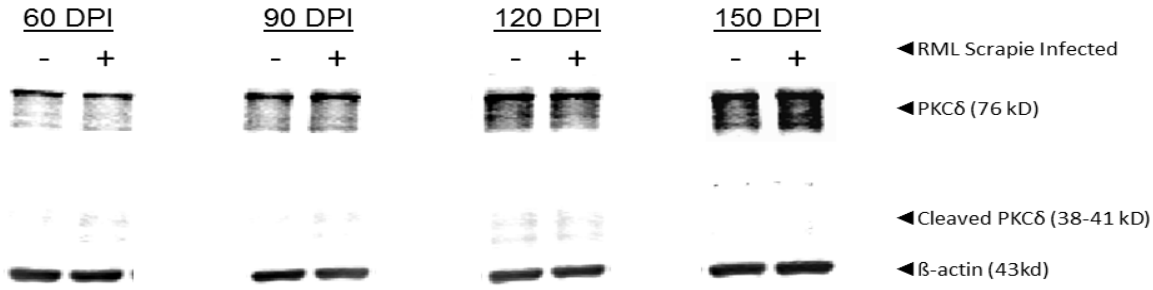


F)

**Native and Cleaved PKCδ Levels in RML Scrapie Infected Cerebellum**

n=3
Fig. 1

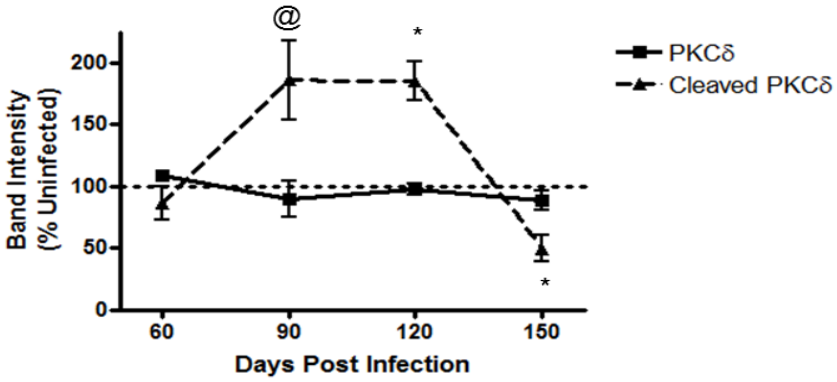


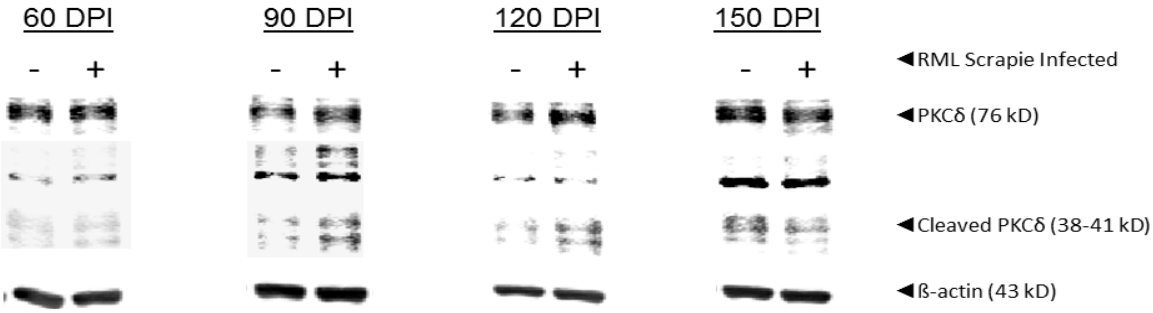

**Figure 1. PKCδ is proteolytically activated during murine scrapie.** The protein levels of native and cleaved of PKCδ were examined by immunoblot in RML scrapie infected mice at 60, 90, 120, and 150 DPI. C57/Bl6 mice were infected by i.c. injection of 30 µl of 1% infected brain homogenate. Control mock inoculations were done with 1% brain homogenate from uninfected mice. A) In motor cortex of infected animals, PKCδ cleavage was slightly increased at 60 DPI and slightly decreased at 150 DPI compared to mock ($p<0.1$ for both). Native PKCδ protein levels were decreased at 150 DPI ($p<0.05$). B) Cleaved PKCδ was significantly increased in the striatum at 120 DPI ($p<0.01$) and decreased at 150 DPI ($p<0.05$). Changes in the native protein level correlated with these changes ($p<0.05$). C) Cleaved PKCδ levels were increased in the thalamus of animals at 90 DPI, and decreased at 120 DPI, though not significantly ($p<0.1$). D) In pons, both native and cleaved levels were significantly reduced at 150 DPI ($p<0.001$ and $p<0.05$, respectively). E) Native PKCδ levels were significantly increased in medulla oblongata at 150 DPI ($p<0.05$). No cleaved PKCδ was detectable levels at any time point. F) In cerebellum, there was increased PKCδ cleaveage PKCδ at 90 ($p<0.1$) and 120 ($p<0.05$) and a significant decrease at 150 DPI ($p<0.05$). Data represent mean ± SEM from densitometric analysis of immunoblots from three separate animals.

n=4 Fig. 2

A)

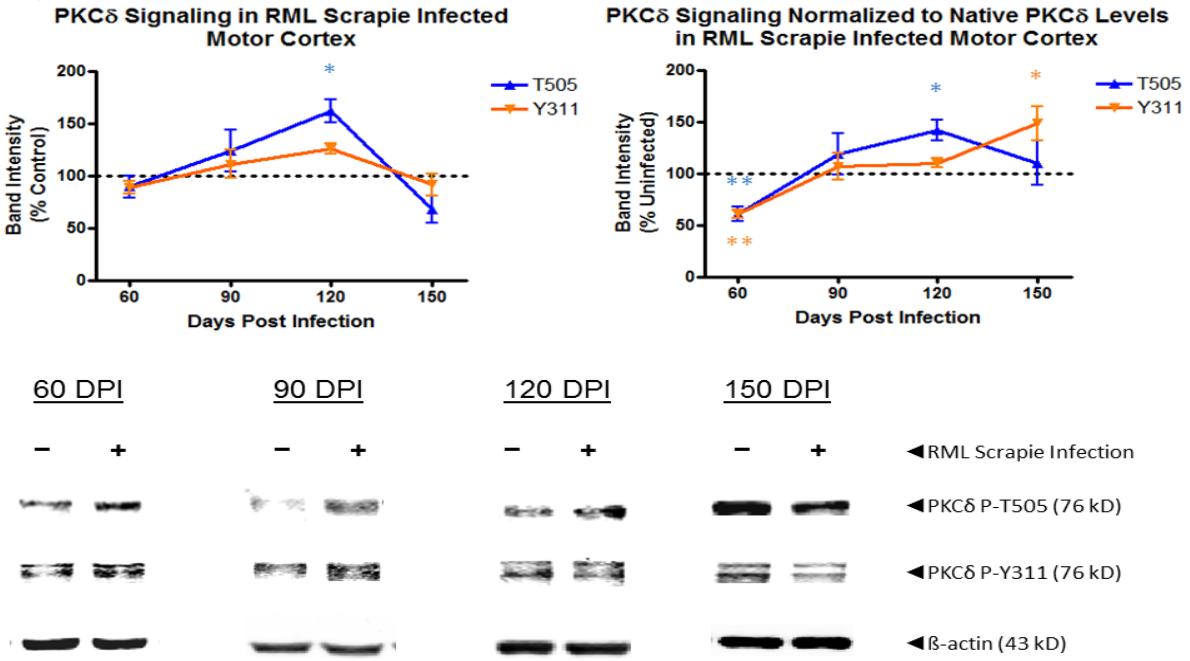


n=4 Fig. 2

B)

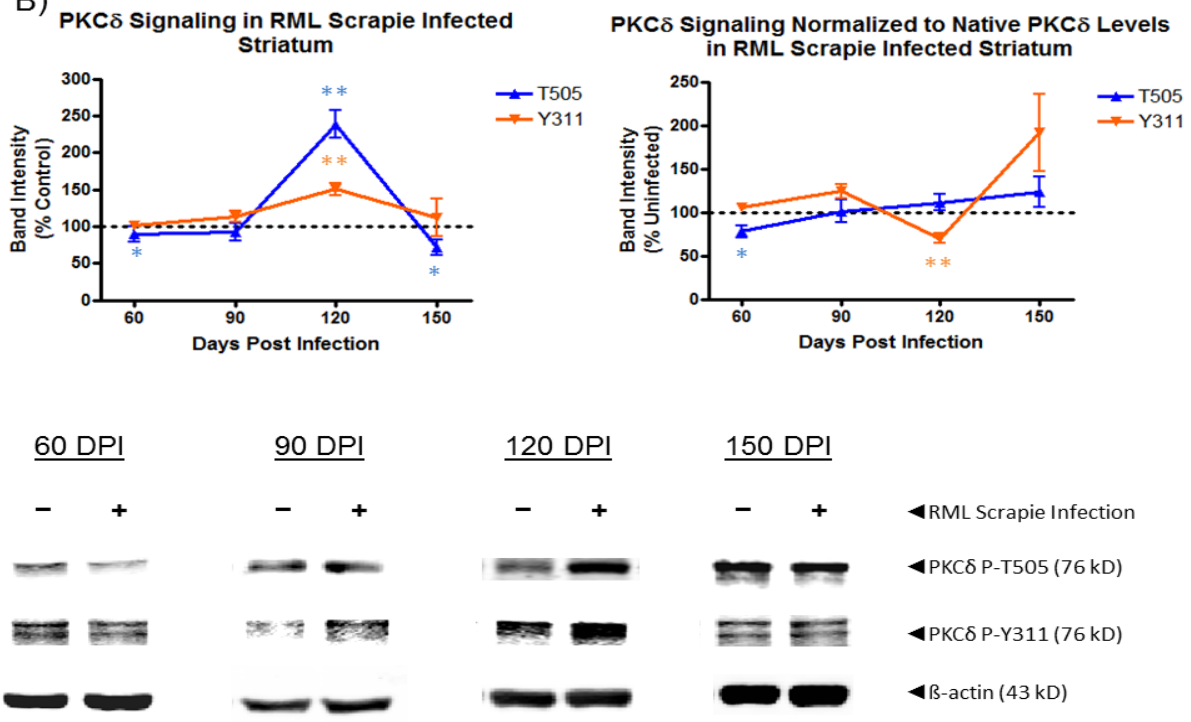

n=4 Fig. 2

C)

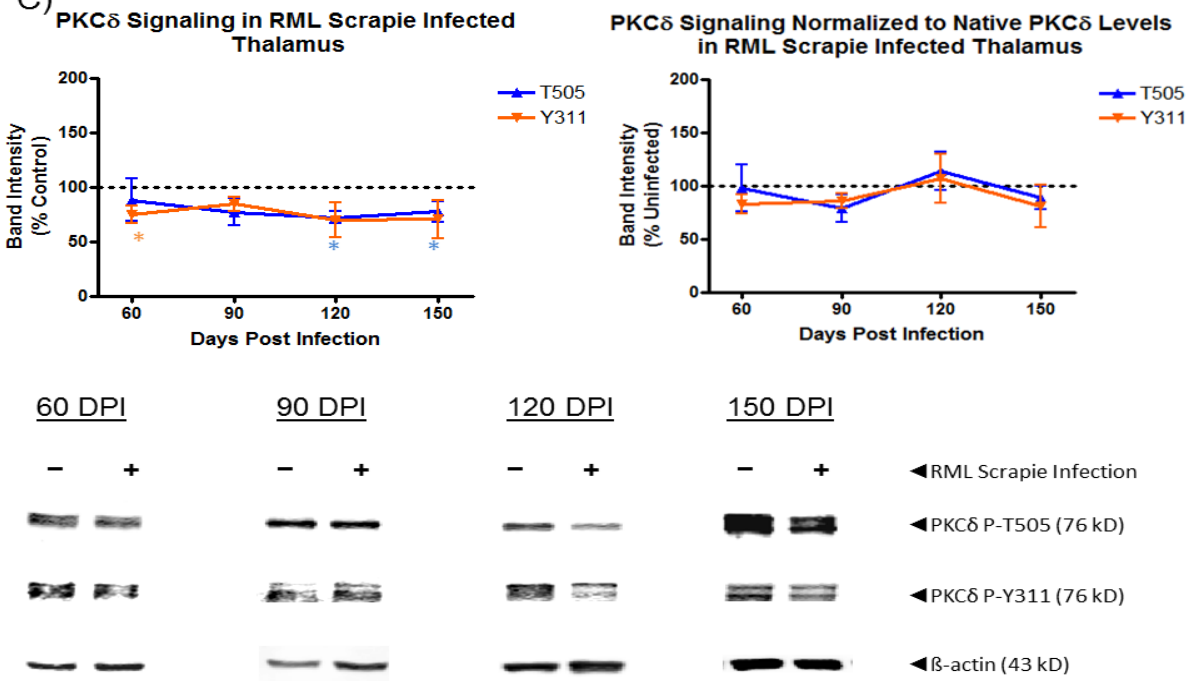


n=4 Fig. 2

D)

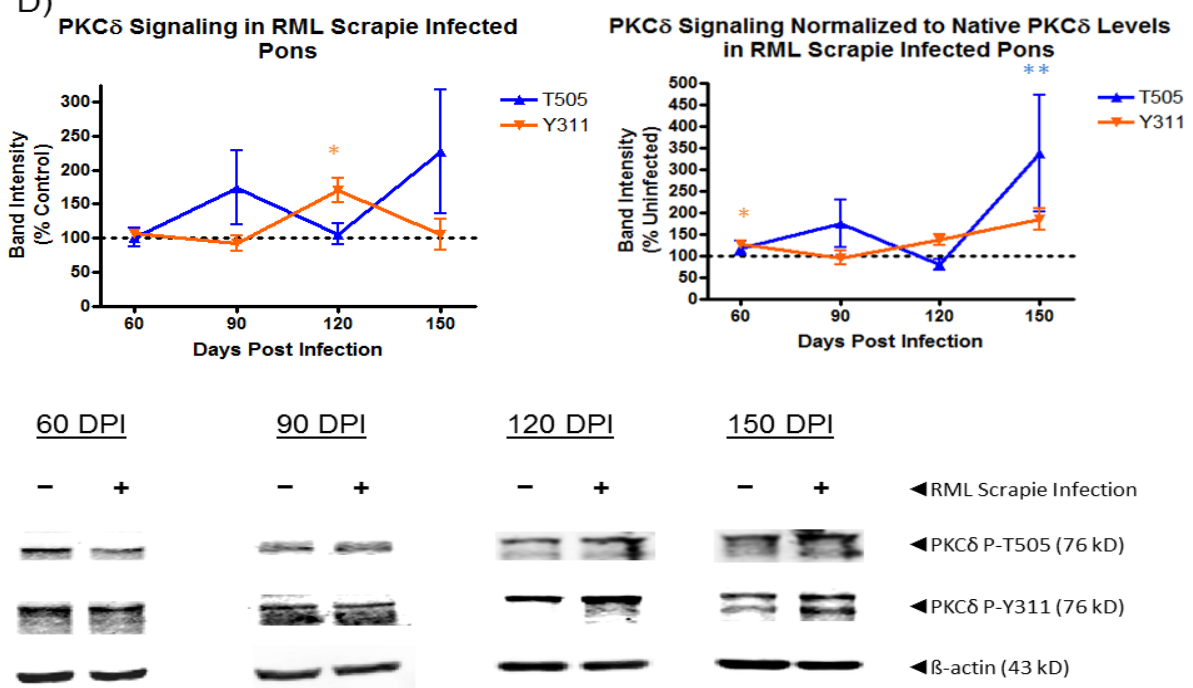

n=4 Fig. 2

E)

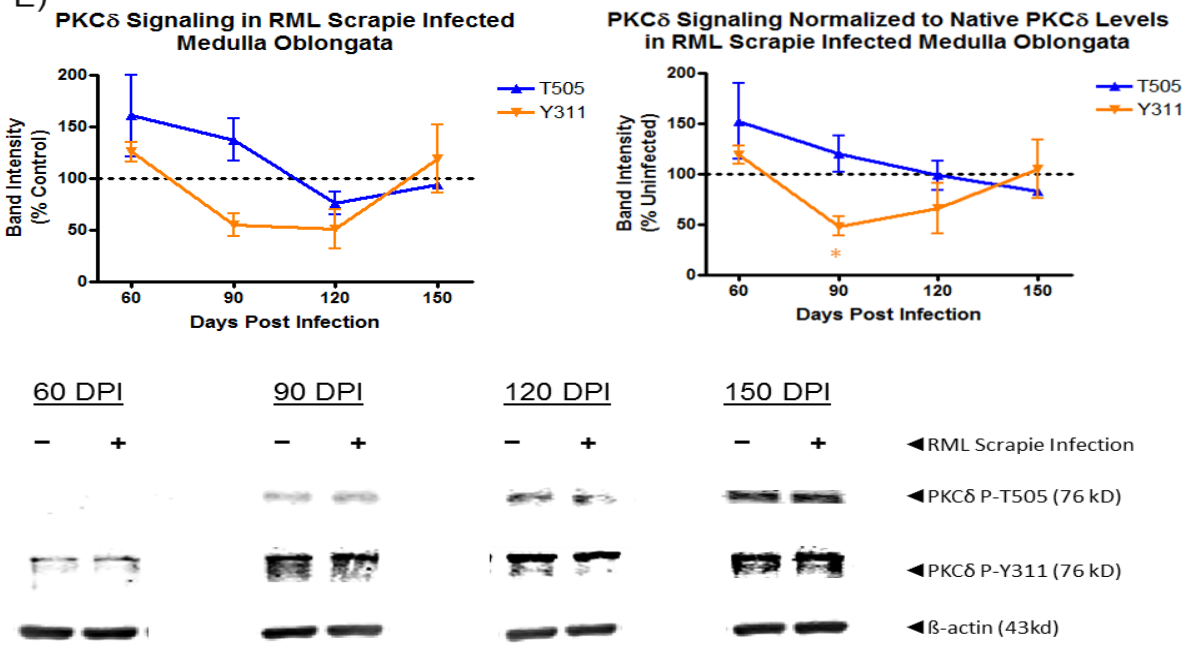


n=4 Fig. 2

F)

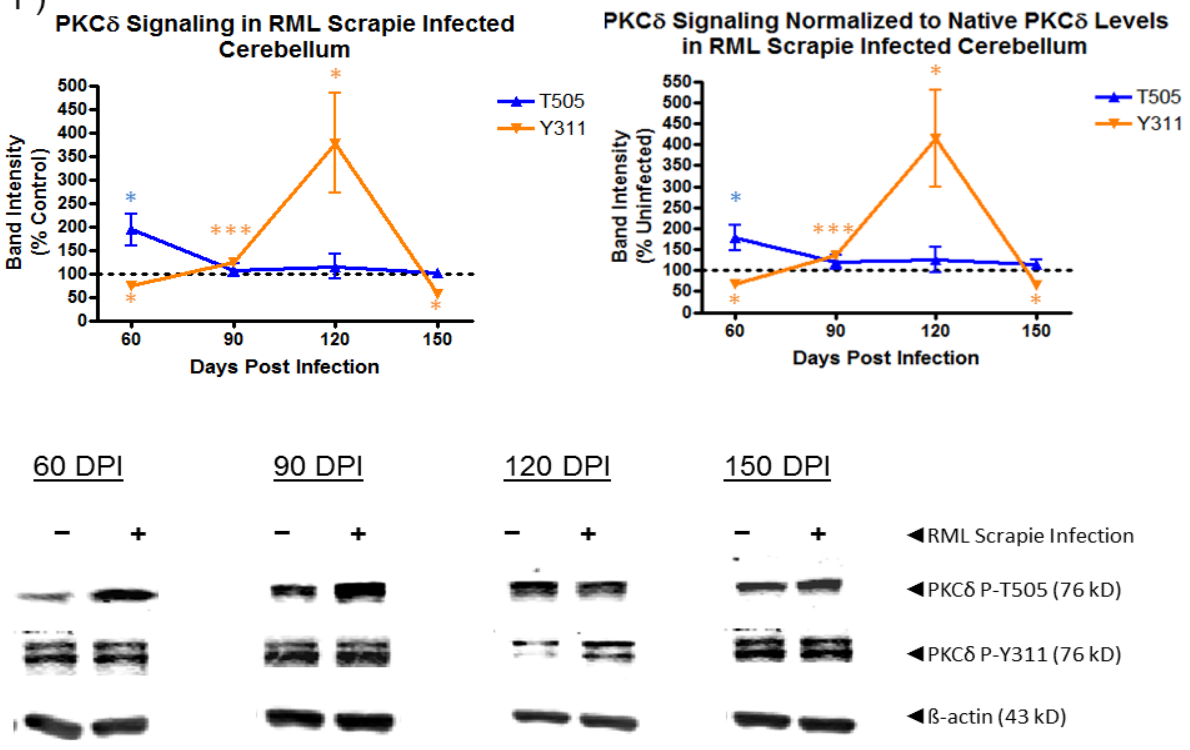

**Figure 2. PKCδ p-T505 and p-Y311 levels in RML scrapie-infected mice.** The phosphorylation of PKCδ at T505 and Y311 was examined by immunoblot in RML scrapie-infected animals at 60, 90, 120, and 150 DPI. C57/Bl6 mice were infected by i.c. injection of 30 µl of 1% infected brain homogenate. Mock inoculations were performed using 1% brain homogenate from uninfected mice. A) The phosphorylation at T505 was increased in the motor cortex of infected animals at 120 DPI ($p<0.05$). When normalized to native protein levels p-T505 levels were significantly lower than mock infected at 60 DPI ($p<0.01$) as was the site at Y311 ($p<0.01$). However, the phosphorylation of Y311 was increased at 150 DPI ($p<0.05$). B) Phosphorylation at T505 was decreased at 60 and 150 DPI in the striatum of infected animals ($p<0.05$). However, both T505 ($p<0.01$) and Y311 ($p<0.01$) were significantly increased at 120 DPI. The increase in p-T505 becomes no change and the increase in p-Y311 becomes a significant reduction ($p<0.01$) when normalized to native protein levels, indicating the specificity of both signals. C) In the thalamus of infected animals, Y311 phosphorylation was decreased at 60 DPI ($p<0.05$), and T505 was decreased at both 120 ($p<0.05$) and 150 DPI ($p<0.05$). D) A significant increase in the pons of infected animals was observed in p-Y311 at 120 DPI ($p<0.05$). When normalized to native protein levels, p-Y311 is slightly but significantly increased at 60 DPI ($p<0.05$). Additionally, p-T505 was increased at 150 DPI but the densitometric value was not significant until normalized to native protein levels ($p<0.01$). This is most likely due to the large variation among animals. E) The only significant change in the medulla oblongata of infected mice was a decrease in

Y311 phosphorylation at 90 DPI when normalized to native protein levels ($p<0.05$). F) There were several changes in cerebellar phosphorylation of PKCδ in infected animals. Y311 phosphorylation was decreased early at 60 DPI ($p<0.05$), but increased at 90 ($p<0.001$) and 120 DPI ($p<0.05$), before again decreasing at 150 DPI ($p<0.05$). These changes corresponded exactly to the cleavage of PKCδ. Additionally, p-T505 was significantly increased at 60 DPI ($p<0.05$). Levels of statistical significance are marked as follows: @ $p<0.1$, * $p<0.05$, ** $p<0.01$ and *** $p<0.001$. Data represent mean ± SEM of densitometric analysis of immunoblots from four separate animals.

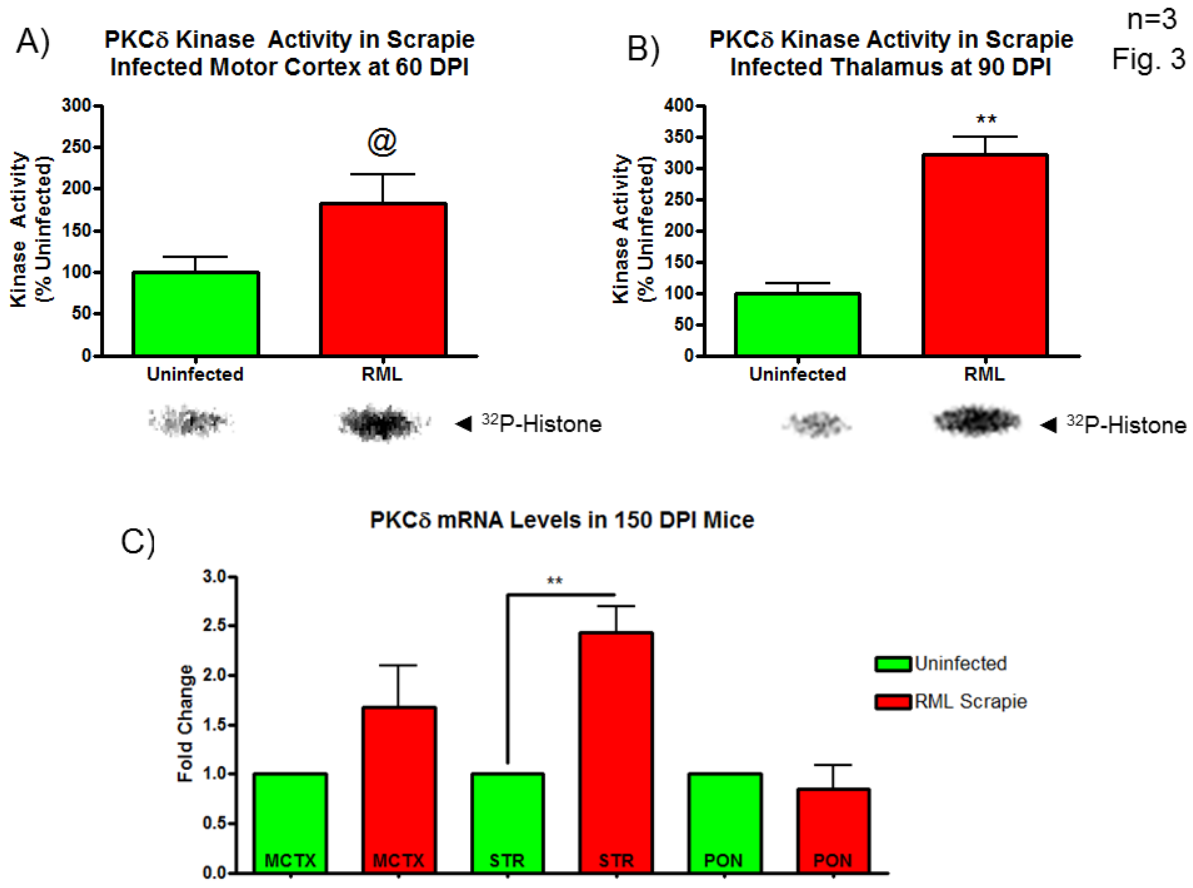

**Figure 3. PKCδ kinase activity is increased in RML scrapie-infected animals and changes in PKCδ native protein level are not transcriptionally regulated.** A-B) Kinase activity was measured by $^{32}P$ kinase assay using PKCδ immunoprecipitated from the motor cortex at 60 DPI and the thalamus at 90 DPI of mock and RML scrapie-infected animals. DAG-independent kinase activity was increased both regions indicating persistent activation of PKCδ; however in motor cortex the p value was slightly above 0.05. Data represent mean ± SEM of densitometric analysis from phosphoimage of three separate animals.C) Total RNA was isolated from uninfected and RML scrapie-infected mouse brain regions at 150 DPI. RNA was quantified by NanoDrop and RNA levels were equalized. Reverse transcription was done to produce cDNA and the level of PKCδ mRNA was assayed by SYBR-green real time quantitative PCR analysis. Although we observed an decrease in the PKCδ native protein levels in the motor cortex and pons, we observed no change in the mRNA levels at 150 DPI. The striatum of RML scrapie-infected mice actually displayed a slight but significant increase in PKCδ mRNA levels despite a significant decrease in protein levels. Asterix indicate statistical significance levels of * $p<0.05$, ** $p<0.01$, and *** $p<0.001$. Data represent mean ± SEM from three individual animals each with two replicates.

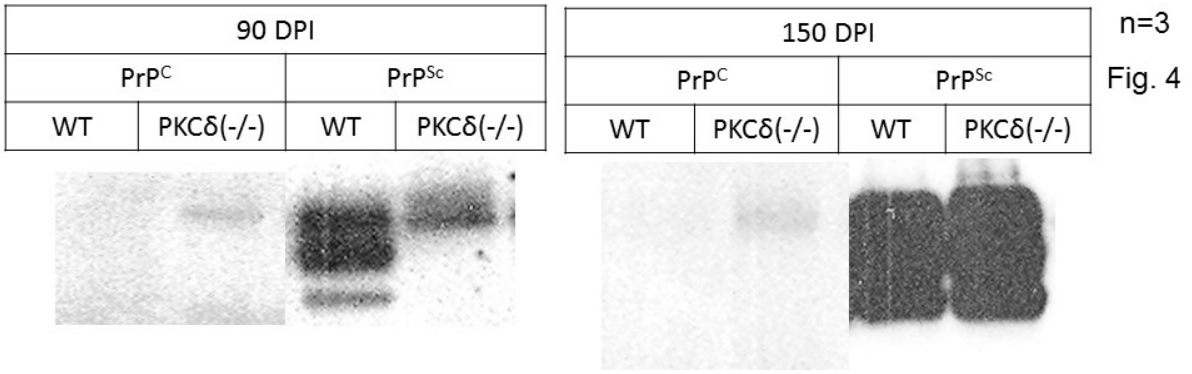


**Figure 4. RML scrapie-infected WT and PKCδ knockout animals accumulate protease resistant $PrP^{Sc}$.** C57Bl/6 and PKCδ(-/-) animals were inoculated i.c. with RML scrapie. At 90 and 150 DPI animals were sacrificed and cortical lysate (not including the motor and frontal cortices) was subjected to limited proteolysis by addition of 20 µg/ml PK and incubation at 37ºC for 1 h. The presence of protease resistant $PrP^{Sc}$ was determined by SDS-PAGE and immunoblot analysis with anti-PrP MAb. In mock inoculated animals, no $PrP^{Sc}$ was observable, while in both WT and PKC(-/-) at 90 (A) and 150 (B) DPI protease resistant $PrP^{Sc}$ was evident. In two of the three PKCδ(-/-) animals assayed at 90 DPI, an altered pattern of protease resistant PrP was observed. At 150 DPI, all RML scrapie-infected animals displayed the same three bands corresponding to the three different glycoforms of $PrP^{Sc}$. Data represent limited proteolysis of three separate animals.

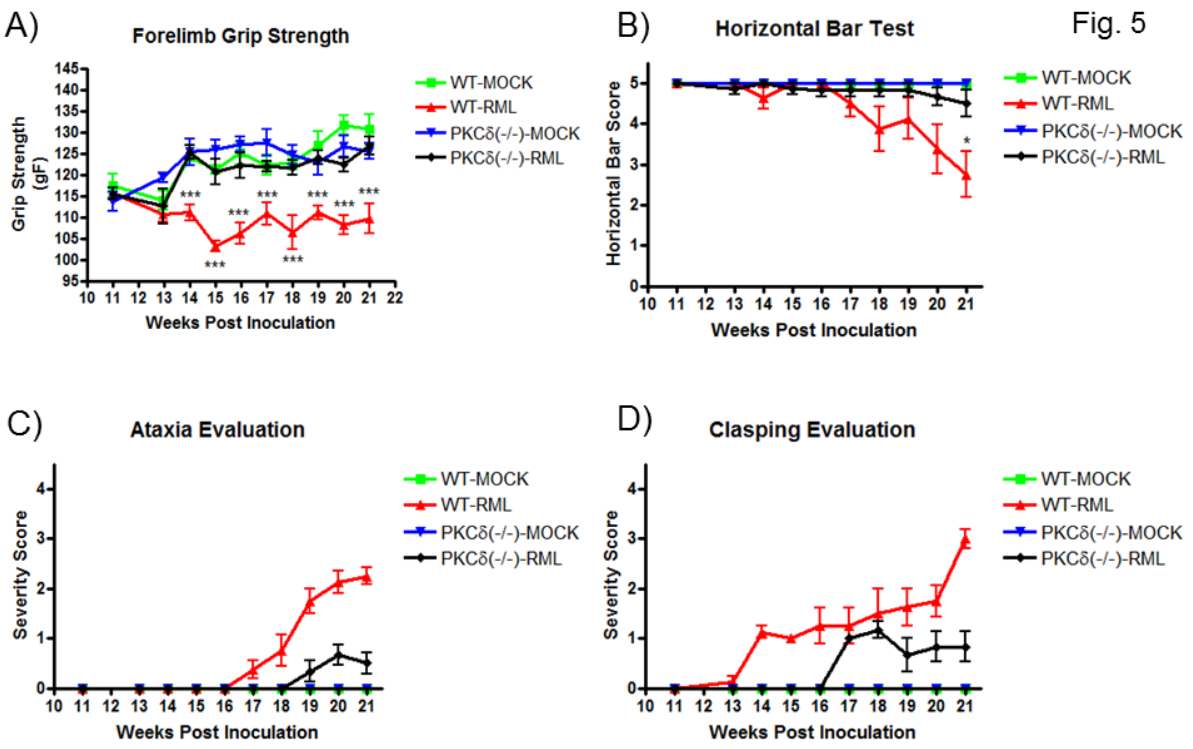


Fig. 5

**Figure 5. PKCδ knockout mice display delayed onset of RML scrapie-related motor symptoms.** RML scrapie-infected WT and PKCδ(-/-) mice were evaluated for motor changes weekly after inoculation. A) Forelimb grip strength was measured using a grip strength meter. WT animals began to display significantly reduced grip strength beginning at 14 weeks. RML scrapie-infected PKC(-/-) animals displayed no significant change from mock infected WT and PKC(-/-) animals throughout the course of infection. B) Motor function was evaluated using the horizontal bar test. WT RML scrapie-infected mice began to show deficits at 17 weeks, and changes became significant at 21 weeks. RML scrapie-infected PKCδ(-/-) mice and mock

infected mice showed no significant changes. Scores were given based on the time each animal could remain hanging from the bar: 0-5s = 1; 6-10s = 2; 11-20s = 3; 21-29s = 4; and 30s or reaching the side support = 5 C) Mice were evaluated for open field ambulation and ability to initiate movement over the course of several minutes. Slight changes in motor function were observed in infected WT mice beginning at 18 weeks and progressed to moderate by 20 weeks. Conversely, PKCδ(-/-) mice displayed a delayed onset in motor signs, and changes remained mild throughout monitoring period. D) The clasping of limbs when held aloft by the tail was evaluated in WT and PKCδ(-/-) mice. Clasping symptoms began in WT mice at 14 weeks and steadily progressed to severe over the course of monitoring. PKCδ(-/-) animals did not begin clasping of limbs until 17 weeks and symptoms did not progress past mild over the course of monitoring. Data represent mean ± SEM with each group containing 6-8 male and female animals.

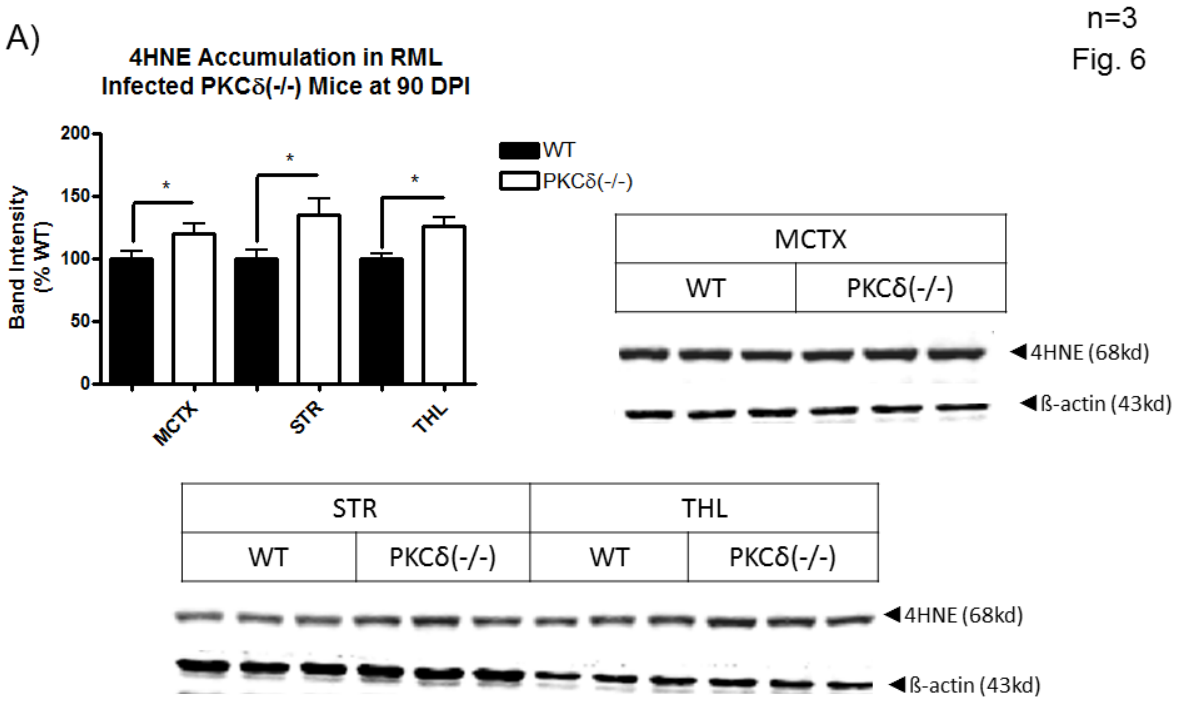


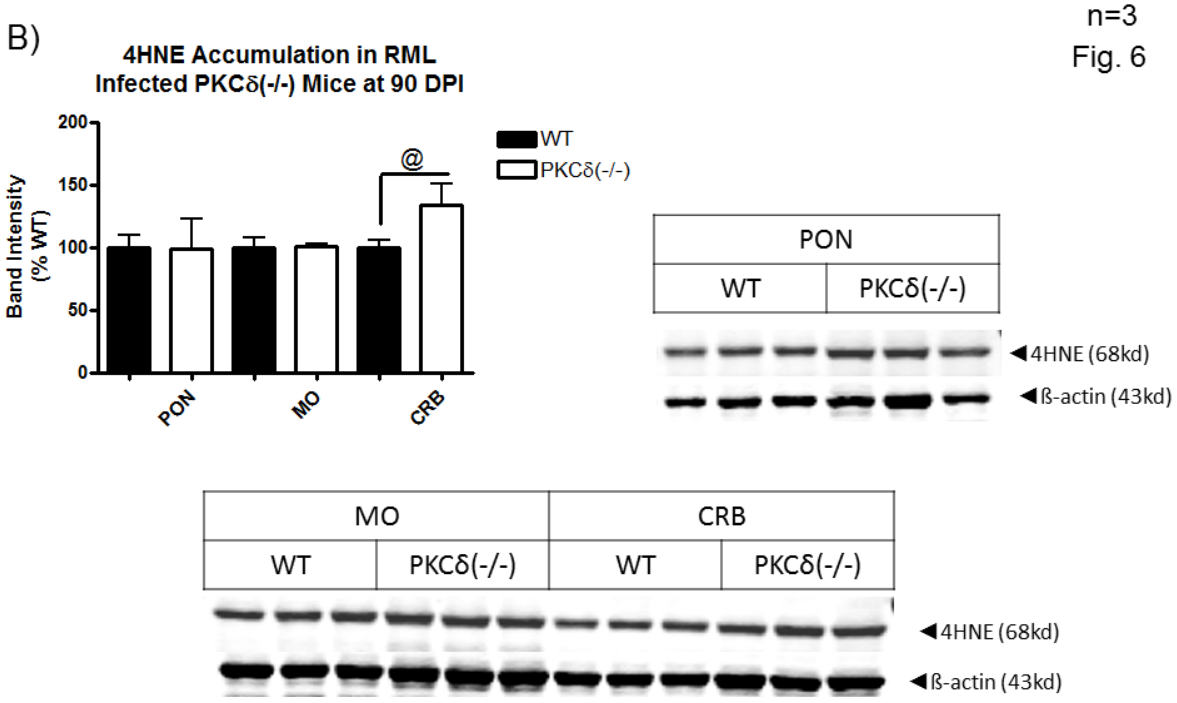

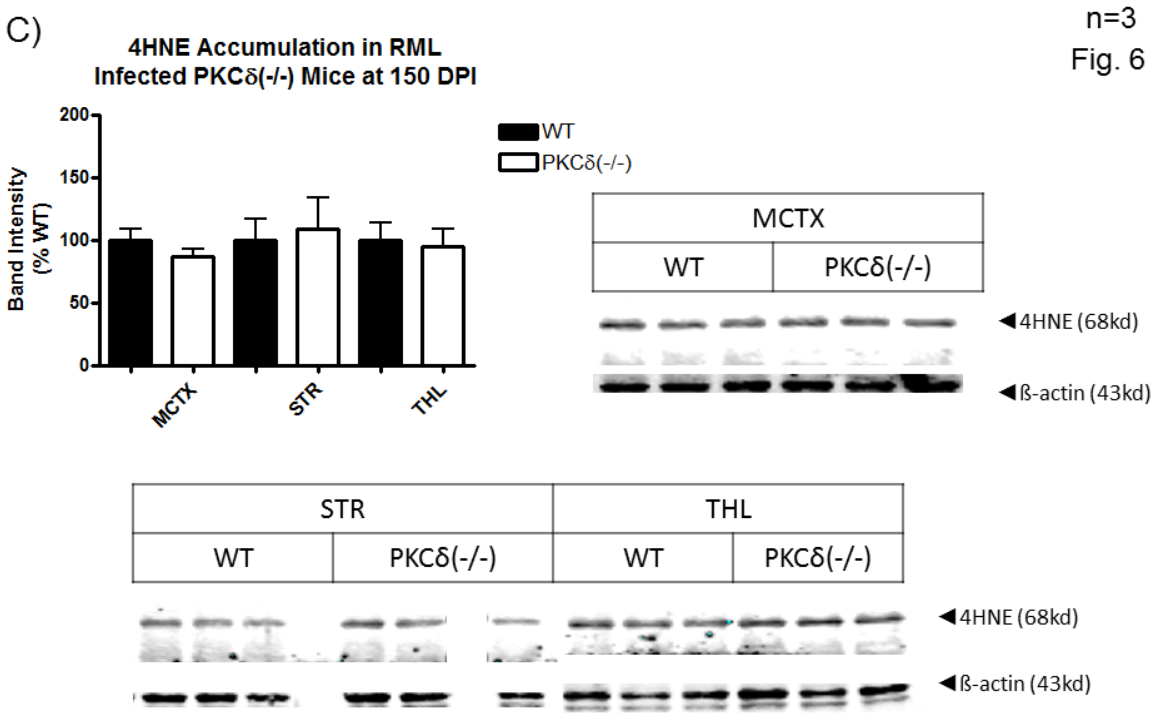


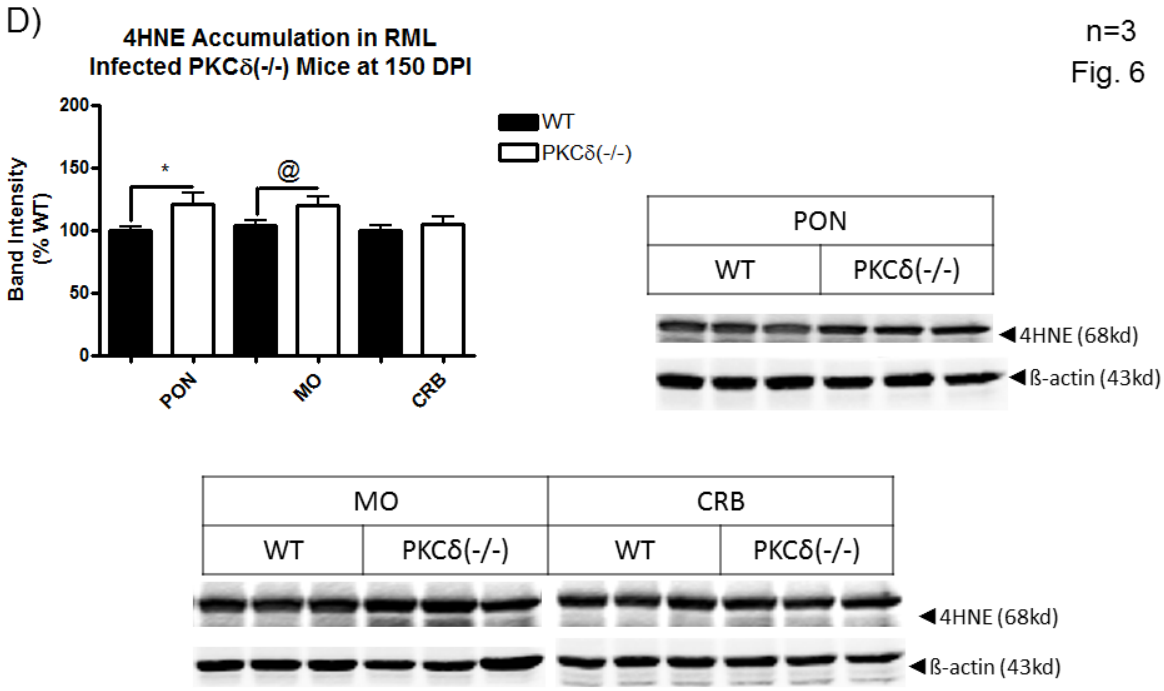

**Figure 6. RML scrapie-infected PKCδ knockout animals display increased markers of oxidative damage.** The level of oxidative damage was evaluated in RML scrapie-infected WT and PKCδ(-/-) animals by immunoblot for 4-HNE, a product of lipid peroxidation. A and B) Significant increases in 4-HNE accumulation were observed in RML scrapie-infected PKCδ(-/-) animals compared to WT in motor cortex, striatum, thalamus, and hippocampus. A slight increase was also observed in cerebellum but was under the level of significance. B and D) A significant increase in oxidative damage was observed in pons in PKCδ(-/-) animals at 150 DPI. A slight but not significant increase was also observed in medulla oblongata. Levels of statistical significance are marked as follows: @ $p<0.1$ * $p<0.05$ ** $p<0.01$ *** $p<0.001$. Data represent mean ± SEM of densitometric analysis from immunoblots of three separate animals.

A)

n=3
Fig. 7

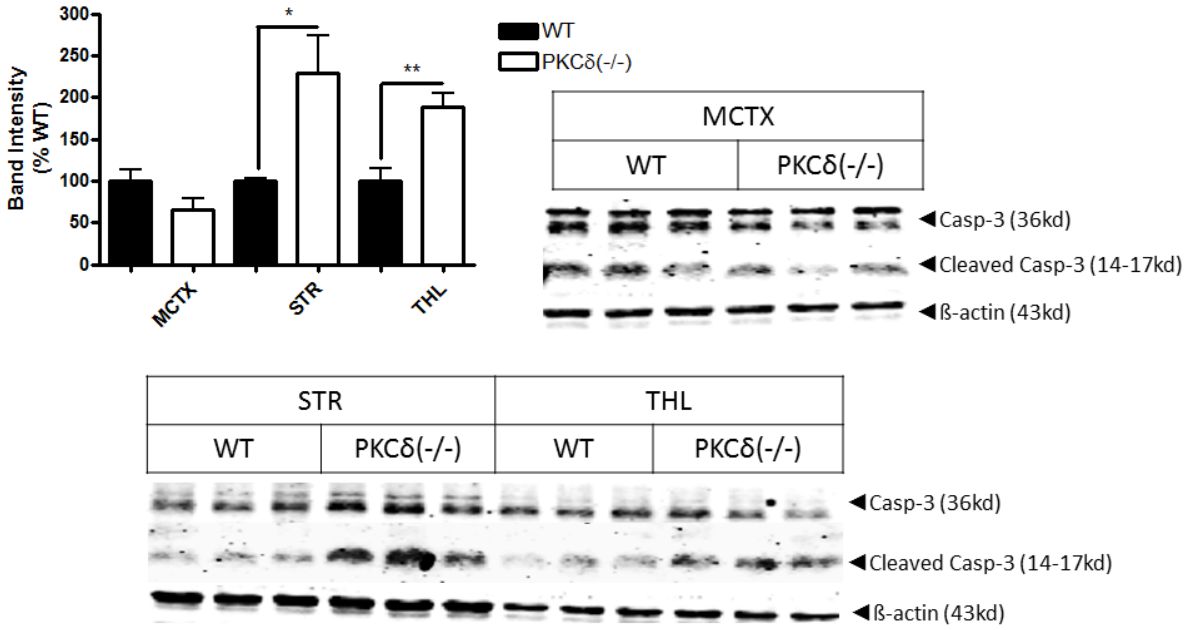


B)

n=3
Fig. 7

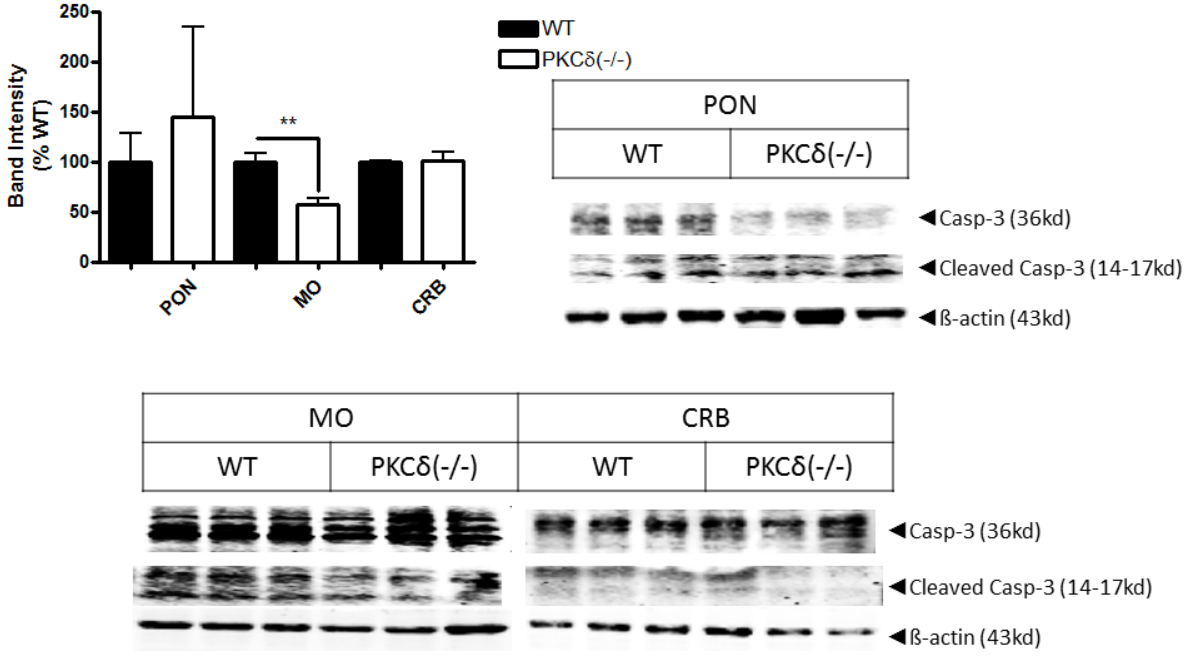

C)

n=3
Fig. 7

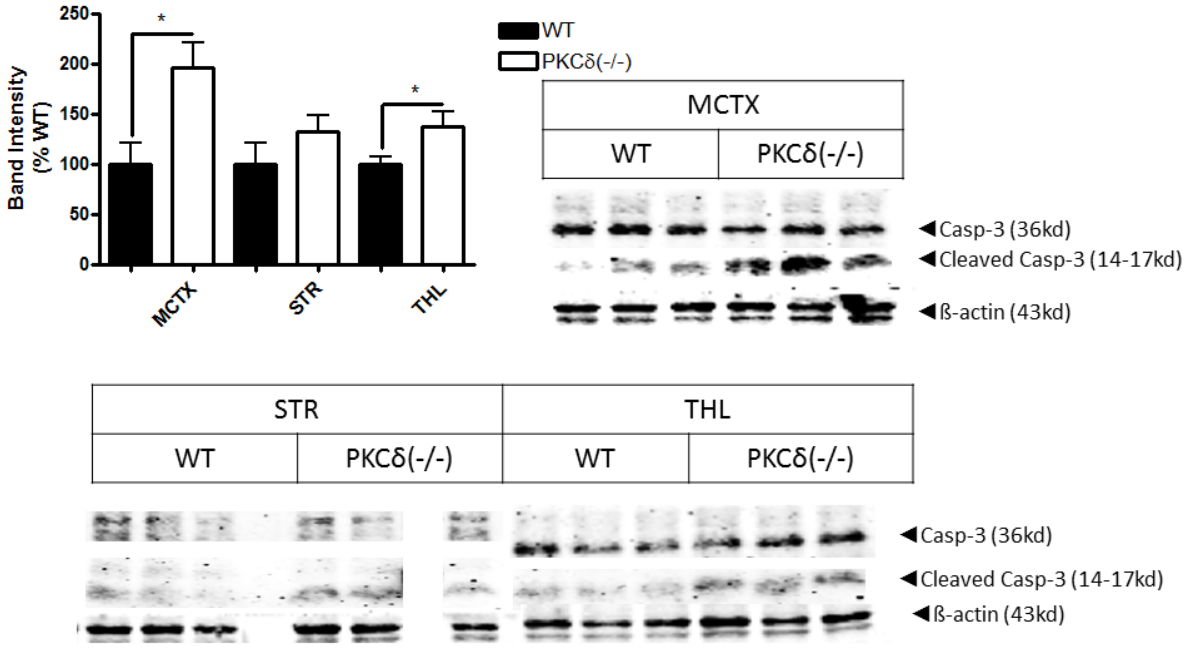


D)

n=3
Fig. 7

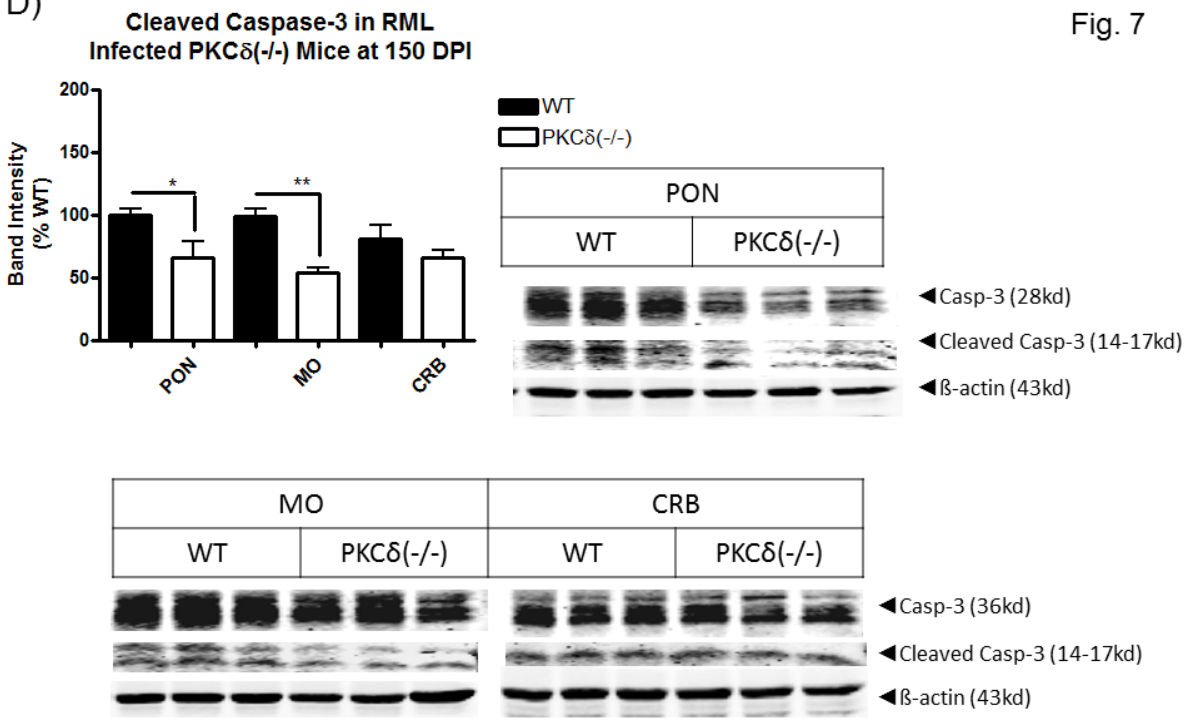

**Figure 7. RML scrapie-infected PKCδ knockout mice have an altered pattern of caspase-3 activation.** RML scrapie-infected WT and PKCδ(-/-) mice were evaluated for activation of caspase-3 by immunoblot analysis for the presence of cleaved caspase-3. A and B) At 90 DPI PKC(-/-) animals have an increase in caspase-3 activation in the striatum and thalamus, but a decrease in the medulla oblongata. C and D) At 150 DPI, PKC(-/-) animals have a similiar increase in caspase-3 activation in the motor cortex and thalamus, but a decrease in the pons as well as the medulla oblongata. Levels of statistical significance are marked as follows: @ $p<0.1$ * $p<0.05$ ** $p<0.01$ *** $p<0.001$. Data represent mean ± SEM of densitometric analysis from immunoblots of three separate animals.

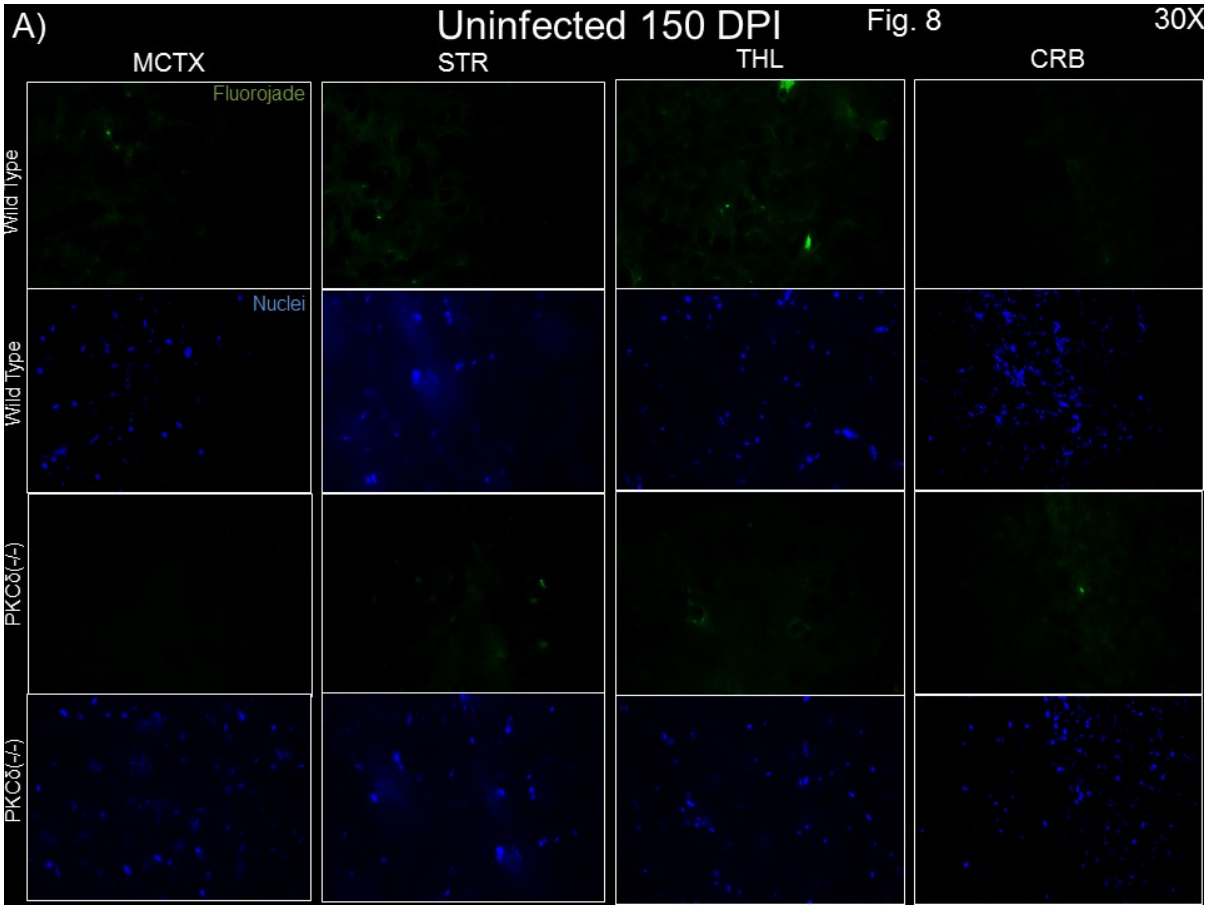

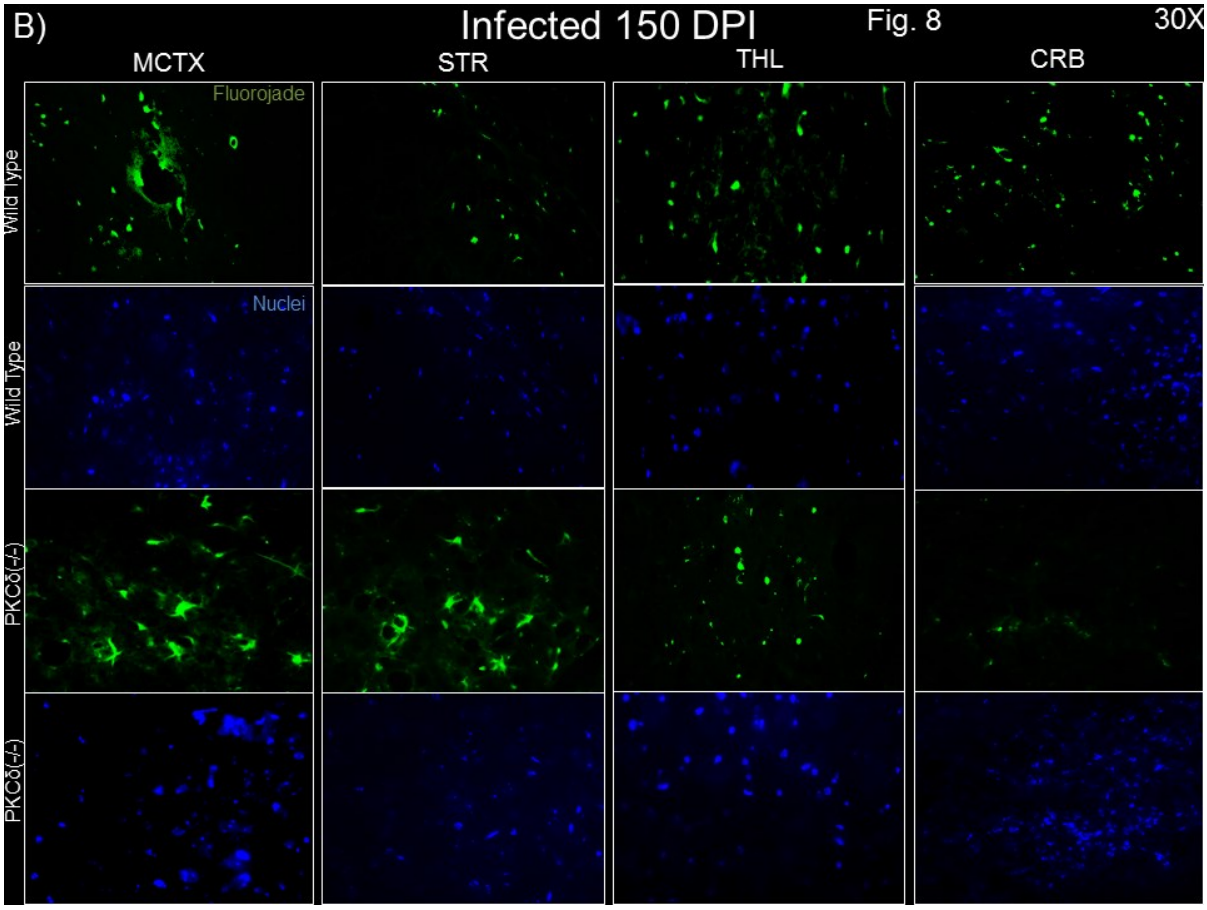


**Figure 8. RML scrapie-infected PKCδ(-/-) mice display an altered pattern of Fluorojade staining.** Degenerating neurons were identified by Fluorojade staining at 150 DPI in mock and RML scrapie-infected WT and PKCδ(-/-) mice. A) Mock infected WT and PKCδ(-/-) mice display little to no Fluorojade staining in all brain regions examined by fluorescent microscope. B) RML scrapie-infected WT animals display widespread Fluorojade staining in all brain regions examined. RML scrapie-infected PKCδ(-/-) mice display strong staining in the motor cortex, striatum, and thalamus but show a reduction in Fluorojade-positive cells in the cerebellum. In the motor cortex and striatum of PKCδ(-/-) many of the Fluorojade positive cells displayed altered morphology compared to WT.

# CHAPTER 5: GENERAL CONCLUSIONS AND FUTURE DIRECTIONS

The results and implications have been presented in each research chapter within this document. This section will provide a broad overview of the findings and suggest possible future studies to continue to elucidate the neurodegenerative mechanisms of TSE.

## Manganese is involved in the pathogenesis of TSE

$PrP^{C}$ readily binds divalent metals, and copper is specifically required during normal functioning of the protein (Brown, 2009). The discovery that Mn was increased during the course of TSE in both humans and animals and that it could replace copper despite an apparent lower affinity implicated this metal in the pathogenesis of the disease (Hesketh et al., 2007; Hesketh et al., 2008; Thackray et al., 2002). Additionally, $PrP^{Sc}$ infected cells were shown to be more susceptible to oxidative stress suggesting the possibility that direct Mn toxicity might be responsible for TSE-related neuronal loss (Milhavet et al., 2000). Instead our findings in cell culture models indicate that $PrP^{Sc}$ infected cells are in fact less susceptible to Mn toxicity. $PrP^{Sc}$ infected CAD5 cells had less caspase-3 activation, DNA fragmentation, and less accumulation of intracellular Mn. These results provide evidence that increased Mn during the course of TSE may affect pathogenesis in some other fashion besides direct toxicity. Truncation studies or mutation of the

active His residues within the metal binding sites would help to identify the role of the specific metal binding sites of PrPC, including the octapeptide repeat domain and the 5$^{th}$ site.

We further found that Mn treatment induces an increase in the cytosolic localization of $PrP^{C}$. This finding is significant because it provides a mechanism whereby cytosolic Mgrn1 and GPI-anchored $PrP^{C}$ could interact during disease pathogenesis. Mgrn1 E3 ubiquitin ligase activity has been implicated in not only polyubiquitination of substrate proteins to signal degradation in the proteasome, but also monoubiquitination and vesicle trafficking (Cooray et al., 2011; Kim et al., 2007; Perez-Oliva et al., 2009). It is important going forward to establish not only the direct cytosolic interaction of Mgrn1 and cytosolic PrP as a result of Mn treatment, but also the attenuation of Mgrn1 E3 ubiquitin ligase activity. A recent study found that the level of Mgrn1 does not affect the progression of mouse adapted scrapie in an animal model of TSE, indicating that Mgrn1 function has redundancy (Silvius et al., 2013). Additionally, it is important to note that both infected and uninfected cells displayed cytosolic PrP at the same time points despite having different tolerances to Mn toxicity. The requirement for the presence of $PrP^{Sc}$ may also be ascertained as well as the specific metal binding site(s) required for this mechanism. While we have discovered that infection with $PrP^{Sc}$ alters a Mn-induced increase in Mgrn1 protein levels in CAD5 cells, additional time points are needed for a detailed qRT-PCR study to clarify the transcriptional regulation of Mgrn1 in response to Mn treatment.

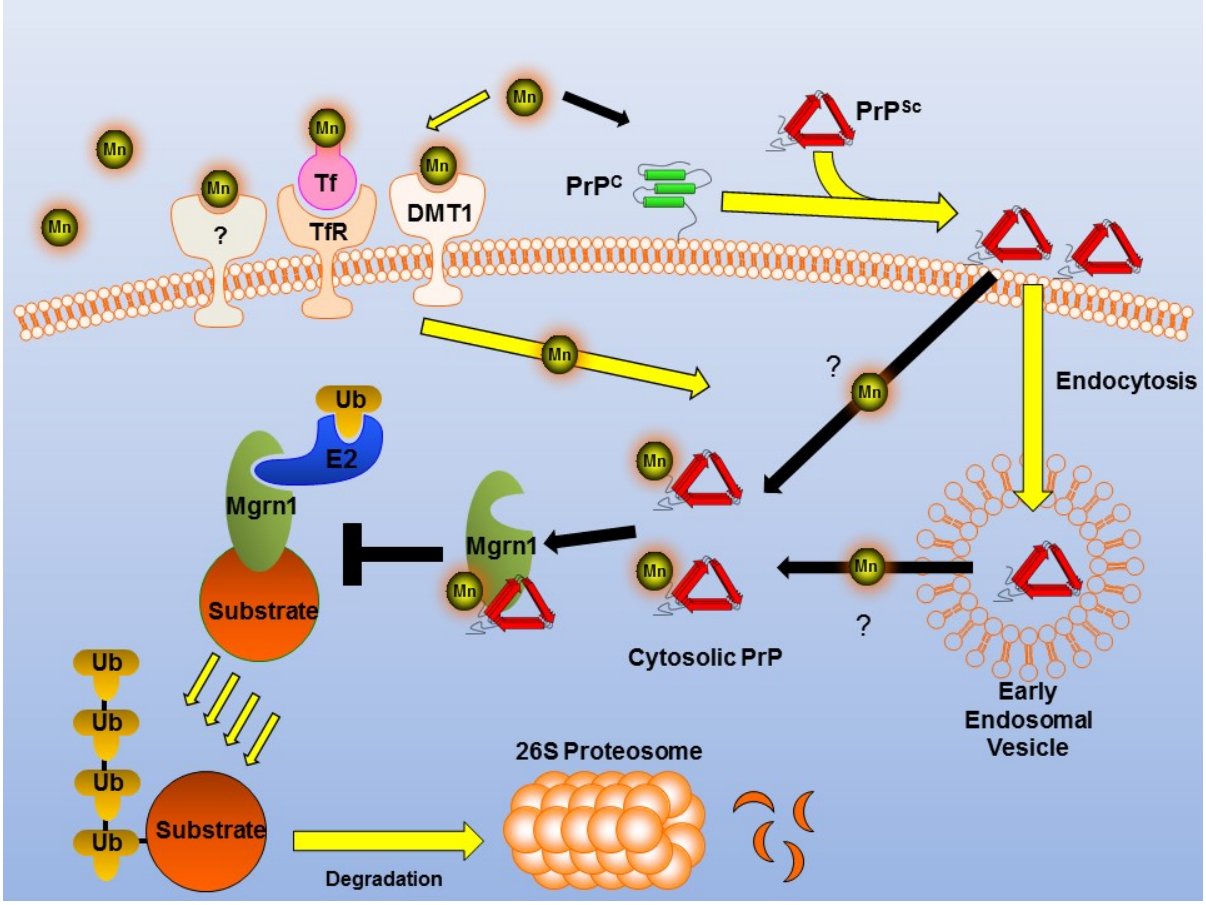


**Figure 1 Hypothetical scheme of Mn-induced cytosolic PrP Interaction with Mgrn1.** Exposure to increased Mn concentrations induces increased cytosolic PrP levels through endocytosis into early endosomal vesicles or another unidentified mechanism. Interaction with cytosolic $PrP^{C}$ or $PrP^{Sc}$ allosterically inhibits the E3 ubiquitin ligase function of Mgrn1 leading to dysfunction of the UPS and spongiform degeneration indicative of TSE.

Kinase signaling modulates TSE neurodegeneration

Our finding that PKCδ is proteolytically activated during TSE draws further connections between prion-like neurodegenerative disorders such as Parkinson's disease and TSE since PKCδ is a key mediator of neuronal apoptosis in dopaminergic neurons (Kanthasamy et al., 2003; Reyland, 2007). Although PKCδ activation may be occurring within degenerating neurons to promote apoptosis in TSE, the possibility remains that these events are also occurring in activated glial cells to promote neuroinflammation. A recent study has shown a connection between caspase-3-mediated cleavage of PKCδ and activation of microglia indicating that glial cells may be a site of cleaved PKCδ (Burguillos et al., 2011). Future studies dedicated to pinpointing the location of PKCδ cleavage and internal phosphorylation events must be done to continue to elucidate the role of this key protein kinase in TSE-related neurodegeneration. A lack of viable *in vitro* model systems that accurately model TSE has hampered more detailed mechanistic investigations. The recent development of murine scrapie infected *ex vivo* brain slice cultures and adult primary culture of neurons that propagate prion infection may allow for more high throughput mechanistic studies (Falsig et al., 2008; Grassmann et al., 2013). Previously, our group has shown that the PKCδ inhibitor rottlerin protected mice treated with the Parkinsonian toxin MPTP, leading to increased locomotor function and dopamine levels (Zhang et al., 2007). Similar studies in models of TSE using rottlerin or its analogs may provide a one of the first viable treatment options for those infected with prion disease.

Overall, the results presented in this document provide some new understanding of the neurodegenerative mechanisms of TSE. Few potential targets for the development of future therapies for TSE in both humans and animals have been presented, and await further studies.

**References**

Brown, D.R., 2009. Brain proteins that mind metals: a neurodegenerative perspective. Dalton Trans. 4069-76.

Burguillos, M.A., et al., 2011. Caspase signalling controls microglia activation and neurotoxicity. Nature. 472, 319-24.

Cooray, S.N., Guasti, L., Clark, A.J., 2011. The E3 ubiquitin ligase Mahogunin ubiquitinates the melanocortin 2 receptor. Endocrinology. 152, 4224-31.

Falsig, J., et al., 2008. A versatile prion replication assay in organotypic brain slices. Nat Neurosci. 11, 109-17.

Grassmann, A., et al., 2013. Cellular aspects of prion replication in vitro. Viruses. 5, 374-405.

Hesketh, S., et al., 2007. Elevated manganese levels in blood and central nervous system occur before onset of clinical signs in scrapie and bovine spongiform encephalopathy. J Anim Sci. 85, 1596-609.

Hesketh, S., et al., 2008. Elevated manganese levels in blood and CNS in human prion disease. Mol Cell Neurosci. 37, 590-8.

Kanthasamy, A.G., et al., 2003. Role of proteolytic activation of protein kinase Cdelta in oxidative stress-induced apoptosis. Antioxid Redox Signal. 5, 609-20.

Kim, B.Y., et al., 2007. Spongiform neurodegeneration-associated E3 ligase Mahogunin ubiquitylates TSG101 and regulates endosomal trafficking. Mol Biol Cell. 18, 1129-42.

Milhavet, O., et al., 2000. Prion infection impairs the cellular response to oxidative stress. Proc Natl Acad Sci U S A. 97, 13937-42.

Perez-Oliva, A.B., et al., 2009. Mahogunin ring finger-1 (MGRN1) E3 ubiquitin ligase inhibits signaling from melanocortin receptor by competition with Galphas. J Biol Chem. 284, 31714-25.

Reyland, M.E., 2007. Protein kinase Cdelta and apoptosis. Biochem Soc Trans. 35, 1001-4.

Silvius, D., et al., 2013. Levels of the Mahogunin Ring Finger 1 E3 ubiquitin ligase do not influence prion disease. PLoS One. 8, e55575.

Thackray, A.M., et al., 2002. Metal imbalance and compromised antioxidant function are early changes in prion disease. Biochem J. 362, 253-8.

Zhang, D., et al., 2007. Neuroprotective effect of protein kinase C delta inhibitor rottlerin in cell culture and animal models of Parkinson's disease. J Pharmacol Exp Ther. 322, 913-22.